Effects of *p*-cresol on oxidative stress, glutathione depletion, and necrosis in HepaRG cells:

comparative effects to other uremic toxins and role of *p*-cresol glucuronide formation

by

Sang Zhu

A thesis submitted in partial fulfillment of the requirements for the degree of

Master of Science

In

Pharmaceutical Sciences

Faculty of Pharmacy and Pharmaceutical Sciences
University of Alberta

Abstract

Background: The toxicological effects of *p*-cresol have primarily been attributed to its metabolism end products; however, very little human toxicological data are available in the key organ (i.e. the liver) responsible for the generation of these metabolites. We hypothesized that *p*-cresol is relatively more toxic than the other protein-bound uremic toxins, and that the glucuronidation of *p*-cresol or the glucuronide end product can lead to toxicities in the human liver. Our objectives were: i) to characterize the concentration- and temporal- effects of *p*-cresol on toxicity markers; ii) to compare the effects of *p*-cresol and other protein bound uremic toxins on toxicity markers in HepaRG cells; iii) to determine the metabolic activities of HepaRG cells in the production of major *p*-cresol conjugated metabolites; and iv) to characterize the effects of exogenously-administered and *in-situ* generated *p*-cresol glucuronide in the manifestation of toxicities in HepaRG cells. Methods: The HepaRG cell line was utilized as the experimental model. The toxicity markers were 2'-7'-dichlorofluorescein (DCF; marker of oxidative stress) formation, total cellular glutathione (GSH) concentration, and lactate dehydrogenase (LDH; marker of cellular necrosis) release. The concentrations of *p*-cresol were measured by ultra-high performance liquid chromatography assay (UPLC). The concentrations of *p*-cresol sulfate and *p*-cresol glucuronide were quantified using ultra-high performance liquid chromatography-tandem mass spectrometry assay (UPLC-MS/MS). Results: *p*-Cresol exposure resulted in concentration- and time-dependent changes in DCF formation, GSH concentration, and LDH release in HepaRG cells at potentially toxicologically relevant conditions. *p*-Cresol was also relatively more toxic than 3-carboxy-4-methyl-5-propyl-2-furanpropanoic acid, indole-3-acetic acid, indoxyl sulfate, kynurenic acid, and hippuric acid on all tested markers. Although the exogenous administration of *p*-cresol sulfate and *p*-cresol glucuronide generated high intracellular concentrations of these metabolites, both metabolites

were significantly less toxic compared to *p*-cresol at equal-molar conditions. Moreover, *p*-cresol glucuronide was the predominant metabolite generated *in situ* from *p*-cresol exposure. The selective attenuation of glucuronidation (without affecting *p*-cresol sulfate formation, while increasing *p*-cresol accumulation) using independent chemical inhibitors (i.e. L-borneol, amentoflavone, or diclofenac) consistently resulted in further increases in LDH release associated with *p*-cresol exposure. Conclusion: These novel data indicated that *p*-cresol was a relatively potent toxicant, and that glucuronidation was unlikely associated with the manifestation of its toxic effects in HepaRG cells.

Preface

This thesis is an original work by Sang Zhu.

Chapters II & III of this thesis are currently being submitted (as one manuscript) for review by a peer-reviewed publication. Sang Zhu (first author) conducted the experiments, collected the data, analyzed the data, wrote the first draft, and prepared subsequent revisions (under assistance of lab member Ms. Yan Rong [second author, PhD candidate in Dr. Kiang's lab] and the supervision of Dr. Kiang). The UPLC and LC/MS/MS analytical assays were initially developed by Ms. Yan Rong under guidance of Dr. Kiang, and Sang Zhu was responsible for validating the UPLC assay and utilizing both assays for her thesis work.

Dedication

My dedications to Ms. Yan Rong for helping me with living arrangements and helping me with laboratory work.

My sincere thanks to my parents for supporting me all the time.

Acknowledgment

Table of Contents:

List of Tables:

List of Figures:

Abbreviations: *ARE/EpRE*, antioxidant/electrophile responsive element; *BCRP*, breast cancer resistance protein; *ciPTEC*, Conditionally immortalized human renal proximal tubule epithelial cells; CKD, chronic kidney disease; *CMPF*, 3-carboxy-4-methyl-5-propyl-2-furanpropionic acid; *CRF*, chronic renal failure; *CYP*, cytochrome P450; *DCF*, 2', 7'-dichlorofluorescein; *DCFDA*, 2', 7'-dichlorofluorescin diacetate; *DMSO*, dimethyl sulfoxide; *DMP*, 2,6-dimethylphenol; *D-PBS*, Dulbecco's phosphate-buffered saline; EC_{50}, half maximal effective concentration; *E. coli*, *Escherichia coli*; *EDTA*, ethylenediaminetetraacetic acid; *eGFR*, estimated glomerular filtration rate; *E1S*, estrone-sulfate; *EMT*, epithelial-to-mesenchymal transition; *ESRD*, end-stage renal disease; *eYFP*, enhanced yellow fluorescent protein; *FBS*, fetal bovine serum; *fMLP*, N-formyl-methionine-leucine-phenylalanine; *GCL*, glutamate-cysteine ligase; *GS*, glutathione synthase; *GSSG*, glutathione disulfide; *GSH*, glutathione; *GSSR*, glutathionylated-cysteine derivative; *GST*, glutathione-S-transferase; *Keap1*, Kelch-like ECH-associated protein 1; *LDH*, lactate dehydrogenase; *MES*, 2-(N-morpholino) ethanesulphonic acid; *MRP4*, multidrug resistance protein 4; *MTT*, 3-(4,5-dimethylthiazol-2-yl)-2,5-diphenyltetrazolium bromide; *MTX*, methotrexate; NAD^+, nicotinamide adenine dinucleotide; $NADP^+$, nicotinamide adenine dinucleotide phosphate; *NADPH*, nicotinamide adenine dinucleotide phosphate; *Nrf2*, the nuclear factor erythroid 2-related factor 2; *OAT*, organic anion transporter; *pCG*, p-cresol glucuronide; *pCS*, p-cresol sulfate; *PMA*, phorbol-12-myristate-13-acetate; *PTH*, parathyroid hormone; *qPCR*, quantitative polymerase chain reaction; *SULT*, sulfotransferase; *t-BOOH*, tert-butyl hydroperoxide; *TCA*, taurocholic acid; *TMRM*, tetramethyl rhodamine methyl ester; *UDPGA*, uridine 5'-diphosphoglucuronic acid; *UGT*, UDP-glucuronosyltransferase; *UPLC-MS/MS*, ultra-high performance liquid chromatography-tandem mass spectrometry assay.

Chapter I : Introduction

1. Uremic toxins

Uremia is a disease condition caused by the accumulation of uremic toxins, which are mainly produced by microbiota in the gut that cannot be removed efficiently from the human body through the kidneys (Prokopienko, Alexander J. and Nolin, 2018). In general, uremic toxins are classified into three categories based on their molecular weights: i) small water-soluble compounds, ii) middle molecules, and iii) protein bound compounds (Vanholder et al., 2003). Small water-soluble compounds are consisted of toxins that are water soluble and have molecular weights less than 500 Daltons (the prototypical substance is urea (Vanholder et al., 2018)). The molecular weights of the middle molecules are usually higher than 500 Daltons with an example being the β_2-microglobulin (Vanholder et al., 2018). For the protein bound uremic toxins, the molecular weights are generally less than 500 Dalton, and *p*-cresol is one of the prototypical examples (Vanholder et al., 2018).

Compared to the small water-soluble and the middle molecule compounds, the removal of protein bound uremic toxins through dialysis is relatively inefficient (Vanholder et al., 2018). Furthermore, subjects with impaired renal functions (e.g. chronic kidney disease [CKD] patients) are likely to "trap" the protein bound uremic toxins within the body (Mutsaers et al., 2015,Poesen et al., 2016), which could lead to the accumulation of protein-bound toxins which have been associated with multi-organ toxicities including kidney dysfunction, cardiovascular disease, and overall mortality (Jourde-Chiche and Burtey, 2020). In addition, the accumulation of protein bound uremic toxins has also been associated with gut microbial dysbiosis and inflammations of organs such as the liver, heart, brain, bone, and blood vessels (Graboski and Redinbo, 2020).

Furthermore, protein bound uremic toxins can be further classified based on their chemical structures (i.e. functional groups) into the following sub-categories: advanced glycation end products, hippurates, indoles, polyamines, phenols, and miscellaneous agents such as 3-carboxy-4-methyl-5-propyl-2-furanpropionic acid (Graboski and Redinbo, 2020). Advanced glycation end products are typically associated with arterial stiffness, diabetic nephropathy, endothelial dysfunctions, and immune system dysregulations; hippurates have been linked to endothelial dysfunctions and renal tubule damage; indoles are correlated with bone disease, cardiovascular disease, endothelial dysfunction, inflammation, muscle weakness or atrophy, neurotoxicity, and oxidative stress; polyamines are associated with anemia; and phenols (e.g. *p*-cresol) have been associated with cardiovascular disease, liver dysfunction, inflammation, oxidative stress, renal fibrosis, vascular remodeling, and ultimately, mortality (Graboski and Redinbo, 2020,Thompson et al., 1994,Weigand et al., 2019,Vanholder et al., 2018,Gryp et al., 2017,Watanabe et al., 2013).

In addition, protein bound uremic toxins have been demonstrated to affect the activities of cytochrome P450, sulfotransferase, and UDP-glucuronosyltransferase enzymes (Prokopienko, Alexander J. and Nolin, 2018). Despite limited data, expressions or activities of transporters such as organic anion transporting polypeptides, organic anion transporters, and breast cancer resistant protein, and multidrug resistance protein 4 can also be modulated by protein-bound uremic toxins (Prokopienko, Alexander J. and Nolin, 2018,Mutsaers et al., 2013,Mutsaers et al., 2015,Weigand et al., 2019). In general, the inhibition or induction of metabolism enzymes and/or transporters can potentially lead to drug-drug interactions in patients with chronic kidney disease, as these patients are very likely to be receiving multiple concurrent medications.

1.1. p-Cresol and its metabolism

p-Cresol is a protein-bound uremic toxin. The major source of *p*-cresol production is the ingestion of dietary proteins as *p*-cresol is mainly produced by bacteria in the large intestines from amino acids such as tyrosine and phenylalanine (Gryp et al., 2017). In addition, *p*-cresol also originates from environmental sources, such as plant extracts, traditional medicines, crude oil, and coal tar (Andersen, 2006,Vanholder et al., 1999). In the production of *p*-cresol, many gut microbiotas such as *Bacteroidaceae*, *Bifidobacteriaceae*, *Eubacteriaceae*, *Lachnospiraceae*, *Porphyromonadaceae*, *Ruminococcaceae*, *Veillonellaceae*, and *Fusobacteriaceae* can be involved, while the *Clostridium* species are identified to be the major bacteria by most studies (Gryp et al., 2017). The primary locations of *p*-cresol metabolism are the human intestine and the liver (Gryp et al., 2017). To our knowledge, there are three metabolic pathways of *p*-cresol in humans, which are oxidation mediated by cytochrome P450 enzymes, and sulfonation or glucuronidation (Prokopienko, Alexander J. and Nolin, 2018) (Figure 1). The major metabolites of *p*-cresol in humans are *p*-cresol sulfate and *p*-cresol glucuronide (Prokopienko, Alexander J. and Nolin, 2018).
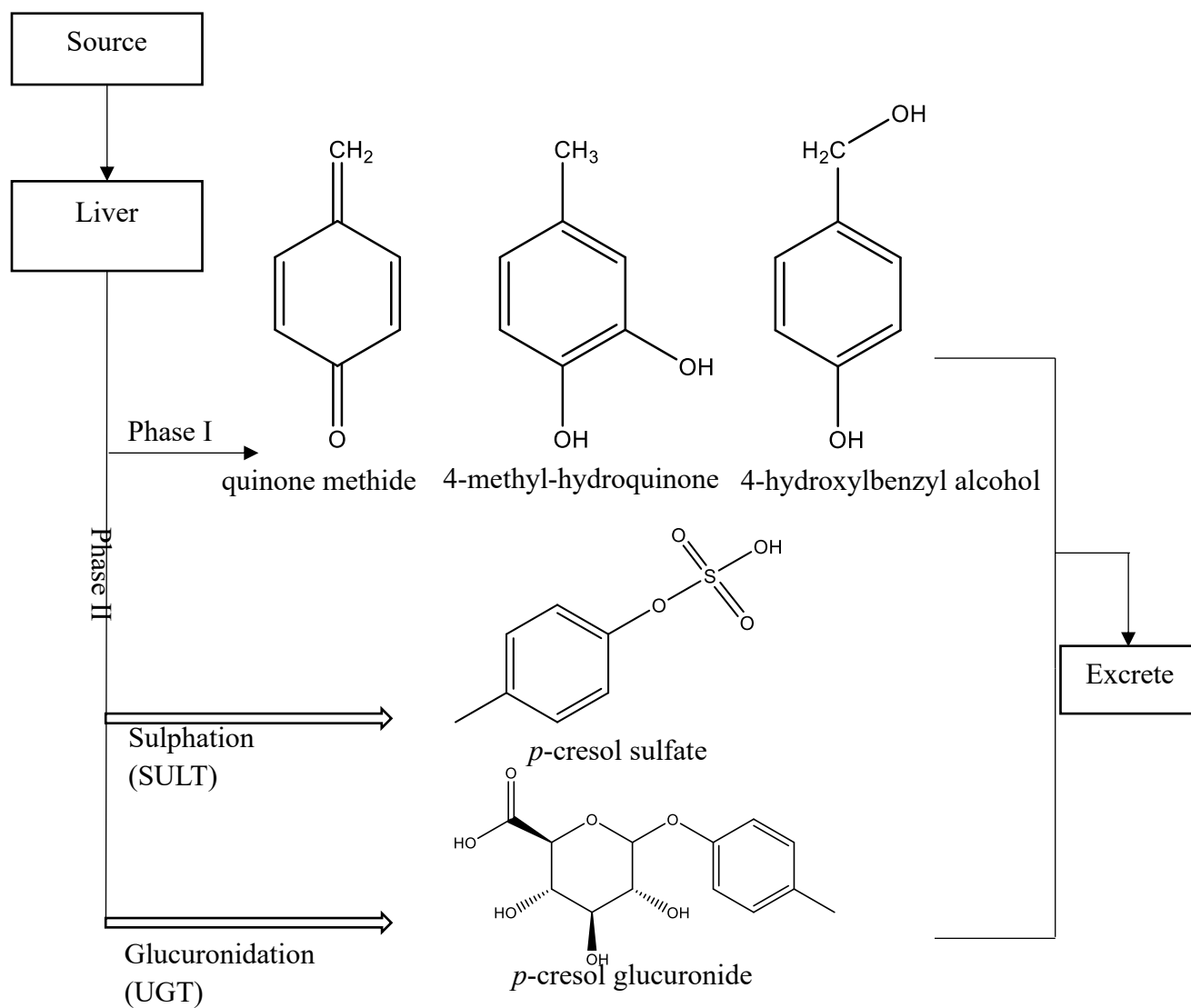
Figure 1. The metabolic fate of *p*-cresol (Yan et al., 2005,Prokopienko, Alexander J. and Nolin, 2018,Gryp et al., 2017,Thompson et al., 1996).

The highest total plasma *p*-cresol concentration observed under uremic conditions is up to 596 µM (Meert et al., 2012) [please see **Table 1**], whereas the highest total concentrations of *p*-cresol sulfate (in plasma) and *p*-cresol glucuronide (in serum) are approximately 1600 µM and 85 µM (Meert et al., 2012,Cuoghi et al., 2012), respectively [please see **Tables 2&3**]. Direct data of *p*-cresol concentrations in the human liver and kidney are limited. However, due to the fact that *p*-cresol is mainly metabolized by the human liver, the sum of *p*-cresol, *p*-cresol sulfate, and *p*-cresol glucuronide concentrations in the human plasma can presumably reflect *p*-cresol exposures in the human liver. Therefore, it is possible that *p*-cresol concentrations can reach mM level in the human liver.

In addition, *p*-cresol sulfate is highly protein-bound (~ 90%); therefore, although the total concentrations of *p*-cresol sulfate are relatively elevated, the free concentrations (which is the pharmacologically-active form) are relatively low in the plasma (Meert et al., 2012,Itoh et al., 2012) (Table 2). To the contrary, the protein binding of *p*-cresol glucuronide is relatively low (~10%). Therefore, although the total plasma concentrations of *p*-cresol glucuronide are lower, the free concentrations of *p*-cresol glucuronide can be similar to or even higher than *p*-cresol sulfate (Meert et al., 2012,Itoh et al., 2012) (Tables 2 & 3). As the free fractions of xenobiotics are biologically active, these data indicate that *p*-cresol glucuronide may exhibit significant biological activities based on its relatively significant unbound plasma concentrations.

Table 1. Summary of plasma concentrations of *p*-cresol in humans

Literature	Matrices	*p*-Cresol concentrations, μM		
(De Smet et al., 1998)	Human blood	Total concentration Normal:4.0-12.7 Outpatients:53.5-148.0 Continuous ambulatory peritoneal dialysispatients:31.2-84.1 Hemodialysis patients:96.1-176.6	Free concentration Normal: NA Outpatients:4.7-11.6 Continuous ambulatory peritoneal dialysispatients:3.2-9.0 Hemodialysis patients:1.8-23.8	Calculated protein binding: Normal:100% Outpatients:86.6-95.3% Continuous ambulatory peritoneal dialysis patients:82.7-93.3% Hemodialysis patients:74.9-95.2%
(Niwa, 1993)	Human serum	Total concentration Normal: 0-9.6 Uremic, pre-hemodialysis: 21-79 Uremic, post-HD: 1-63		
(de Loor et al., 2005)	Human serum	Total concentration Normal: 12.8-21.1 Patients: 201.7-322.3		
(Vanholder et al., 2003)	Human serum	Highest concentration: 376.36		
(Vanholder et al., 2014)	Human plasma	Total concentration: 20.34-430 Free concentration: 5.18-266.32		
(Meert et al., 2007)	Human serum	Total concentration: 263-596		
(Korytowska et al., 2019)	Human plasma	Total concentration: 0.004-0.012		

Table 2. Summary of plasma concentrations of *p*-cresol sulfate in humans

Literature	Matrices	*p*-Cresol sulfate concentrations, μM	
(Prokopienko, Alexander J. and Nolin, 2018)	Human serum	Total concentration (mean): 46-176 Free concentration (mean): 2.9-15.7 Total concentration (highest): 147-289	
(Gryp et al., 2017)	Human plasma	Total concentration: 331-805	
(Prokopienko, A. J. et al., 2019)	Human serum	Total concentration: 117.96	
(Meert et al., 2012)	Human serum	Total concentration (mean): 83.46-252.46 Free concentration (mean): 1.6-24	Total concentration (highest): 483.4 Free concentration (highest): 75.4
(Cuoghi et al., 2012)	Human serum	Total concentration (mean): 170-286 (Martinez et al., 2005) 58-228 (Pham et al., 2008) 105-261 (Meert et al., 2009) 17-211 (Krieter et al., 2010) 37-289 (Liabeuf et al., 2010) 331-805 (Cuoghi et al., 2012) 652-1398 (Cuoghi et al., 2012)	Total concentration (highest): 345 (Martinez et al., 2005) 313 (Pham et al., 2008) 340 (Meert et al., 2009) 307 (Krieter et al., 2010) 560 (Liabeuf et al., 2010) 1049 (Cuoghi et al., 2012) 1664 (Cuoghi et al., 2012)
(Itoh et al., 2012)	Human serum	Total concentration: 124-156 Free concentration: 19-29	

Table 3. Summary of plasma concentrations of *p*-cresol glucuronide in humans

Literature	Matrices	*p*-Cresol glucuronide concentrations, μM
(Meert et al., 2012)	Human serum	Total concentration (mean): 2.8-48.8 Total concentration (highest): 84.8 Free concentration (mean): 2.9-44.5 Total concentration (highest): 79.2
(Itoh et al., 2012)	Human serum	Total concentration: 23.2-26.8 Free concentration: 13-19.4

Theoretically, in addition to the human liver, both the intestines and the kidneys are also exposed to considerable amounts of *p*-cresol. Although the liver is the primary organ for *p*-cresol metabolism (Prokopienko, Alexander J. and Nolin, 2018), intestines can also contribute to the conjugation of *p*-cresol. However, the metabolism end products in the intestines are likely to be excreted directly into the feces and thus would have less influence on the overall systemic concentrations (Rong and Kiang, 2020). In addition, the contributions of human kidneys in *p*-cresol metabolism might also be argued to be less important than the liver, because the overall glucuronidation and sulfation protein contents are lower in the kidneys (Knights et al., 2016,Riches et al., 2009), and by the time blood reaches the kidneys, the majority of *p*-cresol has already been converted to *p*-cresol sulfate and glucuronide (de Loor et al., 2005). This is evident by that fact that free *p*-cresol concentrations in the liver are approximately 2-fold higher than that of human kidneys in data collected from four deceased hemodialysis subjects [i.e. 23.9 µM vs. 10.7 µM (Ikematsu et al., 2019)]. *Based on these assertions, the human liver was the target organ of interest to investigate the p-cresol associate toxicities in our study.*

Data are available on *p*-cresol-induced toxicities in the liver or liver-derived *in vitro* models. Thompson et al. demonstrated increased lactate dehydrogenase (LDH) release in rat liver slices exposed to 2 mM of *p*-cresol for 6 hours (Thompson et al., 1994,Thompson et al., 1996). In addition, the toxicity of *p*-cresol (as demonstrated by intracellular potassium concentration) was significantly reduced by metyrapone (i.e. a cytochrome P450 inhibitor) and increased by phenobarbital (i.e. a cytochrome P450 inducer), indicating a potential role of cytochrome P450 generated toxic *p*-cresol metabolites. Moreover, modulation of cellular glutathione concentrations by N-acetylcysteine or diethyl maleate also affected *p*-cresol mediated LDH release, suggesting a role of glutathione homeostasis in *p*-cresol mediated toxicity (Thompson et al., 1994). The toxicity

of *p*-cresol can be associated with a reactive quinone methide intermediate (the LC_{50} of *p*-cresol was 1.32 mM after 6-hour exposure) in rat liver slice model (Thompson et al., 1996). These data are supported by the production of glutathione adducts of cytochrome P450-generated reactive intermediates in human liver microsomes (Yan et al., 2005). Furthermore, the toxicity of *p*-cresol has also been reported by Abreo et al., who observed an increase in the cellular aluminum concentration in mouse hepatocytes exposed to *p*-cresol at 3 mg/dl for 96 hours (Abreo et al., 1997). As well, *p*-cresol (15 minutes of exposure with 160 mmol/mg microsomal protein) reduced nicotinamide adenine dinucleotide phosphate (NADPH) in isolated rat liver mitochondria, suggesting the induction of toxicity by *p*-cresol in the rat liver (Kitagawa, 2001).

2. Toxicities associated with p-cresol glucuronide

2.1. In vivo studies of p-cresol glucuronide associated toxicity

Based on the published clinical papers, the associations between *p*-cresol glucuronide concentrations and cardiovascular and/or kidney toxicities have been widely established, the papers are summarized in **Table 4** (Poesen et al., 2016,Chinnappa et al., 2018,Liabeuf et al., 2013).

Poesen et al. conducted a prospective investigation on the correlations between *p*-cresol glucuronide concentrations with renal function, cardiovascular disease, and overall mortality (Poesen et al., 2016). Briefly, total and free serum concentrations, 24-hour urinary excretion, protein binding, and renal clearance of *p*-cresol glucuronide were characterized in 203 patients in stages 1-5 of pre-dialysis CKD (120 males, 83 females) (See **Table 6** for definitions of stages of CKD). The median concentrations of albumin and creatinine were 4.51 g/dL and 1.81 mg/dL, respectively. The median estimated glomerular filtration rate (eGFR), creatinine clearance, and 24-hour proteinuria were 34 mL/min per 1.73 m^2, 40 mL/min, and 0.31 g, respectively. Serum

samples of eight healthy volunteers were also collected as the control group. In CKD patients, the total and free median concentrations of *p*-cresol glucuronide were 0.22 μM and 0.13 μM, respectively. Increased serum total and free concentrations of *p*-cresol glucuronide were associated with reduced eGFR (p<0.001). Moreover, the median amount of 24-hour urinary excreted *p*-cresol glucuronide was ~4 μM and well correlated with eGFR (rho=-0.25, p<0.001). With respect to protein binding, the serum from uremic patients exhibited significantly elevated unbound fractions of *p*-cresol glucuronide (88.1±3.7%, mean±SD) compared to healthy serum (74.5±3.3%) (p<0.001). Based on linear regression analysis, eGFR was identified as one of the significant variables predicting the unbound fraction of *p*-cresol glucuronide (p<0.001). Moreover, the median total and free renal clearance of *p*-cresol glucuronide were 98.9 mL/min and 136.5 mL/min, respectively, which were positively correlated with eGFR (p<0.001). Furthermore, the ratios of *p*-cresol sulfate to *p*-cresol glucuronide were calculated and utilized as markers of metabolism in correlation analyses. Both total and free ratios of *p*-cresol sulfate/glucuronide were positively correlated with eGFR (total: rho=0.23, p=0.001; free: rho=0.20, p=0.005). Likewise, increased ratios of 24-hour urinary excreted *p*-cresol sulfate to glucuronide were related to elevated eGFR (rho=0.32, p<0.001). In addition, Cox proportional hazards analysis was performed to evaluate the effects of *p*-cresol sulfate/glucuronide ratios on the risks of cardiovascular disease and overall mortality. For cardiovascular disease, the hazard ratio of [*p*-cresol sulfate/glucuronide] was 0.55 (p<0.001). In terms of overall mortality, hazard ratio of [*p*-cresol sulfate/glucuronide] was 0.65 (p<0.01). In general, Poesen et al. demonstrated that the shift from *p*-cresol sulfation to *p*-cresol glucuronidation was associated with the severity of renal dysfunction (as evident by decreased eGFR), and this shift was linked to cardiovascular disease and overall mortality.

Chinnappa et al. evaluated the effects of total and free serum concentrations of *p*-cresol glucuronide on cardiac performance using correlational analysis (Chinnappa et al., 2018). The patient population consisted of 56 male CKD patients in stages 2-5 before dialysis who were asymptomatic, and who lacked the diagnosis of fulminant cardiac disease and/or diabetes. The average age was 46.8 ± 12.5 years (mean±standard deviation), with eGFR of 38.5 ± 24.1 mL/min per 1.73 m^2. The enrolled patients were further divided into four subgroups based on their CKD stages. The renal functions (as indicated by eGFR) were significantly different in the four subgroups: 73.5 ± 7.9 mL/min per 1.73 m^2, 43.2 ± 7.9 mL/min per 1.73 m^2, 21.5 ± 4.3 mL/min per 1.73 m^2, and 11.9 ± 2.4 mL/min per 1.73 m^2 in CKD stages 2, 3, 4, and 5, respectively ($p < 0.001$). The concentrations of creatinine, urea, calcium, phosphate, bicarbonate, uric acid, parathyroid hormone, and hemoglobin were also different in the individual subgroups ($p < 0.05$). In addition, cardiac function as demonstrated by peak cardiac output, peak heart rate, peak cardiac power, and peak O_2 consumption were significantly different amongst patients at different stages of CKD ($p < 0.05$). In the cohort of 56 patients, the median total and free *p*-cresol glucuronide concentrations were 0.013 mg/dL and 0.011 mg/dL, respectively. Increased total concentration of *p*-cresol glucuronide was associated with reduced peak cardiac power (r [correlation coefficient]=-0.52, $p < 0.01$), peak cardiac output (r=-0.45, $p < 0.01$), peak mean arterial pressure (r=-0.30, $p < 0.05$), peak heart rate (r=-0.41, $p < 0.01$), aerobic exercise capacity (r=-0.43, $p < 0.01$), and arteriovenous O_2 difference (r=-0.26, $p < 0.05$). Likewise, elevated free concentration *p*-cresol glucuronide was associated with decreased peak cardiac power (r=-0.52, $p < 0.01$), peak cardiac output (r=-0.45, $p < 0.01$), peak mean arterial pressure (r=-0.29, $p < 0.05$), peak heart rate (r=-0.41, $p < 0.01$), and aerobic exercise capacity (r=-0.42, $p < 0.01$). Overall, based on correlational analyses in patients at various CKD stages, *p*-cresol glucuronide concentrations were linked to compromised cardiac

functions, suggesting important roles of *p*-cresol glucuronide in mediating cardiac-related toxicities.

Liabeuf et al. investigated the associations between *p*-cresol glucuronide concentrations and cardiovascular and/or overall mortalities (Liabeuf et al., 2013). The patient cohort included 139 Caucasians with CKD stages from 2-5. Most patients (n=94) were pre-dialysis, while n=45 CKD stage 5 patients were on dialysis. The average age was 67±12 years (mean±SD). Sex distribution in the study population was 60% male and 40% female. eGFR, one of the indicators of renal function, was 35±19 mL/min per 1.73 m^2. The total and free serum concentrations of *p*-cresol glucuronide were 0.29±0.54 mg/dL and 0.27±0.54 mg/dL, respectively. The patients were further divided into two subgroups based on free serum levels of *p*-cresol glucuronide: free *p*-cresol glucuronide concentration≤0.041 mg/dL (n=70) and free *p*-cresol glucuronide concentration > 0.041 mg/dL (n=69). Free *p*-cresol glucuronide concentration was significantly higher in patients at CKD stage 5 on dialysis compared to patients in earlier stages or without dialysis (p<0.0001). In addition, "free *p*-cresol glucuronide concentration > 0.041mg/dL" was significantly associated with cardiovascular (p=0.01) and overall (p=0.002) mortalities based on data collected in 38 deceased patients. Moreover, free *p*-cresol glucuronide concentrations were significant predictive markers of cardiovascular (p=0.003) and overall (p=0.004) mortalities.

Meert et al. evaluated *p*-cresol glucuronide concentrations in CKD patients on hemodialysis compared to healthy subjects (Meert et al., 2012). The serum samples were collected from 77 CKD patients on dialysis (50 males and 27 females) and 15 heathy volunteers (11 males and 4 females). The average age (±standard deviations) were 69±14 years and 26±4 years, respectively. The total serum concentration of *p*-cresol glucuronide in CKD patients was 7.3±6.5 mg/L, which was significantly higher than that in healthy subjects (0.35±0.03 mg/L).

Mutsaers et al. assessed the total plasma p-cresol glucuronide concentrations in chronic renal failure (n=79) and pre-dialysis end-stage renal disease (n=12) patients (Mutsaers et al., 2015). The mean age (mean±SD) were 59±14 years and 55±14 years, respectively. Sex distribution in the study population was 29% female in chronic renal failure patients and 22% female in pre-dialysis end-stage renal disease patients. The concentrations of urea and creatinine were 12±4 mmol/L and 171±58 μmol/L in chronic renal failure patients, respectively; and 21±7 mmol/L and 774±242 μmol/L in pre-dialysis end-stage renal disease patients, respectively. Four healthy subjects served as the control group. The total plasma concentrations of p-cresol glucuronide in healthy subjects, chronic renal failure patients, and pre-dialysis end-stage renal disease patients were 0.3 μM, 1 μM, and 30 μM, respectively. The total plasma concertation of p-cresol glucuronide was significantly increased in end-stage renal disease (ESRD) patients (30 μM) compared to healthy controls (0.3 μM, $p < 0.05$). The percentage of p-cresol glucuronide in pre-dialysis end-stage renal disease patients (i.e. 21%) was significantly increased compared to healthy subjects (i.e. 1.5%) and chronic renal failure patients (i.e. 1.3%, $p < 0.05$), indicating a shift toward p-cresol glucuronide (with corresponding decrease in p-cresol sulfate) formation as renal function becomes progressively worsened.

2.2. In vitro studies of p-cresol glucuronide associated toxicity

There were several *in vitro* studies demonstrating the toxicity of p-cresol glucuronide using various human cellular models (**Table 5**). The liver toxicity of p-cresol glucuronide was characterized in human primary hepatocytes and the kidney toxicity of p-cresol glucuronide was characterized in human embryonic kidney 293 cells or human conditionally immortalized renal proximal tubule epithelial cells.

Weigand et al. (Weigand et al., 2019) investigated the toxicity of p-cresol glucuronide using primary human hepatocytes, which were isolated from patients undergoing hepatectomy. Hepatocytes were treated with 500 µM p-cresol glucuronide for 96 hours at 37 °C, and the p-cresol glucuronide generated effects were compared to the solvent control. Cell viability was determined by the Hoechst 33342 marker; cellular ATP was represented by the bioluminescence signal; and membrane potential was characterized by the tetramethyl rhodamine methyl ester marker. p-Cresol glucuronide significantly decreased cell viability ($p<0.001$), cellular ATP ($p<0.05$), and membrane potential ($p<0.05$) by 40%, 50%, and 10%, respectively.

London et al. compared the toxicity of p-cresol glucuronide vs. its parent surrogate p-cresol in the human embryonic kidney 293 cell line (London et al., 2020). Cells were treated with 0-100 µM p-cresol or p-cresol glucuronide (in calcium and sodium salt forms) for 7 days at 37 °C. Cell viability was determined using crystal violet staining assay, and the absorbance of crystal violet colony formation was measured at 590 nm. At concentrations of 0-100 µM, both forms of p-cresol glucuronide exhibited similar suppression effects on the formation of crystal violet colony compared to p-cresol. The calcium form of p-cresol glucuronide at 100 µM decreased crystal violet colony formation to a similar extent as the same concentration of p-cresol (approximately 26%). On the other hand, the sodium form of p-cresol glucuronide reduced colony formation to a lesser extent compared to the calcium salt of p-cresol glucuronide or p-cresol.

Meert et al. assessed the toxicity of p-cresol glucuronide in human leucocytes isolated from blood samples of 8 healthy volunteers (Meert et al., 2012). Leucocytes were stimulated with N-formyl-methionine-leucine-phenylalanine (0.83 µM), *E. coli* (1.66×10^8 cells/mL), and phorbol-12-myristate-13-acetate (1.35 µM). Both unstimulated (i.e. the baseline) and stimulated leucocytes were further classified as monocytes, granulocytes, and lymphocytes by flow cytometry. Human

whole blood was incubated with saline control solutions, 48 mg/L *p*-cresol glucuronide alone, or combinations of 48 mg/L *p*-cresol glucuronide and 108 mg/L *p*-cresol sulfate (deemed physiological concentrations) for 10 minutes at 37 °C. Oxidative burst activities were measured by percentages of rhodamine-positive cells (after fMLP stimulation) and mean fluorescence intensity per cell (after *E. coli* and PMA stimulation). *p*-Cresol glucuronide alone had no effects on oxidative burst activity in all baseline or stimulated leucocytes; however, the combination of *p*-cresol glucuronide and *p*-cresol sulfate increased oxidative burst activities in all treatment conditions compared to the control (p<0.05 or 0.01), except for E. *coli*-stimulated lymphocytes.

Mutsaers et al. determined the effects of *p*-cresol glucuronide on mitochondrial succinate dehydrogenase activities in human conditionally immortalized renal proximal tubule epithelial cells (Mutsaers et al., 2013). Cells were treated with medium control, 2 mM of *p*-cresol, and *p*-cresol glucuronide for 48 hours at 37 °C. The activities of mitochondrial succinate dehydrogenase were determined using the 3-(4,5-dimethylthiazol-2-yl)-2,5-diphenyltetrazolium bromide (MTT) assay. The absorbance of purple formazan salt formation was measured at 570 nm. Overall, mitochondrial succinate dehydrogenase activities were significantly reduced by 2 mM *p*-cresol (28%, p<0.05) and 2 mM *p*-cresol glucuronide (14%, p<0.05), compared to the medium control.

Mutsaers et al. also investigated the toxic effects of *p*-cresol glucuronide in human conditionally immortalized renal proximal tubule epithelial cells (Mutsaers et al., 2015). Cells were treated with 0-2 mM *p*-cresol glucuronide or control solution for 48 hours at 37 °C. Epithelial-to-mesenchymal transition was characterized by vimentin (a mesenchymal marker), E-cadherin (an epithelial marker), and Snail (transcription factor) using quantitative polymerase chain reactions. Cell injury was characterized by tubular damage markers such as kidney injury molecule-1 and vanin-1. Overall, exposure of *p*-cresol glucuronide (at 2 mM) significantly

increased vimentin expression (p<0.05) while decreasing mRNA expression of Snail and kidney injury molecule-1 (p<0.05), suggesting the induction of epithelial-to-mesenchymal transition indicative of overall toxic effects on these cells.

Overall, the toxicities of *p*-cresol glucuronide have been demonstrated in various *in vitro* or clinical investigations. However, these *ex vivo* or *in vitro* studies have used super-physiological concentrations of exogenously-administered *p*-cresol glucuronide (**Tables 4&5**), while the clinical data were mostly based on correlational analyses (i.e. could not establish cause-effect relationships). Therefore, despite convincing evidence supporting the toxicology of *p*-cresol glucuronide in various models, there data did not provide definitive evidence suggesting direct *p*-cresol glucuronide-associated organ toxicities. *Therefore, we aimed to focus on the toxicity of p-cresol glucuronide, using mechanistic approaches, in my thesis.*

Table 4. *In vivo* studies of *p*-cresol glucuronide toxicity

Study population	Study design	*p*-Cresol glucuronide concentration	Outcome(s)	Reference
Population: CKD patients at stages 1–5 before dialysis Sample size: 203 Age (median [range]): 60 [47-72] years Gender: 120 males and 83 females Albumin (median [range]): 4.51 [4.20-4.68] g/dL Creatinine (median	Prospective, correlational analysis Control group: 8 healthy subjects	Total serum concentration (median [range]): 0.22 [0.08–0.60] µM Free serum (median [range]): 0.13 [0.05–0.50] µM	↑eGFR, ↑ratios of *p*-cresol sulfate/*p*-cresol glucuronide (total serum: rho=0.23, p=0.001; free serum: rho=0.20, p=0.005; 24-hour urinary excretion: rho=0.32, p<0.001). ↓serum ratio of *p*-cresol sulfate/*p*-cresol glucuronide, ↑cardiovascular disease (hazard ratio per SD higher 0.55, p<0.001). ↓serum ratio of *p*-cresol sulfate/*p*-cresol glucuronide, ↑mortality (hazard ratio 0.65, p<0.01).	(Poesen et al., 2016)

[range]): 1.81 [1.29-2.50] mg/dL eGFR (median [range]): 34 [23-56] mL/min per 1.73 m^2 Creatinine clearance (median [range]): 40 [27-61] mL/min 24-h proteinuria (median [range]): 0.31 [0.11-1.13] g				
Population: CKD patients at stages 2–5 before dialysis, asymptomatic, lack of diagnosis of	Cross-sectional, correlational analysis	Total serum concentration (median [25th-75th percent]): 0.013 (0.004-0.035) mg/dL	Free serum concentrations of *p*-cresol glucuronide in CKD-stage 5 patients were significantly higher than other stages. ↑**total** *p*-cresol glucuronide, ↓peak cardiac power (r	(Chinnappa et al., 2018)

cardiac disease or diabetes Sample size: 56 Age (mean±SD): 46.8±12.5 years Gender: 56 males eGFR (mean±SD): 38.5±24.1 mL /min per 1.73 m^2		Free serum concentration (median [25th-75th percent]): 0.011 (0.002-0.029) mg/dL	[correlation coefficient]=-0.52, p<0.01); ↓peak cardiac output (r=-0.45, p<0.01); ↓peak mean arterial pressure (r=-0.30, p<0.05); ↓peak heart rate (r=-0.41, p<0.01); ↓aerobic exercise capacity (r=-0.43, p<0.01); ↓peak arteriovenous O$_2$ difference (r=-0.26, p<0.05). ↑**free** *p*-cresol glucuronide, ↓peak cardiac power (r=-0.52, p<0.01); ↓peak cardiac output (r=-0.45, p<0.01); ↓peak mean arterial pressure (r=-0.29, p<0.05); ↓peak heart rate (r=-0.41, p<0.01); ↓aerobic exercise capacity (r=-0.42, p<0.01).	
Population: CKD patients at stages 2-5 (most patients were before dialysis, 45 patients in stage 5 were on dialysis); Caucasian	Prospective correlation analysis	Total serum concentration (mean±SD): 0.29±0.54 mg/dL Free serum concentration (mean±SD): 0.27±0.54 mg/dL	Free *p*-cresol glucuronide concentration was significantly higher in CKD patients at stage 5 on dialysis compared to patients at earlier stages or without dialysis (p<0.0001). ↑free *p*-cresol glucuronide, ↓eGFR in CKD patients at stages 2-5 before dialysis (r^2=0.34, p<0.0001).	(Liabeuf et al., 2013)

Sample size: 139 Age (mean±SD): 67±12 years Gender: 84 males, 55 females eGFR (mean±SD): 35±19 mL /min per 1.73 m^2 (calculated only in patients before dialysis)			Free *p*-cresol glucuronide>0.041mg/dL was significantly associated with cardiovascular (p=0.01) and overall (p=0.002) mortalities. Free *p*-cresol glucuronide concentrations were significant predictive markers of cardiovascular (p=0.003) and overall (p=0.004) mortalities.	
Population: CKD patients on dialysis Sample size: 77 Age (mean or median [not	Correlation analysis Control group: 15 healthy subjects	Total serum concentration (mean±SD, [range]): 7.3±6.5 mg/L, [0.4-24.0 mg/L]	Total serum concentrations of *p*-cresol glucuronide in CKD patients on dialysis were ~20 fold higher than that in healthy subjects (0.35±0.03 mg/L).	(Meert et al., 2012)

specified]±SD): 69±14 years Gender: 50 males and 27 females		Free serum concentration (mean±SD, [range]): 6.7±5.9 mg/L, [0.4-22.4 mg/L]		
Patient: patients with chronic renal failure and pre-dialysis end-stage renal disease Sample size: 79 for chronic renal failure patients and 12 pre-hemodialysis end-stage renal disease patients Age (mean±SD): 59±14 years	Correlation analysis Control group: 4 healthy subjects	Total plasma concentration in chronic renal failure patients (mean): 1 μM Total plasma concentration in pre-dialysis end-stage renal disease patients (mean): 30 μM	Total plasma concentrations of p-cresol glucuronide in pre-dialysis end-stage renal disease patients (i.e. 30 μM) was significantly increased compared to healthy subjects (i.e. 0.3 μM) ($p<0.05$). The percentage of p-cresol glucuronide in pre-dialysis end-stage renal disease patients (i.e. 21%) was significantly increased compared to healthy subjects (i.e. 1.5%) and chronic renal failure patients (i.e. 1.3%) ($p<0.05$), indicating a shift from p-cresol sulfonation to glucuronidation.	(Mutsaers et al., 2015)

in chronic renal failure patients; 55±15 years in pre-dialysis end-stage renal disease patients Gender: 56 males，23 females (chronic renal failure patients); 9 males, 3 females (pre-dialysis end-stage renal disease patients) eGFR (mean±SD): 37±14 mL /min per 1.73 m^2 in chronic renal failure patients (data				

are not available in pre-dialysis end-stage renal disease patients)				

Abbreviation(s): *CKD*, chronic kidney disease; *eGFR*, estimated glomerular filtration rate; *PTH*, parathyroid hormone; *SD*, standard deviation

Table 5. *In vitro* studies of *p*-cresol glucuronide toxicity

Model	Experimental design	Outcome	Reference
Primary human hepatocytes isolated from patients undergoing hepatectomy	Control and experimental groups: • solvent control • *p*-cresol glucuronide (500 µM) The control and experimental groups were incubated with hepatocytes for 96 hours at 37 °C Assessment maker(s): cell viability was determined by Hoechst 33342; cellular ATP was determined by the bioluminescence signal; membrane potential was determined by tetramethylrhodamine methyl ester	*p*-cresol glucuronide significantly decreased cell viability ($p<0.001$), cellular ATP ($p<0.05$) and membrane potential ($p<0.05$) by approximately 40%, 50%, and 10%, respectively.	(Weigand et al., 2019)
Human embryonic kidney 293 cell	Control and experimental groups: • medium control • *p*-cresol (0-100 µM)	*p*-Cresol glucuronide exhibited similar trend on the formation of crystal violet colony as *p*-cresol.	(London et al., 2020)

	• the sodium form of *p*-cresol glucuronide (0-100 µM) • the calcium form of *p*-cresol glucuronide (0-100 µM) The control and experimental groups were incubated with cells for 7 days at 37 °C. Assessment maker(s): cell viability was determined by a crystal violet cell viability assay. The absorbance of crystal violet colony formation was measured at 595 nm.	The calcium form of *p*-cresol glucuronide (100 µM) decreased the crystal violet colony formation to a similar extent as *p*-cresol (at the same concentration, approximately 26%).	
Human leucocytes isolated from blood samples from 8 healthy volunteers Human leucocytes were stimulated with fMLP (0.83 µM), *E. coli* (1.66×10^8 cells/mL), and PMA (1.35 µM).	Control and experimental groups: • saline control solutions • *p*-cresol glucuronide alone (48 mg/L) • combination of *p*-cresol glucuronide and	*p*-Cresol glucuronide alone had no effects on oxidative burst activities in all baseline or stimulated leucocytes. Combinations of *p*-cresol glucuronide and sulfate increased oxidative burst activities in all cell types	(Meert et al., 2012)

Both unstimulated (i.e. the baseline) and stimulated leucocytes were further classified to monocytes, granulocytes, and lymphocytes.	*p*-cresol sulfate (see text for concentrations) The control and experimental treatment groups were incubated with whole blood for 10 minutes at 37 °C. Assessment maker(s): oxidative burst activity as measured by percentage of rhodamine-positive cells (after fMLP stimulation) and mean fluorescence intensity per cell (after *E. coli* and PMA stimulation).	except for *E. coli*-stimulated lymphocytes, compared to the control ($p<0.05$ or <0.01); combinations of both *p*-cresol sulfate and *p*-cresol glucuronide also increased the activities in all baseline leucocytes ($p<0.01$) and fMLP-stimulated granulocytes ($p<0.01$), compared to *p*-cresol sulfate alone.	
Human conditionally immortalized renal proximal tubule epithelial cell	Control and experimental groups: • medium control • *p*-cresol (2 mM) • *p*-cresol glucuronide (2 mM) Cell were incubated with control and experimental groups for 48 hours at 37 °C.	Mitochondrial succinate dehydrogenase activities were significantly reduced by *p*-cresol (28%, $p<0.05$) and *p*-cresol glucuronide (14%, $p<0.05$) vs. medium control.	(Mutsaers et al., 2013)

	Assessment maker(s): Mitochondrial succinate dehydrogenase activity was determined by 3-[4,5-dimethylthiazol-2-yl]-2,5-diphenyl tetrazolium bromide (MTT) assay. The absorbance of purple formazan salt formation was measured at 570 nm.		
Human conditionally immortalized renal proximal tubule epithelial cell	Control and experimental groups: • salt control solution • *p*-cresol glucuronide (0-2 mM) Cell were incubated with control and experimental groups for 48 hours at 37 °C. Assessment maker(s): EMT induction was determined by mesenchymal marker vimentin, epithelial marker E-cadherin, and	Exposure of *p*-cresol glucuronide (2 mM) significantly increased vimentin expression ($p<0.05$) and decreased mRNA expression of snail and kidney injury molecule-1 ($p<0.05$).	(Mutsaers et al., 2015)

	transcription factor snail; cell injury was indicated by tubular damage markers kidney injury molecule-1 and vanin-1.		

Abbreviation(s): *BCRP*, breast cancer resistance protein; *E. coli*, *Escherichia coli*; *E1S*, estrone-sulfate; *EMT*, epithelial-to-mesenchymal transition; *eYFP*, enhanced yellow fluorescent protein; *fMLP*, N-formyl-methionine-leucine-phenylalanine; *MRP4*, multidrug resistance protein 4; *MTT*, 3-(4,5-dimethylthiazol-2-yl)-2,5-diphenyltetrazolium bromide; *MTX*, methotrexate; *pCG*, *p*-cresol glucuronide; *pCS*, *p*-cresol sulfate; *PMA*, phorbol-12-myristate-13-acetate; *qPCR*, quantitative polymerase chain reaction; *TCA*, taurocholic acid.

Table 6. The stages of chronic kidney disease (Levey et al., 2005)

Stage	eGFR, mL/min per 1.73 m^2
1	≥90
2	60-89
3	30-59
4	15-29
5	<15 (or dialysis)

3. Experimental model

The HepaRG cell line was utilized as the main tool in our experiments (please see more experimental details in **Chapter II**). Originally, HepaRG cells were derived from a female patient who was diagnosed with hepatocarcinoma and hepatitis C virus infection (Gripon et al., 2002). The cells were initially isolated from the patient's liver tumor and differentiated using dimethyl sulfoxide (DMSO) (Gripon et al., 2002). Subsequently, the cells were selected based on "induction of cell differentiation" and "partial purification of the differentiated cells" procedures (Gripon et al., 2002). In general, HepaRG cells exhibit four important features making them a suitable experimental model: i) fully developed human hepatocyte functions (e.g. metabolism enzymes, transporter activities, and cellular regulation pathways), ii) the presence of bile canaliculi structures, iii) characteristics of "immortalized" stem cells, and iv) abilities to differentiate into functional liver cells (Biopredic International, 2016). Microscopic representations of undifferentiated and differentiated HepaRG cells are illustrated in Figure 2 (images taken in our laboratory).

Figure 2A)
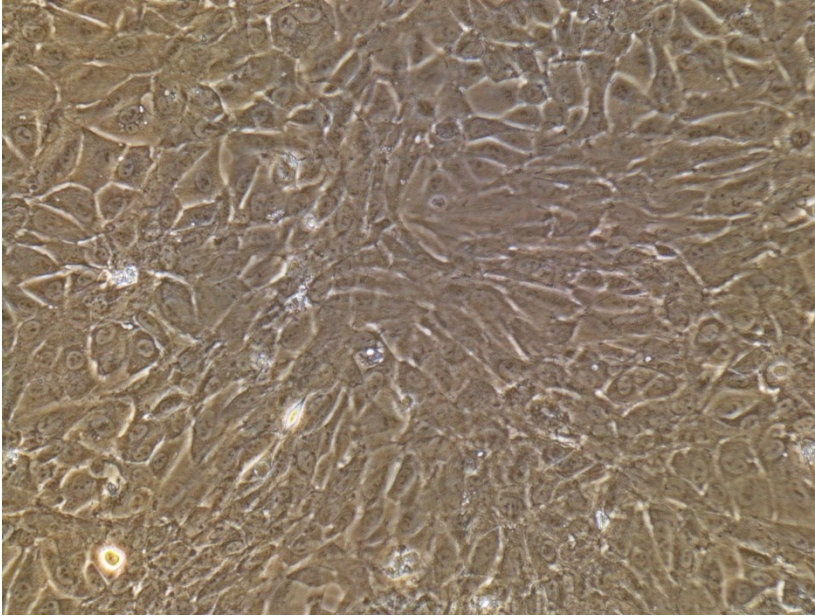
Figure 2B)
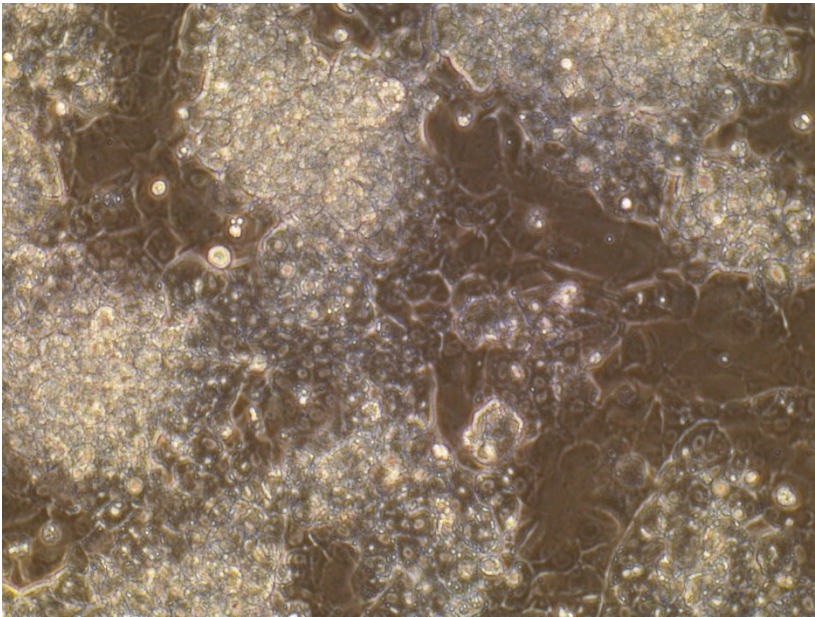
Figure 2. Sample images were taken from our laboratory representing A) undifferentiated HepaRG cells at passage 17 and B) differentiated HepaRG cells at passage 18 (both under 20X microscope). Taken on March 6, 2020.

Compared to primary human hepatocytes, similar expressions of Phase I, II, and III enzymes in HepaRG cells make this cell line an ideal tool for metabolism-mediated xenobiotic toxicity studies (Gripon et al., 2002,Ashraf et al., 2019,Guillouzo et al., 2007). The gene expression profiles in differentiated HepaRG cells are generally comparable with primary human hepatocytes with respect to Phase I (e.g. alcohol dehydrogenases [ADH]1A, ADH1B, ADH1C, ADH4]; aldehyde dehydrogenases [ALDH]1L1, ALDH1L2, ALDH9A1; and cytochrome P450 [CYP]1A2, CYP2B6, CYP2C9, CYP3A4, CYP3A5, CYP2A6, CYP2C19, CYP3A7, CYP2D6, CYP2C8, CYP2E1) and Phase II (e.g. uridine 5'-diphospho-glucuronosyltransferase [UGT]1A1, UGT1A6, UGT2A3, UGT2B4, UGT2B15, UGT2B17, UGT2B28, UGT3A1, UGT8; sulfotransferase [SULT]1A1, SULT1A2, SULT1C2, SULT1C4, SULT1B1, SULT1E1, SULT2A1; N-acetyltransferases [NAT]1, NAT2; and glutathione S-transferases [GST]A1, GSTA3, GSTK1) metabolism enzymes. Likewise, comparable mRNA expressions are evident in HepaRG cells compared to human hepatocytes in regards to various uptake and efflux transporters (e.g. ATP-binding cassette family [ABC]B1, ABCB4, ABCC10; and solute carrier organic anion transporter family [SLCO]2B1) (Hart et al., 2010). In addition, the mRNA expressions of proteins maintaining normal hepatocyte functions including aldolase B, haptoglobin, and albumin in undifferentiated HepaRG cells were also similar to human primary hepatocyte (Guillouzo et al., 2007). However, in the differentiated HepaRG cells, the expressions of haptoglobin and albumin were relatively higher than that in human primary hepatocyte (Guillouzo et al., 2007).

There are already several examples in the literature utilizing HepaRG cells in the study of metabolism-mediated toxicities. For instance, Yokoyama et al. assessed the enzyme activities of CYP1A2, CYP2B6, CYP2C9, CYP2C19, CYP2D6, CYP3A4, SULTs, and UGTs in HepaRG cells, compared to HepG2 and human hepatocytes. They found the enzyme activities in HepaRG

cells were comparable to human hepatocytes, and much higher than HepG2 cells (Yokoyama et al., 2018). Furthermore, Yokoyama et al. also compared the toxic effects of acetaminophen in HepaRG cells and human hepatocytes (Yokoyama et al., 2018). Acetaminophen is known to be metabolized by CYP2E1, CYP3A4 and CYP1A2 in the formation of the toxic product N-acetyl-p-benzoquinone imine (Ashraf et al., 2019). Based on Yokoyama et al., the IC_{50} and cytotoxicity of acetaminophen in HepaRG cells were similar to primary human hepatocytes (Yokoyama et al., 2018). In addition, Guillouzo et al. determined the toxicities of aflatoxin B_1 (which is known to exert its hepatotoxicity by generating the 8,9-epoxide metabolite mediated by CYP1A2 and CYP3A4) in HepaRG cells and primary human hepatocytes using the MTT assay. It was also demonstrated that the IC_{50} values identified in both systems were comparable, indicating that the HepaRG is a suitable model for investigating metabolism-mediated toxicity (Guillouzo et al., 2007). Overall, these examples demonstrated the suitability of the HepaRG cell line for investigating CYP-mediated livery injury. *However, the suitability of HepaRG cells for phase II-metabolism mediated toxicities still remain to be established. The latter will be further investigated as part of my thesis.*

In general, there are several advantages for using the HepaRG cell line as the experimental model. i) Fully differentiated HepaRG cells contain both hepatocyte-like and biliary canalicular-like cell types with similar morphology as human hepatocytes (Figure 2) (Gripon et al., 2002). ii) The expression levels of major metabolism enzymes and transporters are generally comparable between HepaRG cells and primary human hepatocytes (e.g. our data presented in Chapter II further confirm the enzyme activities of select phase II UGT and SULT enzymes) (Gripon et al., 2002,Ashraf et al., 2019,Guillouzo et al., 2007). iii) The costs for obtaining and maintaining HepaRG cells are more affordable compared to primary human hepatocytes. iv) HepaRG cells can

be cultured for an extended duration after differentiation (Gripon et al., 2002). However, the model does have some limitations. For example, the HepaRG cell line is derived from a single female with hepatocarcinoma and infection of hepatitis C virus; therefore, it may exhibit physiological changes associated with these conditions and does not allow us to characterize inter-individual variability. Overall, the beneficial characteristics make HepaRG cell line a suitable model for the current study.

4. Rationale and hypothesis

Hypothesis: the overall aim of my thesis was to characterize the toxicities of *p*-cresol and determine the role of *p*-cresol glucuronide in mediating the toxicity of *p*-cresol in a human hepatic model. I hypothesized that *p*-cresol is relatively more toxic than the other protein-bound uremic toxins [therefore warranting a focused investigation of this protein-bound uremic toxin], and that the glucuronidation of *p*-cresol or the glucuronide end product can lead to toxicities in the human liver.

Rationale: *p*-cresol is a protein-bound uremic toxin mainly produced by bacteria in the large intestines from amino acids such as tyrosine and phenylalanine (Prokopienko, Alexander J. and Nolin, 2018). *p*-Cresol undergoes hepatic metabolism (Gryp et al., 2017) through three main pathways: phase I CYP450, phase II sulphation (in the formation of *p*-cresol sulfate), and phase II glucuronidation (in the formation of *p*-cresol glucuronide) (Prokopienko, Alexander J. and Nolin, 2018). The highest total concentrations of *p*-cresol, *p*-cresol sulfate, and *p*-cresol glucuronide in human plasma/serum under uremic conditions are 596 µM, 1664 µM, and 85 µM, respectively (Meert et al., 2012,Cuoghi et al., 2012), which suggest that similar concentrations can be attained in the liver, the primary sources of these species in the plasma. *p*-Cresol has been associated with hepatotoxicity as evident by data in rat liver models (Thompson et al., 1994,Thompson et al., 1996,Kitagawa, 2001) and mouse hepatocytes (Abreo et al., 1997). *However, the data on the hepatotoxicity potential of p-cresol in human models are limited.* In addition, *p*-cresol glucuronide has been associated with toxicity in various liver, kidney, and cardiac models based on published i*n vivo* and *in vitro* studies (Poesen et al., 2016,Chinnappa et al., 2018,Liabeuf et al., 2013,Mutsaers et al., 2015,Meert et al., 2012,Weigand et al., 2019,London et al., 2020,Mutsaers et al., 2013), although at physiologically unobtainable conditions. On the other hand, data are also available

suggesting *p*-cresol glucuronide was relatively less toxic compared to *p*-cresol in *in vitro* kidney models (London et al., 2020,Mutsaers et al., 2013). Moreover, to my knowledge, no data are yet available on the role of *in situ (i.e. physiologically relevant)* generated *p*-cresol glucuronide in mediating the organ injury. As well, there is very little data comparing the relative toxic effects of *p*-cresol to *p*-cresol sulfate, *p*-cresol glucuronide, or other common uremic toxins in a human liver model.

5. Objectives

To test the overall hypothesis, there are four independent objectives:

1. To characterize the concentration- and temporal- effects of *p*-cresol on markers of oxidative stress (2', 7' –dichlorofluorescein, DCF formation), total cellular glutathione (GSH) depletion, and lactate dehydrogenase (LDH) release in HepaRG cells.

2. To compare the effects of *p*-cresol and other protein bound uremic toxins on toxicity markers in HepaRG cells.

3. To determine the metabolic activities of HepaRG cells in the production of major *p*-cresol conjugated metabolites (i.e. *p*-cresol sulfate and *p*-cresol glucuronide).

4. To characterize the effects of exogenously-administered and *in-situ* generated *p*-cresol metabolites (i.e. *p*-cresol glucuronide) in the manifestation of toxicities in HepaRG cells.

Chapter II : Experimental Data

1. Introduction

p-Cresol, a part of the protein-bound uremic toxin milieu, is derived from colonic amino acids tyrosine and phenylalanine (Vanholder et al., 1999). The toxicological effects of *p*-cresol have primarily been attributed to its metabolism end products (Vanholder et al., 2018), which are considered relatively important toxic species amongst a large variety of uremic toxins known to date (Vanholder et al., 2018,Glorieux et al., 2021). *p*-Cresol is extensively conjugated in enterocytes and hepatocytes in the formation *p*-cresol sulfate and *p*-cresol glucuronide (Gryp et al., 2017,Vanholder et al., 1999). Under typical uremic conditions, sulfonation is the predominant pathway as evident by the relatively higher plasma total concentrations of *p*-cresol sulfate in various clinical reports (Poesen et al., 2016,Liabeuf et al., 2013,Mutsaers et al., 2015,Itoh et al., 2012,Chinnappa et al., 2018,Meert et al., 2012). However, due to differences in protein binding, the biologically active unbound concentrations of *p*-cresol glucuronide and *p*-cresol sulfate are comparable (Itoh et al., 2012,Liabeuf et al., 2013,Mutsaers et al., 2015,Chinnappa et al., 2018), with some studies suggesting higher plasma concentrations of the free glucuronide (e.g. (Meert et al., 2012)). Furthermore, a shift to the production of *p*-cresol glucuronide from *p*-cresol sulfate has been observed in patients with advanced kidney disease (Poesen et al., 2016,Mutsaers et al., 2015), indicating glucuronidation might be an important pathway for *p*-cresol metabolism at *higher p*-cresol concentrations where the toxicity is more likely manifested.

p-Cresol glucuronide has been implicated in cardiovascular toxicity and overall mortality in human models. Liabeuf et al (Liabeuf et al., 2013) was the first to establish an association between serum *p*-cresol glucuronide concentrations and total or cardiac-related mortality, highlighting similar predictive powers of the glucuronide compared to the sulfate metabolite.

Consistent observations were also reported by Glorieux et al (Glorieux et al., 2021) in chronic kidney disease patients not yet on hemodialysis, where both plasma concentrations of total and unbound *p*-cresol glucuronide were correlated with total mortality. In patients with advanced chronic kidney disease, the plasma ratio of *p*-cresol glucuronide to *p*-cresol sulfate is progressively increased (Poesen et al., 2016,Mutsaers et al., 2015), and this apparent shift in metabolic profile from sulfonation to glucuronidation has also been associated with cardiac disease and mortality (Poesen et al., 2016). A role of *p*-cresol glucuronide in early stages of cardiac disease progression has also been suggested in chronic kidney disease patients without full-blown cardiac dysfunction, where both free and total serum *p*-cresol glucuronide concentrations have been associated with decreased peak cardiac power, peak cardiac output, mean arterial pressure, peak heart rate, and aerobic exercise capacity (Chinnappa et al., 2018). Furthermore, experimental data supported the nephrotoxic effects of the glucuronide metabolite. Exogenously administered *p*-cresol glucuronide (2 mM) generated mitochondrial toxicity (Mutsaers et al., 2013) and altered gene expressions associated with epithelial-to-mesenchymal transition (Mutsaers et al., 2015) in conditionally immortalized human renal proximal tubule epithelial cells. In human embryonic kidney 293 cells, exposure of 100 µM of *p*-cresol glucuronide for seven days also resulted in modest reductions in cell viability (London et al., 2020). In addition, toxicity data of *p*-cresol glucuronide are also available in other human tissues. In an *ex-vivo* model, leukocytes isolated from the whole blood of healthy subjects exposed to 48 mg/L of *p*-cresol glucuronide for 10 minutes further enhanced the oxidative burst activities associated with *p*-cresol sulfate (Meert et al., 2012). In primary cultures of human hepatocytes, the viability, cellular ATP concentration, and mitochondrial membrane potential were significantly reduced in cells exposed to 0.5 mM of *p*-cresol glucuronide for 96 hours (Weigand et al., 2019).

While these data collectively suggested the potential toxicity profiles of *p*-cresol glucuronide, the clinical studies were primarily correlational in nature, and most *in vitro*/*ex-vivo* experimental models have utilized exogenously administered *p*-cresol glucuronide at relatively high concentrations. Very few studies have also provided direct comparisons on the toxic effects of *p*-cresol (i.e. pre-cursor) to its metabolites, where the limited available data appeared to suggest that *p*-cresol was equally, if not more toxic, than its glucuronide (Mutsaers et al., 2013,London et al., 2020). Furthermore, despite evidence supporting the toxicity of *p*-cresol glucuronide and *p*-cresol sulfate, very little human data are available in the key organ (i.e. liver) responsible for the generation of these metabolites. Although *p*-cresol induced liver injury has already been documented in several pre-clinical animal studies (Kitagawa, 2001,Abreo et al., 1997,Thompson et al., 1994,Thompson et al., 1996), the relative toxic effects of *p*-cresol (which is more abundant than its conjugated metabolites in the human liver (Ikematsu et al., 2019)) and the role of *in situ*-generated metabolites in the manifestation of toxicity in a human experimental hepatic model have not yet been systematically characterized.

To further elucidate the toxicological importance of *p*-cresol in a liver model and determine whether the glucuronidation of *p*-cresol constituted a *toxification* or a *detoxification* pathway, our objectives were to i) systematically characterize the effects of *p*-cresol in comparison to other protein-bound uremic toxins and its metabolites on markers of oxidative stress (2'-7'-dichlorofluorescein, DCF, formation), total cellular glutathione (GSH) concentration, and cellular necrosis (lactate dehydrogenase, LDH, release), which are toxicity endpoints known to be associated with *p*-cresol or its metabolites in various other liver experimental models (e.g. (Thompson et al., 1994,Thompson et al., 1996,Weigand et al., 2019,Yan et al., 2005); ii) determine the metabolic profiles of *p*-cresol in the generation of its conjugated metabolites; and iii)

characterize the role of *in situ*-generated *p*-cresol glucuronide in the manifestation of toxicities. We utilized a human primary hepatoma liver cell line (i.e. HepaRG) which is metabolically competent (i.e. allowing the *in situ* generation and the mechanistic modulation of *p*-cresol metabolites) and known to be suitable for toxicity studies (Ashraf et al., 2019,Gripon et al., 2002,Guillouzo et al., 2007).

2. Materials and methods

2.1. Chemicals and reagents

Ammonium acetate (catalogue# 1220-1-70) was obtained from Caledon Laboratories Ltd (Ontario, Canada) and further passed through Millipore™ Millex™ 0.45 µM filters from Fisher Scientific (Ontario, Canada) before being added to mobile phases. Glutathione assay kit (catalogue# 703002) was purchased from Cayman chemicals (Michigan, USA). Amentoflavone (catalogue# 40584), 3-carboxy-4-methyl-5-propyl-2-furanpropionic acid (CMPF, catalogue# 90833), 2', 7'-dichlorofluorescin diacetate (DCFDA, catalogue# D6883), diclofenac (catalogue# D6899), 2,6-dimethylphenol (DMP, catalogue# D174904), formic acid (catalogue# F0507), hydrocortisone 21-hemisuccinate sodium salt (catalogue# H2270), hippuric acid (catalogue# 112003), indole-3-acetic acid (catalogue# I2886), indoxyl sulfate potassium salt (catalogue# I3875), kynurenic acid (catalogue# K3375), lactate dehydrogenase cytotoxicity detection kit (catalogue# 4744926001), L-borneol (catalogue# 15598), meta-phosphoric acid (catalogue# 239275), methanol (catalogue# 34860), tert-butyl hydroperoxide (t-BOOH, catalogue# 416665), triethanolamine (catalogue# T58300), Triton X-100 (catalogue# T8787), *p*-cresol (catalogue# C85751), penicillin-streptomycin (catalogue# P0781), and water (catalogue# 270733) were purchased from Sigma-Aldrich (Ontario, Canada). *p*-Cresol glucuronide (catalogue# C782005), *p*-

cresol glucuronide-d$_7$ (catalogue# C782007), *p*-cresol sulfate potassium salt (catalogue# T536805), and *p*-cresol sulfate potassium salt-d$_7$ (catalogue# T536802) were purchased from Toronto Research Chemicals (Ontario, Canada). Dimethyl sulfoxide (DMSO, catalogue# D2650), Dulbecco's phosphate-buffered saline (D-PBS, catalogue# 14190-144), fetal bovine serum (FBS, catalogue# 12483-020), human recombinant insulin (catalogue# 12585-014), L-glutamine (GlutaMax, catalogue# 35050-061), trypsin (0.05%)/ethylenediaminetetraacetic acid (EDTA, catalogue# 25300-062), and Williams' E medium (catalogue# 12551-032) were purchased from Thermo Fisher Scientific (Ontario, Canada). Sodium EDTA (catalogue# CH110) was purchased from Truin Science (Alberta, Canada).

2.2. HepaRG cell maintenance and differentiation

HepaRG is a hepatic tumor cell line that was established from a female subject infected with hepatitis C virus (Gripon et al., 2002). The HepaRG cell line exhibits comparable metabolic activities to primary human hepatocytes, making it a suitable tool for metabolism and xenobiotic toxicity studies (Gripon et al., 2002,Ashraf et al., 2019,Guillouzo et al., 2007). HepaRG cells were obtained from Biopredic International (Rennes, France) via a material transfer agreement with Inserm Transfert (Paris, France). Cells were maintained and differentiated according to Biopredic International's and Gripon et al.'s protocols (Gripon et al., 2002,Rong and Kiang, 2019,Biopredic International, 2016). William's E medium was supplemented with 10% FBS, 100 units/mL penicillin, 100 µg/mL streptomycin, 5 µg/mL insulin, 5×10^{-5} M hydrocortisone hemisuccinate, and 1% glutamine to obtain the *growth medium*. HepaRG cells were cultured at a density of 0.5×10^6 cells per 25 cm^2 flasks (Corning, New York, USA) with the growth medium refreshed every 72 hours. Cells were passaged every 2 weeks until being subjected to differentiation using the

differentiation medium (i.e. growth medium with 2% DMSO, v/v). After plating onto 24-well culture plates (BioLite, Thermo Fisher Scientific, Ontario, Canada) using a density of 0.4×10^6 cells/well in 500 μL of differentiation medium, cells were further acclimatized for 12 days before treatment. For all of these procedures, cells were maintained in a 37°C incubator with 5% CO_2 (Steri-Cycle CO_2 incubator, Thermo Fisher Scientific, Ontario, Canada).

2.3. HepaRG cell treatment

All experiments were conducted in differentiated HepaRG cells at passage #18 for consistency. All chemicals described below were soluble in the differentiation medium. Initial control experiments exposed HepaRG cells to a known hepatotoxicant in various liver cellular models, t-BOOH (specific conditions presented below) (e.g. (Liang et al., 2018,Kiang et al., 2010,Kiang et al., 2011)), to verify the responsiveness of the HepaRG model. To characterize the cellular responses to *p*-cresol, concentration- and time-dependent effects were initially characterized. The stock solution of *p*-cresol (100 mM) was freshly prepared before each treatment and further diluted to treatment concentrations in the differentiation medium. For concentration-response experiments, cells were treated with 0 to 2 mM of *p*-cresol for 24 hours. For time-course experiments, cells were treated with 0.75 mM or 1 mM of *p*-cresol for 0 to 24 hours (concentrations selected based on linearity in concentration-response data). As *p*-cresol has not been comparatively investigated against other uremic toxins in a hepatic model, an initial experiment determined the toxic effects of *p*-cresol in relation to other protein-bound uremic solutes deemed toxicologically relevant (Prokopienko, Alexander J. and Nolin, 2018,Vanholder et al., 2018) (chemical structures shown in Figure 3) to assess the suitability of a focused investigation on *p*-cresol alone. Cells were treated with the differentiation medium (i.e. the vehicle control), 1 mM each of *p*-cresol, 3-

carboxy-4-methyl-5-propyl-2-furanpropanoic acid, indole-3-acetic acid, indoxyl sulfate, kynurenic acid, or hippuric acid for 24 hours. The effects of these treatments on markers of cellular toxicity (i.e. DCF, GSH, and LDH assays) and *p*-cresol metabolite formations were determined (please see individual toxicity markers and metabolite characterizations below).

To determine the relative effects of exogenously administered *p*-cresol metabolites (Figure 3), cells were exposed to equal-molar concentrations (i.e. 1 mM) of *p*-cresol, *p*-cresol sulfate, and *p*-cresol glucuronide for 24 hours prior to toxicity and metabolite assay characterizations. To determine the effects of *in situ*-generated *p*-cresol glucuronide in the manifestation of cellular toxicity, chemical inhibitors were utilized to selectively attenuate its formation in HepaRG cells. Control experiments were conducted to optimize the specificity (toward *p*-cresol glucuronide formation), potency, and toxicity of several chemical inhibitors: HepaRG cells were pre-treated with blank cell differentiation medium (i.e. the vehicle control), or several concentrations of L-borneol, amentoflavone, or diclofenac for 30 minutes; then each inhibitor was co-treated with blank cell differentiation medium or 0.75 mM of *p*-cresol for 24 hours. These chemical inhibitors were selected based on known depletion effects of uridine 5'-diphosphoglucuronic acid (UDPGA) (i.e. L-borneol) (Watkins and Klaassen, 1983) or inhibitory effects toward UDP-glucuronosyltransferase (UGT)1A6 (i.e. amentoflavone and diclofenac) (Lv et al., 2018,Uchaipichat et al., 2004,Rong and Kiang, 2020), the latter being the primary enzyme responsible for the production of *p*-cresol glucuronide in human liver microsomes (Rong and Kiang, 2020). The optimized inhibitor concentrations (i.e. 0.75 mM L-borneol, 75 μM amentoflavone, and 100 μM diclofenac, to be discussed further in Results) that did not generate cellular toxicity (by LDH assay) were utilized in subsequent modulation experiments. *p*-Cresol at 0.75 mM was selected for inhibition experiments based on linear responses in the individual

toxicity assays observed in concentration and time-course experiments. The effects of these treatments on markers of cellular toxicities (i.e. DCF, GSH, and LDH assays) were characterized. Concentrations of *p*-cresol, *p*-cresol sulfate, and *p*-cresol glucuronide in culture were also measured as part of control experiments.

Figure 3
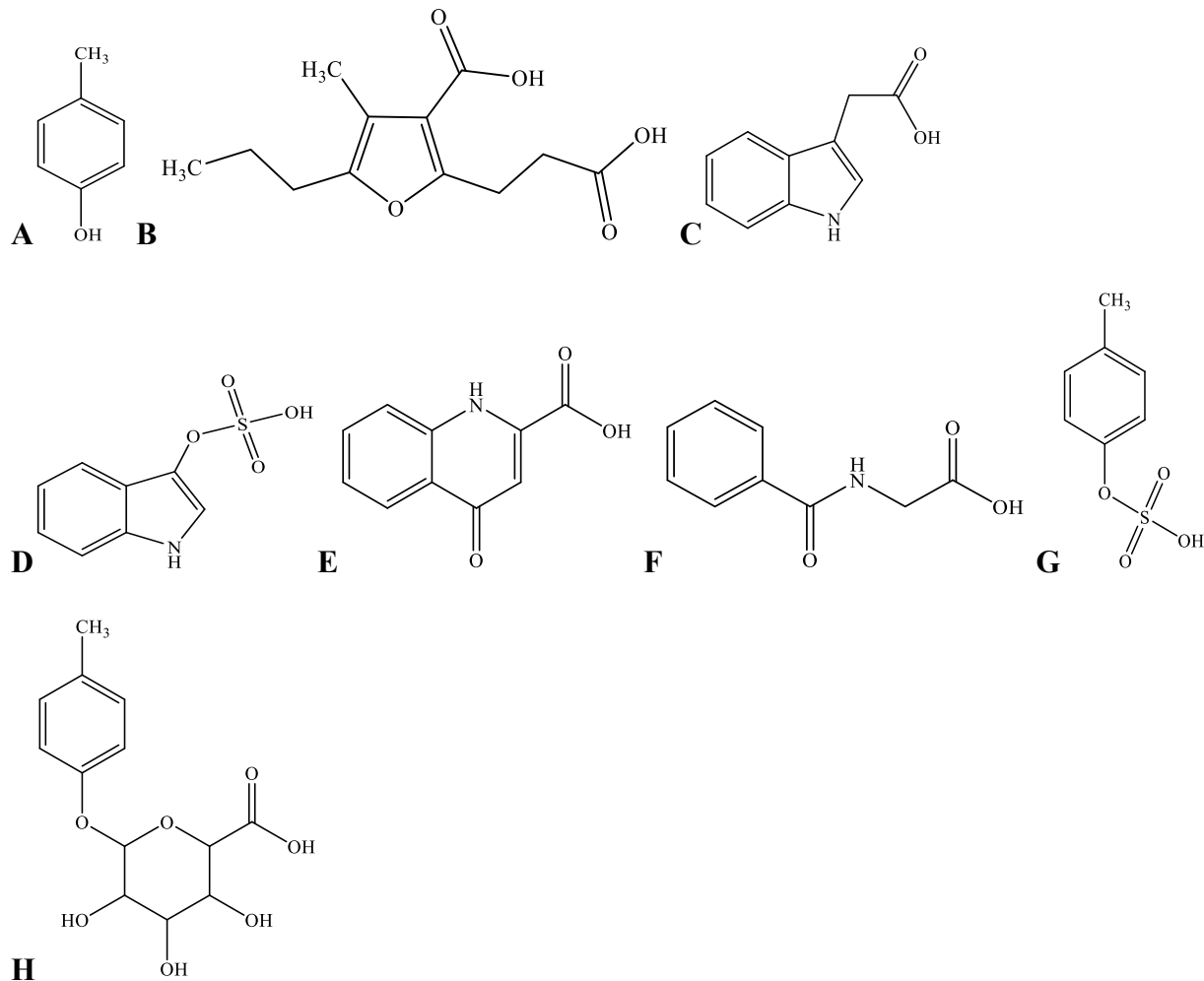
Figure 3. Chemical structures of (A) *p*-cresol (CAS# 106-44-5), (B) CMPF (CAS# 86879-39-2), (C) indole-3-acetic acid (CAS# 87-54-1), (D) indoxyl sulfate (CAS# 487-94-5), (E) kynurenic acid (CAS# 492-27-3), (F) hippuric acid (CAS# 495-69-2), (G) *p*-cresol sulfate (CAS# 3233-58-7), and (H) *p*-cresol glucuronide (CAS# 17680-99-8). *CMPF, 3-carboxy-4-methyl-5-propyl-2-furanpropanoic acid.*

2.4. DCF assay for the measurement of cellular oxidative stress

The formation of the fluorescent DCF from 2', 7'-dichlorofluorescin diacetate (DCFDA) is considered a non-specific marker representative of cellular oxidative stress (Chen et al., 2010). Following treatment (as described above in *2.3. HepaRG cell treatment*), cells were washed twice with 500 μL D-PBS (room temperature [i.e. 23.5°C]) and exposed to 2 μM DCFDA in 500 μL D-PBS (Kiang et al., 2010). The fluorescence intensity of the DCF product was measured at excitation and emission wavelengths of 485 nm and 530 nm, respectively, every 3 minutes up to 30 minutes to ensure the linearity of DCF formation (SpectraMax M2, Molecular Devices, California, USA). This process was shielded from laboratory incandescent lighting to minimize artefactual DCF formation (Chen et al., 2010). DCF formation in treated cells was expressed as a percentage of the vehicle control, after subtracting background fluorescence intensity at 0 minutes of incubation (which exhibited comparable DCF fluoresce values as cell-free medium). t-BOOH (5 mM, exposed for 10 minutes to HepaRG cells) was used as the positive control for DCF formation.

2.5. GSH assay for the measurement of total cellular glutathione concentration

Total cellular GSH concentration was determined using the manufacturer's protocol (Cayman Chemical, 2016) as described by Kiang et al (Kiang et al., 2011). Following cell treatment (as described above in *2.3. HepaRG cell treatment*), cells were washed twice with 500 μL D-PBS (25°C) and homogenized in 250 μL cold 50 mM 2-(N-morpholino) ethanesulphonic acid (MES) buffer containing 0.25 mM EDTA. The resulting cell suspension was sonicated (75D ultrasonic cleaner, VWR International, Alberta, Canada) for 5 minutes in ice water, vortexed (Vortex-Genie 2, Thermo Fisher Scientific) for 5 seconds, and centrifuged (centrifuge 5424 R,

Eppendorf, Ontario, Canada) at 10,000 g for 15 minutes at 4°C. Subsequently, 200 µL of the supernatant was de-proteinated using 200 µL of meta-phosphoric acid (100 mg/mL) for 5 minutes and centrifuged at 2,300 g for 3 minutes at room temperature (i.e. 23.5°C). The resulting protein-free supernatant (200 µL) was neutralized with 10 µL of 4 M triethanolamine and incubated (50 µL/well in 96-well plate) with 150 µL of assay reaction mixture on an orbital shaker (VWR Standard Orbital Shaker 3500, Edmonton, Alberta) shielded from light at room temperature for 5 minutes. The assay reaction mixture consisted of 5, 5'-dithiobis-2-nitrobenzoic acid, $NADP^+$, glucose-6-phosphate, glutathione reductase, glucose-6-phosphate dehydrogenase, and water in MES buffer (Cayman Chemical, 2016). The blank control was 50 mM MES buffer. The absorbance of the reaction product, 5-thio-2-nitrobenzoic acid, was measured at 412 nm (Cayman Chemical, 2016) every 3 minutes up to 30 minutes to ensure the linearity of product formation (SpectraMax M2 plate reader, Molecular Devices, California, USA). GSH concentration was calculated using a standard curve ranging from 0-12.5 µM prepared from glutathione disulfide analytical standards (Cayman Chemical, 2016). Total cellular GSH concentration in treated cells were expressed as percentages of the vehicle control. t-BOOH (5 mM, exposed for 24 hours to HepaRG cells) was used as the positive control for total cellular glutathione depletion.

2.6. LDH assay for the measurement of cellular necrosis

Cellular LDH release as a marker of necrosis was determined using the manufacture's protocol (Roche, 2016) as described previously (Kiang et al., 2010,Rong and Kiang, 2019). Following cell treatment (as described above in *2.3. HepaRG cell treatment*), cell supernatant was collected and stored on ice. Cells were incubated in 500 µL lysis buffer (i.e. cell differentiation medium with 2% v/v Triton X-100 and 20 mM EDTA) for 5 minutes at room temperature (i.e.

23.5°C) to facilitate cell detachment. The resulting cell suspension was vortexed for 30 seconds and centrifuged at 20,000 g at 4°C for 10 minutes to release cellular LDH. Subsequently, 50 µL each of cell supernatant or processed cell lysates were incubated with 100 µL of the assay reaction mixture (i.e. 200 µL catalyst [i.e. NAD^+ and diaphorase] and 9000 µL dye solution [i.e. iodotetrazolium chloride and sodium lactate]) in 96-well plates to start the enzyme reaction. The differentiation medium was used as the blank control of which absorbance was subtracted from all measurements. The absorbance of the reaction product, a red formazan salt, was measured at wavelength of 490 nm (Roche, 2016) every 3 minutes for up to 30 minutes to ensure linear enzymatic conditions (SpectraMax M2, Molecular Devices, California, USA). LDH in the cell supernatant was expressed as a percentage of the sum total of LDH quantified from both supernatant and cell lysates (Kiang et al., 2010). t-BOOH (50 mM, exposed for 24 hours to HepaRG cells) was used as the positive control for cellular necrosis.

2.7. Quantification of p-cresol sulfate and p-cresol glucuronide concentrations in HepaRG cell culture

An ultra-high performance liquid chromatography-tandem mass spectrometry assay (UPLC-MS/MS, Shimadzu LC-MS 8050, Kyoto, Japan) was developed and validated in our lab to quantify the concentrations of *p*-cresol sulfate and *p*-cresol glucuronide in HepaRG cell culture, based on a previously published assay (Rong and Kiang, 2020). Briefly, culture supernatant (30 µL) or lysates (obtained after removing supernatant, washing cells twice with 500 mL of 37°C D-PBS, and harvesting cells with 500 mL of 37°C culture medium) was collected and deproteinated with a mixture of 1 µg/mL *p*-cresol sulfate-d7 and *p*-cresol glucuronide-d7 (i.e. internal standards) in 90 µL methanol (i.e. extraction solvent) (Cuoghi et al., 2012). Analyte extraction was shielded

from light at room temperature (i.e. 23.5°C) for 20 minutes. In order to precipitate proteins, the mixture was vortexed, sonicated (each for 30 seconds), and centrifuged at 4,000 g for 10 minutes at 4°C. Five µL of the resulting supernatant was injected into the autosampler (ShimadzuSIL-30 AC, Kyoto, Japan) for analysis. A biphenyl column (2.7 µM particle size, 2.1 mm inner diameter, 100 mm length, Restek Corporation, Pennsylvania, USA) was utilized to separate p-cresol sulfate and p-cresol glucuronide using an isocratic condition with a flow rate of 0.3 mL/min (at 30°C). The mobile phase consisted of water and methanol (10:90, v/v) supplemented with 2 mM ammonium acetate and 0.1% formic acid. Analyte identifications were achieved with negative electrospray ionization with multiple reaction monitoring of the following mass transitions: p-cresol sulfate (mass to charge ratio [m/z]: 187.00→107.00), p-cresol glucuronide (m/z: 282.85→106.95), p-cresol sulfate-d$_7$ (m/z: 194.10→114.15), and p-cresol glucuronide-d$_7$ (m/z: 290.00→114.00). The assay was validated following the United States Food and Drug Administration (FDA)'s guidance document (US Food and Drug Administration., 2018).

2.8. Quantification of p-cresol concentrations in HepaRG cell culture

An ultra-high performance liquid chromatography assay (UPLC, Shimadzu Nexera-i LC-2040 C, Kyoto, Japan) was developed and validated to quantify the concentrations of p-cresol in HepaRG cell culture. Thirty µL of cell supernatant or lysates was collected and deproteinated with 90 µL methanol (containing 50 µg/mL 2,6-dimethylphenol (DMP), the internal standard). The mixture was protected from light during sample extraction at room temperature (i.e. 23.5°C) for 20 minutes. After extraction, the mixture was vortexed and sonicated at room temperature for 30 seconds and centrifuged at 4,000 g at 4°C for 10 minutes. Subsequently, the supernatant (50 µL) was injected into the autosampler and separated using the Zorbax Eclipse XDB-C18 analytical

column (5 μm particle size, 4.6 mm inner diameter, 250 mm length; Agilent Technologies, Ontario, Canada) at a temperature of 40°C. The mobile phase consisted of water and methanol (26:74, v/v) supplemented with 0.5 mM ammonium acetate and 0.025% formic acid at an isocratic flow rate of 0.3 mL/minute. The wavelength of the ultraviolet detector was 280 nm for both *p*-cresol and DMP, which was pre-optimized based on control spectral scans (Shimadzu UV-2600i, Kyoto, Japan). The assay was validated following the United States Food and Drug Administration (FDA)'s guidance document (US Food and Drug Administration., 2018).

2.9. Statistical analysis

Only non-parametric testing with more stringent thresholds were utilized. The Mann-Whitney rank sum test was used to compare two groups, and the Kruskal-Wallis analysis of variance on ranks followed by Student-Newman-Keuls *post hoc* test were used to compare multiple groups (SigmaStat 3.5, Systat Software, California, USA) (Kiang et al., 2010,Kiang et al., 2011,Surendradoss et al., 2014). A p value <0.05 was deemed *a priori* as the threshold for significance. The half maximal effective concentrations (EC_{50}) were determined by sigmoidal 3-parameter fitting ($y = \frac{a}{1+\exp\left(\frac{X_0 - X}{b}\right)}$) (SigmaPlot 14.0, Systat Software, California, USA).

3. Results

3.1. Positive control and concentration / time-course responses of p-cresol in HepaRG cells

t-BOOH was utilized as an assay-based positive control for each toxicity marker (Liang et al., 2018,Kiang et al., 2010,Kiang et al., 2011). t-BOOH increased DCF formation (with 5 mM, 10 minutes of exposure; by $297.0\pm31.8\%$, n=3, p<0.05), decreased total cellular GSH (with 5 mM, 24 hours of exposure; by $100.0\pm0.4\%$, n=3, p<0.05), and increased LDH release (with 50 mM, 24

hours of exposure; by 87.8±2.7%, n=3, p<0.05) (please see Supplementary Materials, Figures S1-S3) compared to the vehicle control, confirming the known toxic effects of the hydroperoxide in other liver cellular models (e.g. (Liang et al., 2018,Kiang et al., 2010,Kiang et al., 2011)). *p*-Cresol exposure resulted in concentration-dependent increases in DCF formation (EC_{50}=0.64±0.37 mM, Figure 4A), decreases in total cellular GSH concentration (EC_{50}=1.00±0.07 mM, Figure 4B), and increases in LDH release (EC_{50}=0.85±0.14 mM, Figure 4C) after 24 hours of exposure. The minimum concentration of *p*-cresol causing significant toxicity was 0.25 mM (DCF formation), 0.75 mM (GSH depletion), and 0.5 mM (LDH release) (Figure 4). Based on the EC_{50} values generated from concentration-response experiments, 1 mM of *p*-cresol (representing near maximum but still linear toxicity responses) was utilized to establish the time-dependent effects for each toxicity marker. *p*-Cresol (1 mM) significantly increased DCF formation at ≥ 6 hours of exposure (Figure 5A), depleted total cellular GSH at ≥ 6 hours of exposure (Figure 5B), and increased LDH release at ≥ 12 hours of exposure (Figure 5C), indicating possible temporal relationships between *p*-cresol-associated oxidative stress, GSH depletion, and cellular necrosis.

Figure 4A)

Figure 4B)

53
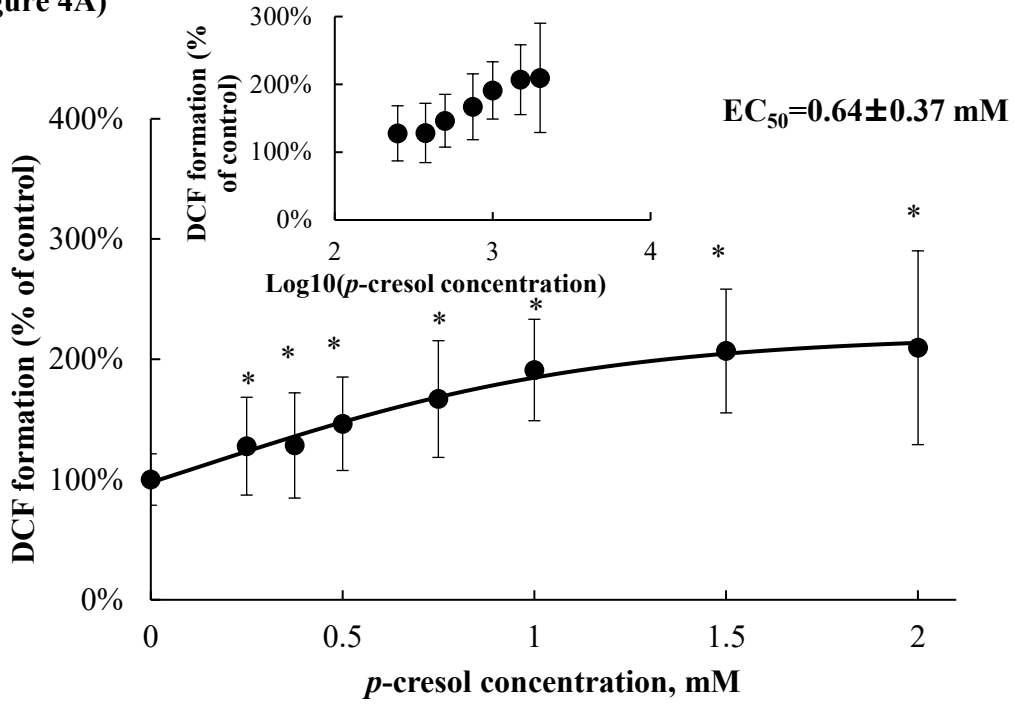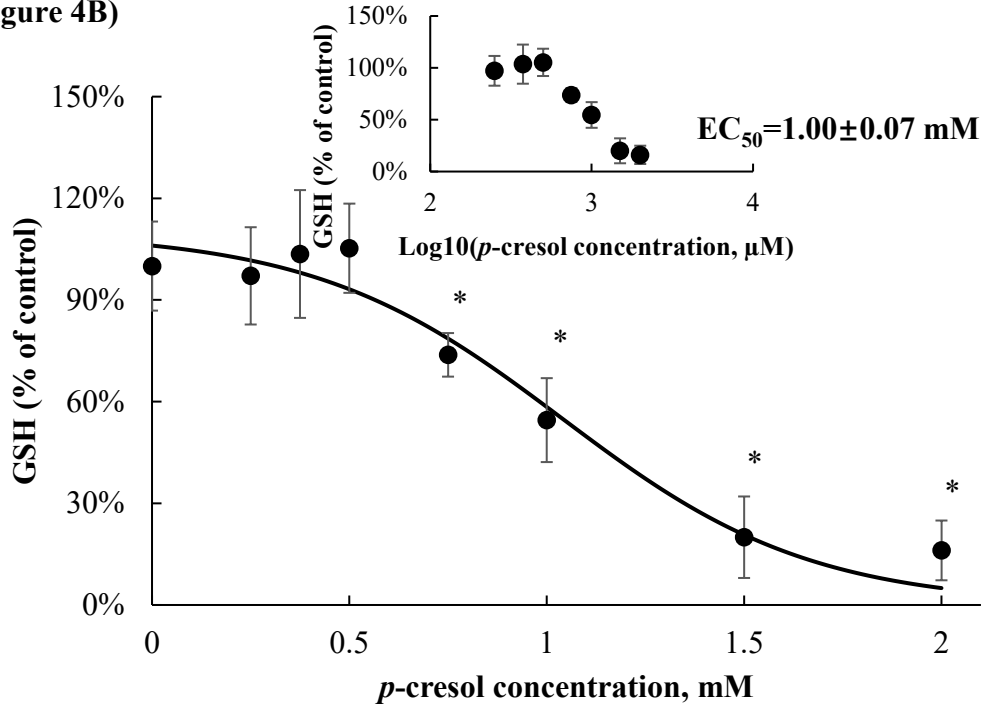
Figure 4C)

Figure 4. Concentration-responses of *p*-cresol in A) DCF formation, B) total cellular GSH depletion, and C) LDH release in HepaRG cells (0.4 million cells/well). Cells were treated with 0 to 2 mM of *p*-cresol for 24 hours as described in Materials and Methods. DCF formation (n=18) and total cellular GSH depletion (n=12) were expressed as percentages of the vehicle control (i.e. the HepaRG differentiation medium). LDH release (n=8) was calculated as the percentage of activity in the cell supernatant to that of the sum of cell supernatant and cell lysates. The EC_{50} values were calculated based on sigmoidal, 3-parameter fitting (SigmaPlot 14.0). Data are presented as mean ± standard deviation. *p<0.05 versus the vehicle control using the Mann-Whitney rank sum test. *DCF, 2', 7' –dichlorofluorescein; EC_{50}, half maximal effective concentration; GSH, total cellular glutathione; LDH, lactate dehydrogenase.*

Figure 5A)

Figure 5B)

Figure 5C)

Figure 5. Time-dependent effects of *p*-cresol in (A) DCF formation, (B) total cellular GSH depletion, and (C) LDH release in HepaRG cells (0.4 million cells/well). Cells were treated with 1 mM *p*-cresol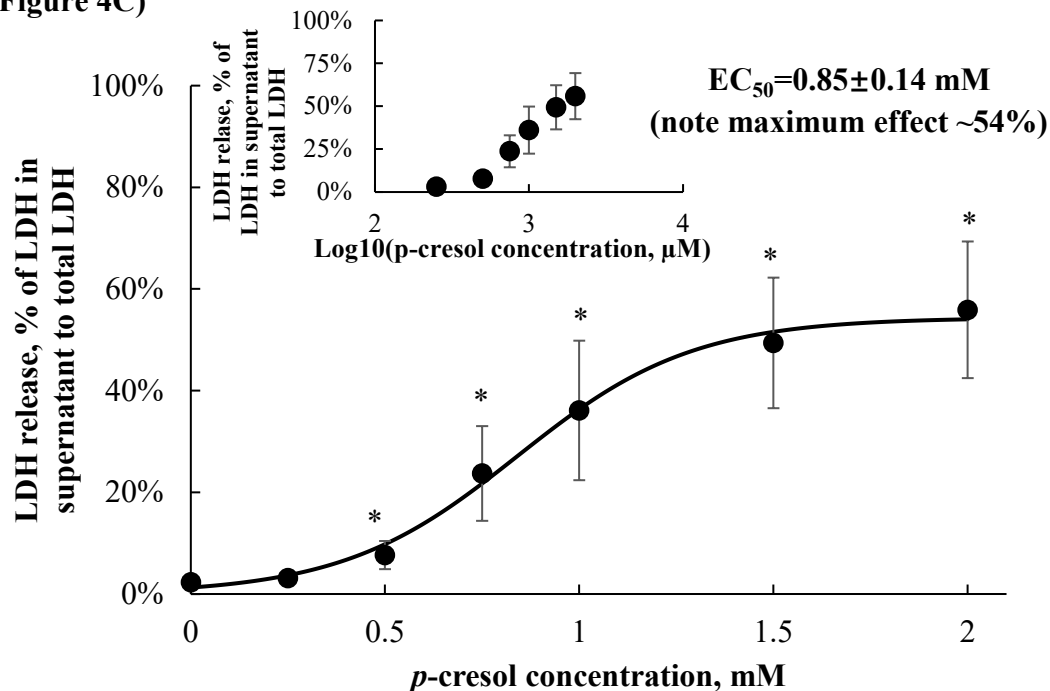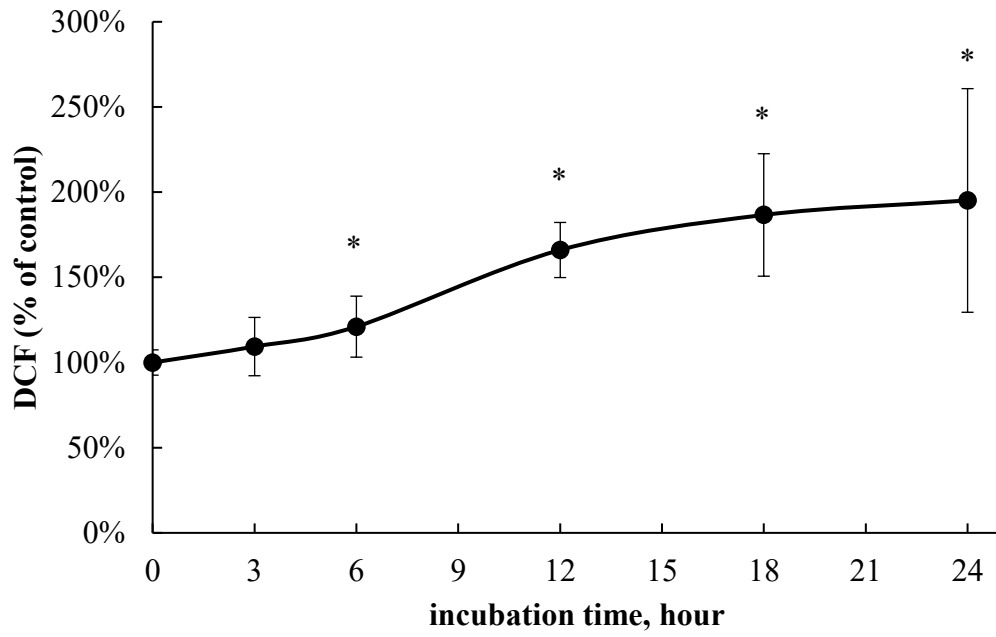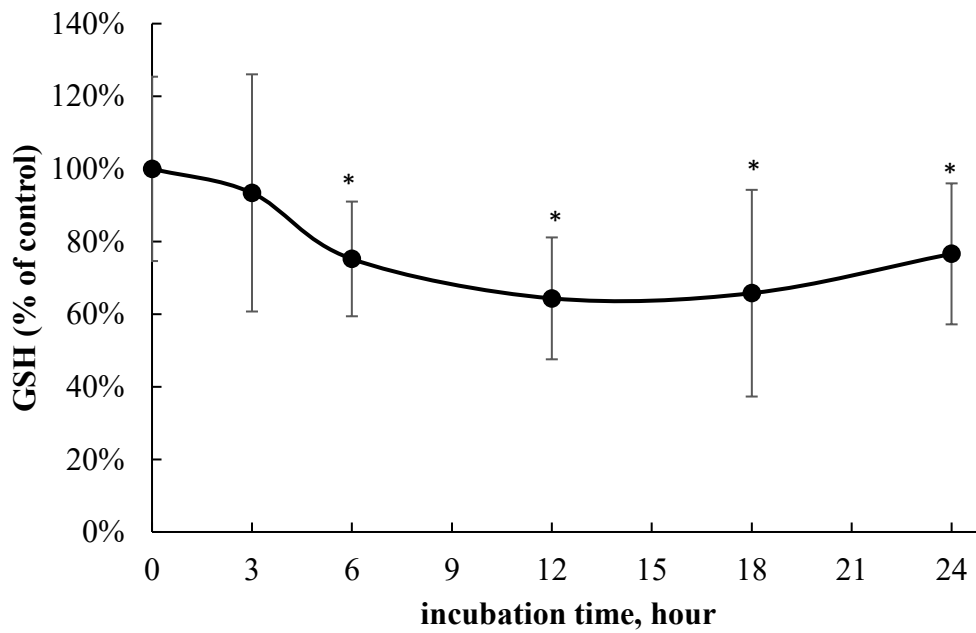 for 0, 3, 6, 12, 18, and 24 hours as described in Materials and Methods. DCF formation (n=12) and total cellular GSH depletion (n=10) were expressed as percentages of their vehicle controls (i.e. the HepaRG differentiation medium) at corresponding treatment times. LDH release (n=4) was initially calculated as the percentage of activity in the cell supernatant to that of the sum of cell supernatant and cell lysates, and further expressed as a percentage of the vehicle control at the corresponding treatment times. Data are presented as mean ± standard deviation. *p<0.05 versus the vehicle control using the Mann-Whitney rank sum test. *DCF, 2', 7' – dichlorofluorescein; GSH, total cellular glutathione; LDH, lactate dehydrogenase.*

3.2. Relative toxic effects of p-cresol in comparison to other uremic toxins in HepaRG cells

p-Cresol is a part of a large milieu of uremic toxins, and the toxic effects of *p*-cresol compared to other toxicologically important protein-bound uremic solutes (Prokopienko, Alexander J. and Nolin, 2018,Vanholder et al., 2018) have not been systematically characterized in a hepatic model. The relative effects of *p*-cresol and other protein-bound uremic toxins on the DCF, GSH, and LDH markers were determined using equal molar conditions (i.e. 1 mM exposure for 24 hours). Our data indicated *p*-cresol to be the most toxic with respect to each marker compared to all tested uremic toxins in HepaRG cells (Figure 6). Overall, CMPF, indole-3-acetic acid, indoxyl sulfate, kynurenic acid, and hippuric acid had little effects on DCF increase, GSH depletion, or LDH release when compared to the vehicle control (Figure 6). While it is ideal to consider the concurrent effects of the entire uremic milieu when assessing toxicity (Cohen et al., 2007), these data supported further *targeted* investigations of *p*-cresol as a potent uremic toxicant in this experimental model.
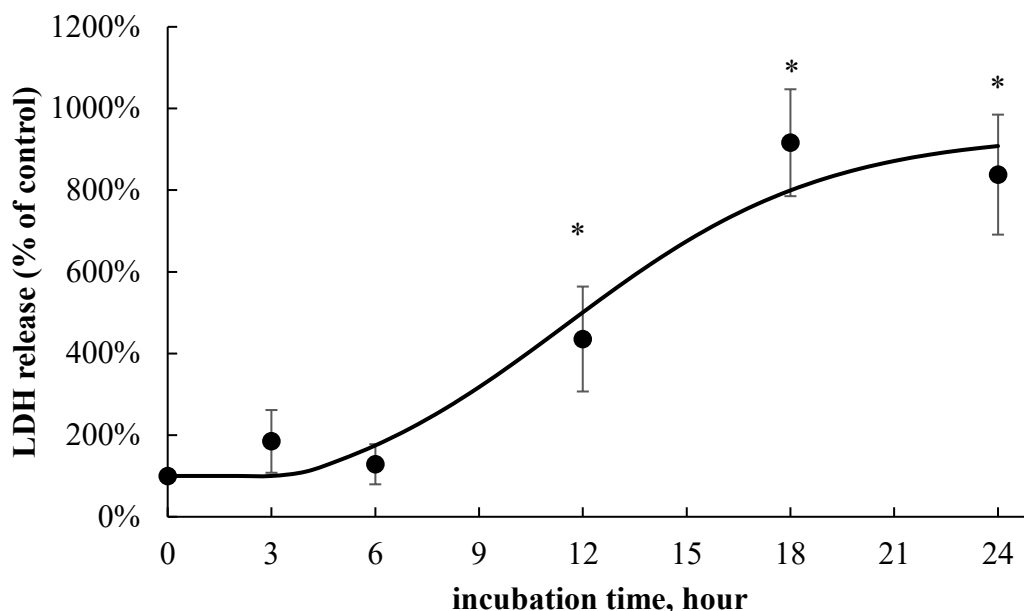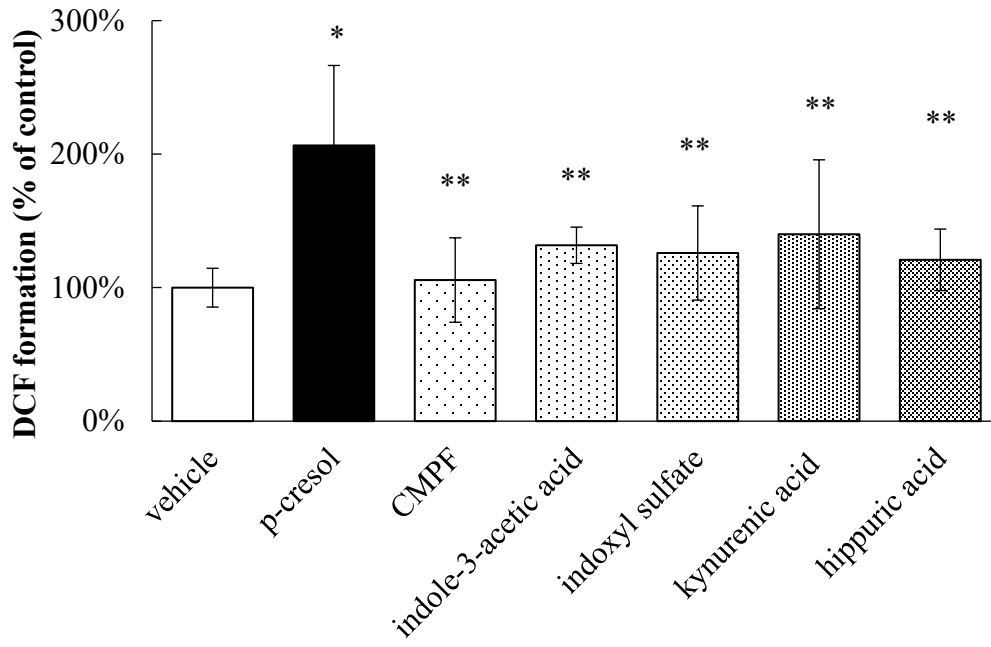
Figure 6A)

Figure 6B)
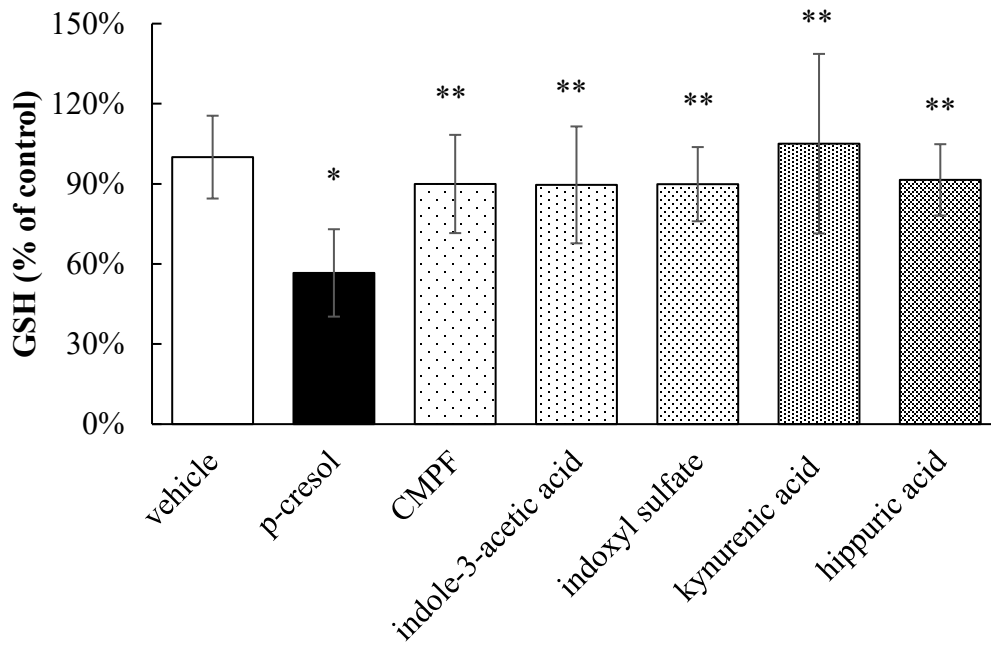
Figure 6C)
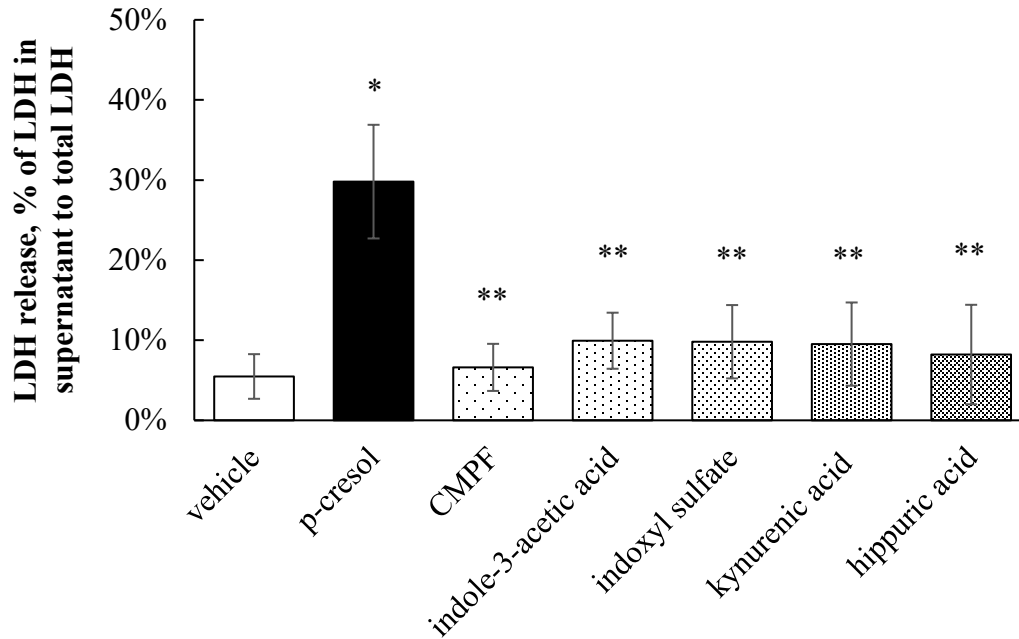
Figure 6. Relative effects of uremic toxins on (A) DCF formation, (B) total cellular GSH depletion, and (C) LDH release in HepaRG cells (0.4 million cells/well). Cells were treated with equal-molar (i.e. 1 mM) concentrations of *p*-cresol, CMPF, indole-3-acetic acid, indoxyl sulfate, kynurenic acid, or hippuric acid for 24 hours as described in Materials and Methods. DCF formation and total cellular GSH depletion were expressed as percentages of the vehicle control (i.e. the HepaRG differentiation medium). LDH release was calculated as the percentage of activity in the cell supernatant to that of the sum of cell supernatant and cell lysates. Data are presented as mean ± standard deviation from n=8 determinations. *$p < 0.05$ versus the vehicle control using ANOVA on ranks; **$p < 0.05$ versus *p*-cresol. *CMPF, 3-carboxy-4-methyl-5-propyl-2-furanpropanoic acid; DCF, 2', 7' –dichlorofluorescein; GSH, total cellular glutathione; LDH, lactate dehydrogenase.*

3.3. p-Cresol sulfate and glucuronide concentrations in HepaRG cells treated with p-cresol

The formation of *p*-cresol sulfate and *p*-cresol glucuronide were approximately linear (as evident in the culture supernatant) at *p*-cresol concentrations ≤ 1000 µM after 24 hours of exposure (Figures 7A&7B). The maximum *p*-cresol sulfate and *p*-cresol glucuronide concentrations generated were 27.2 ± 6.2 µM and 277.3 ± 12.3 µM in the culture supernatant, respectively, achieved at 1000 µM of *p*-cresol exposure. In contrast to the culture supernatant, low concentrations of *p*-cresol sulfate and *p*-cresol glucuronide were found in the cell lysates (i.e. $1.7\pm1.5\%$ for *p*-cresol sulfate and $3.3\pm1.0\%$ for *p*-cresol glucuronide as percentages of the sum of cell lysates and supernatant from averages of all tested concentrations) (Figures 7C&7D). Based on these findings, only the culture supernatant was utilized for metabolite quantification for subsequent chemical modulation experiments (please see section 3.6 below). The observation of metabolites being found primarily in culture supernatant is consistent with other analytes in the HepaRG model (Rong and Kiang, 2019) or in different *in vitro* hepatocyte models (Surendradoss, Chang, & Abbott, 2014). Furthermore, metabolite concentrations declined at *p*-cresol concentration > 1 mM (Figure 7), possibly due to cellular toxicity as evident by LDH release ($EC_{50}\sim$1mM, Figure 4C).

Concentrations of *p*-cresol sulfate and *p*-cresol glucuronide in the culture supernatants of cells treated with 0.75 mM or 1.0 mM of *p*-cresol increased linearly as a function of incubation time from 0 to 24 hours (Figures 8A&8B). Consistent with our concentration-response experiments, metabolite concentrations in cell lysates were consistently low (i.e. $5.3\pm3.7\%$ for *p*-cresol sulfate and $3.3\pm1.4\%$ for *p*-cresol glucuronide as percentages of total metabolites generated in cells treated with 1.0 mM of *p*-cresol using all tested time points, Figures 8C&8D); however, the increases in cell lysate metabolite concentrations were slightly curve linear. Taken together, these data confirmed the suitability of our experimental conditions (i.e. 750 µM or 1000 µM of *p*-

cresol exposure for 24 hours) for modulation or comparative experiments. Furthermore, *p*-cresol glucuronide was the predominant metabolite at these toxic conditions in this model (Figures 7&8). The glucuronidation pathway was the focus of our subsequent mechanistic modulation experiments.

Figure 7A)
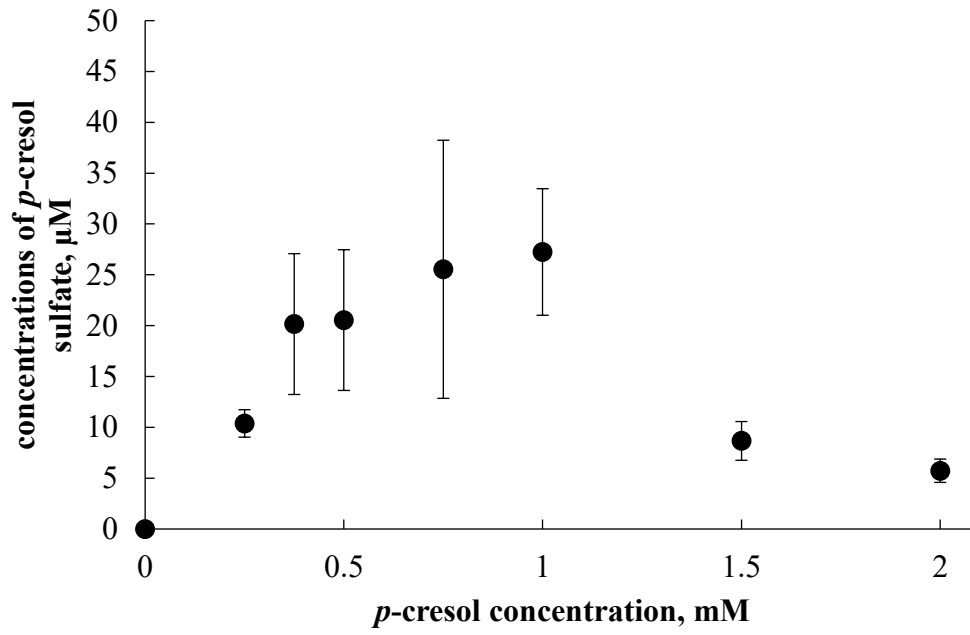
Figure 7B)
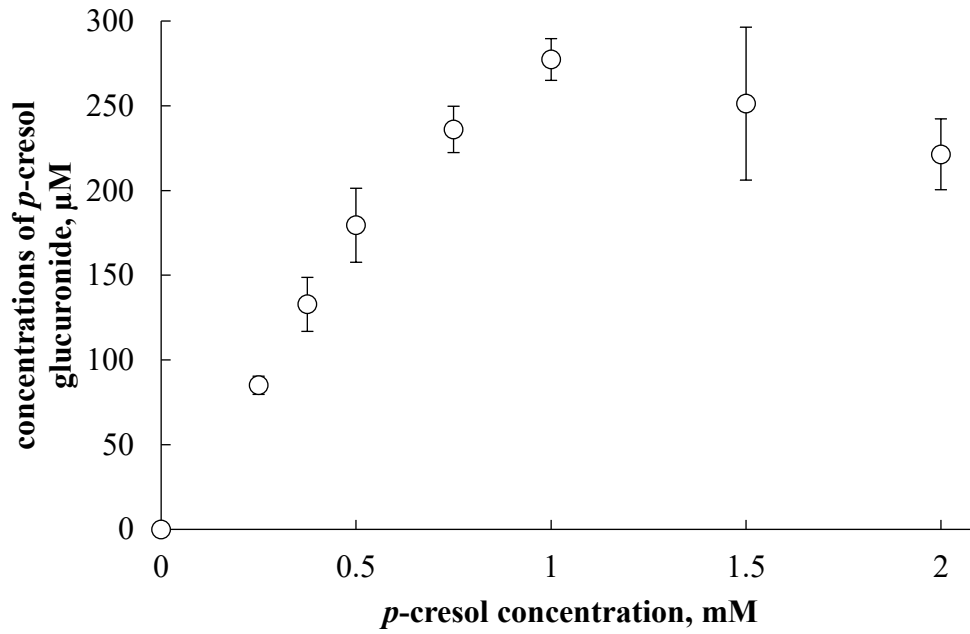
Figure 7C)
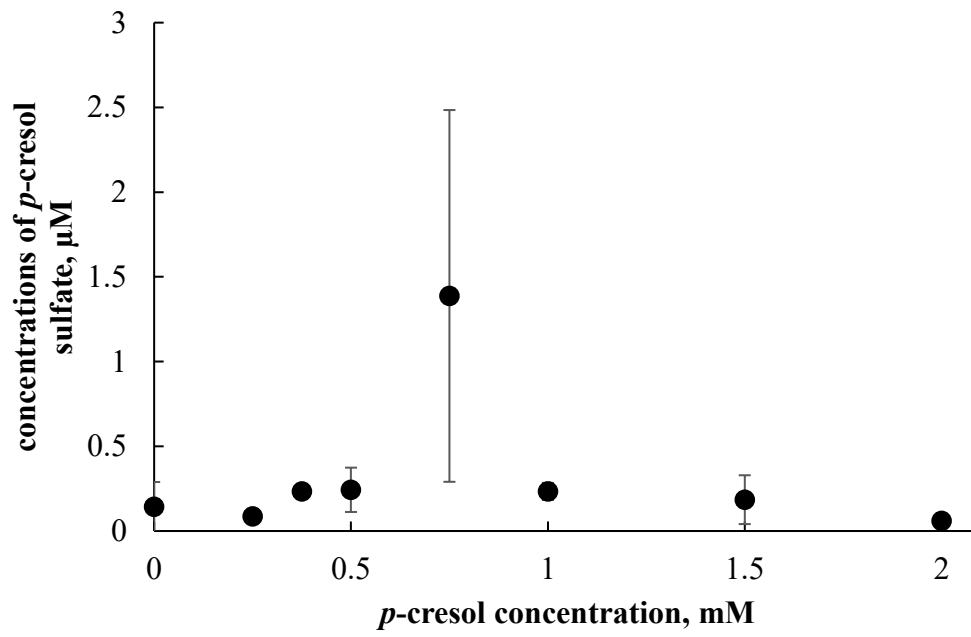
Figure 7D)
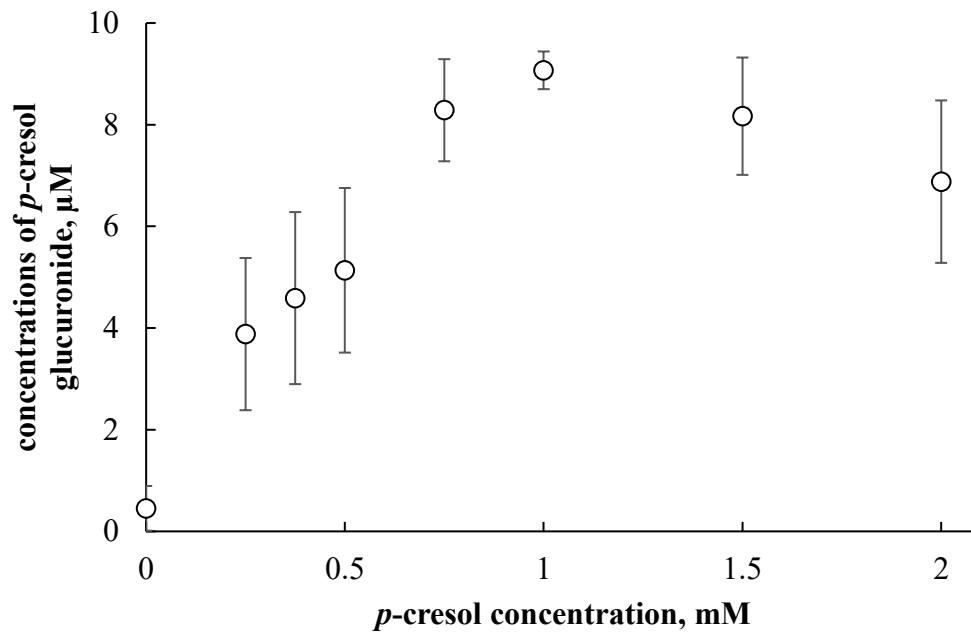
Figure 7. Concentration-dependent effects of *p*-cresol (0 to 2 mM, 24 hours of exposure) on the formation of A) *p*-cresol sulfate in culture supernatant, B) *p*-cresol glucuronide in culture supernatant, C) *p*-cresol sulfate in cell lysates, and D) *p*-cresol glucuronide in cell lysates in HepaRG cells (0.4 million cells/well). Concentrations of *p*-cresol sulfate and *p*-cresol glucuronide were determined as described in Materials and Methods. The concentrations of metabolites decreased after 1 mM treated *p*-cresol because of likely cell death as illustrated in **Figure 4**. Data are presented as mean ± standard deviation from n=3 determinations.

Figure 8A)

0.75 mM p-cresol   1 mM p-cresol

Figure 8B)

0.75 mM p-cresol   1 mM p-cresol
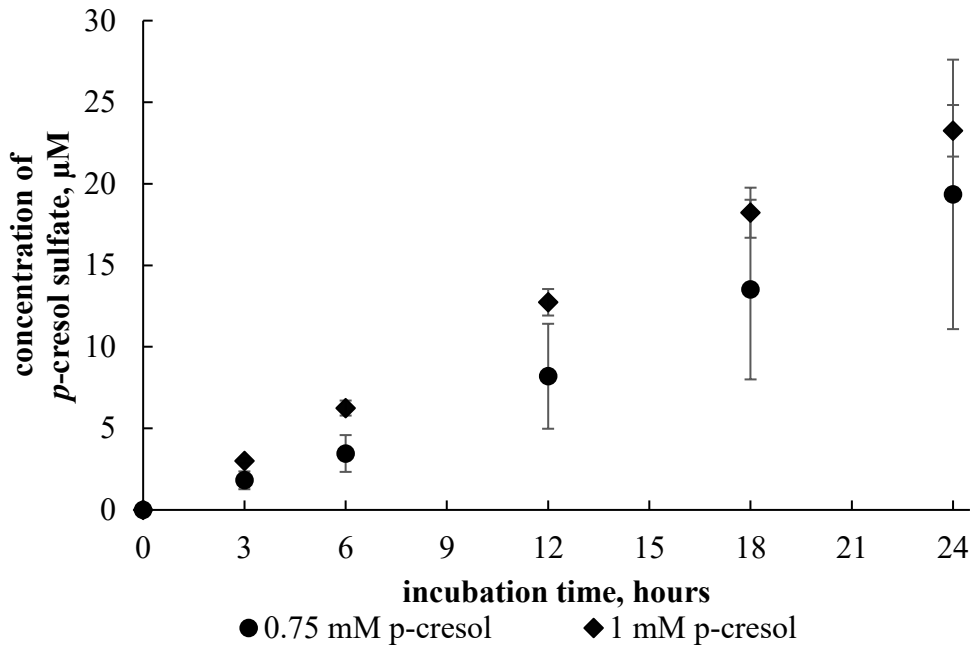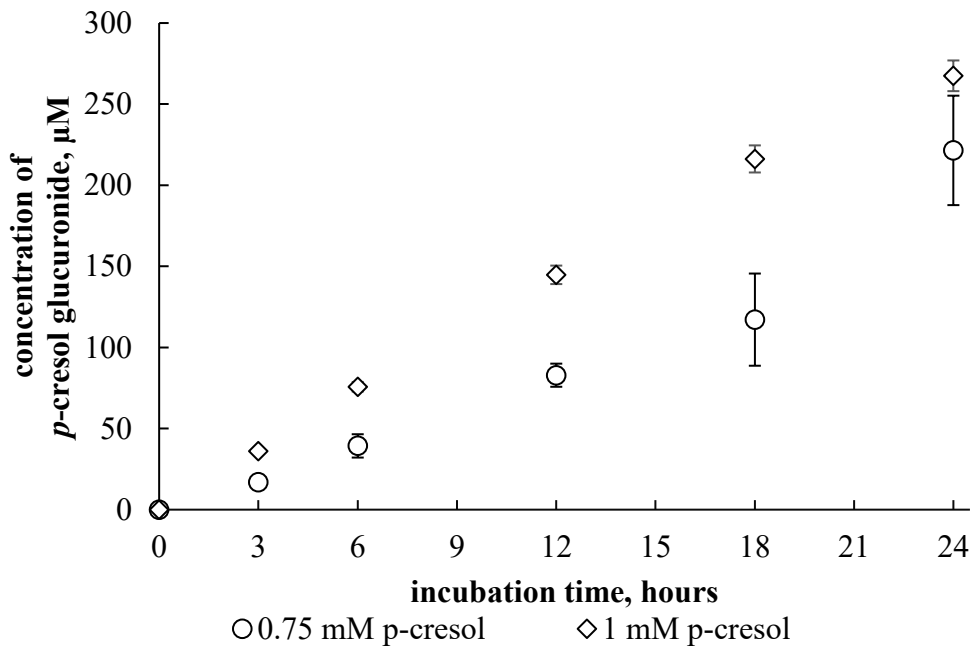
Figure 8C)

Figure 8D)

Figure 8. Time-dependent formation of A) *p*-cresol sulfate in culture supernatant, B) *p*-cresol glucuronide in culture supernatant, C) *p*-cresol sulfate in cell lysates, and D) *p*-cresol glucuronide in cell lysates in HepaRG cells (0.4 million cells/well) treated with 0.75 or 1 mM of *p*-cresol. Concentrations of *p*-cresol sulfate and *p*-cresol glucuronide were determined as described in Materials and Methods. Two concentrations tested in this experiment were used for subsequent toxicity comparison and modulation experiments. Data are presented as mean ± standard deviation from n=4 determinations.

3.4. Relative toxic effects of p-cresol and p-cresol conjugated metabolites

At equal-molar concentrations (1 mM, 24 hours of exposure), exogenously-administered *p*-cresol sulfate and *p*-cresol glucuronide were less effective (i.e. less toxic) compared to *p*-cresol in generating DCF formation (by 31.9±75.8% and 71.8±23.8%, respectively, p<0.05, Figure 9A), depleting total cellular GSH (by 16.5±22.1% and 40.0±19.8%, p<0.05, Figure 9B), and increasing LDH release (by 23.4±2.8% and 24.3±1.8%, p<0.05, Figure 9C). *p*-Cresol sulfate reduced total cellular GSH concentration (by 30.5±13.6%, p<0.05, Figure 9B), whereas both *p*-cresol sulfate and *p*-cresol glucuronide slightly increased LDH release compared to the vehicle control (Figure 9C). These findings indicated that *p*-cresol was relatively more potent than its conjugated metabolites when added exogenously at equal-molar concentrations with respect to the induction of oxidative stress, depletion of GSH, and generation of necrosis in HepaRG cells. Moreover, at these conditions, *p*-cresol sulfate was also consistently more toxic than *p*-cresol glucuronide (Figure 9).

Figure 9A)
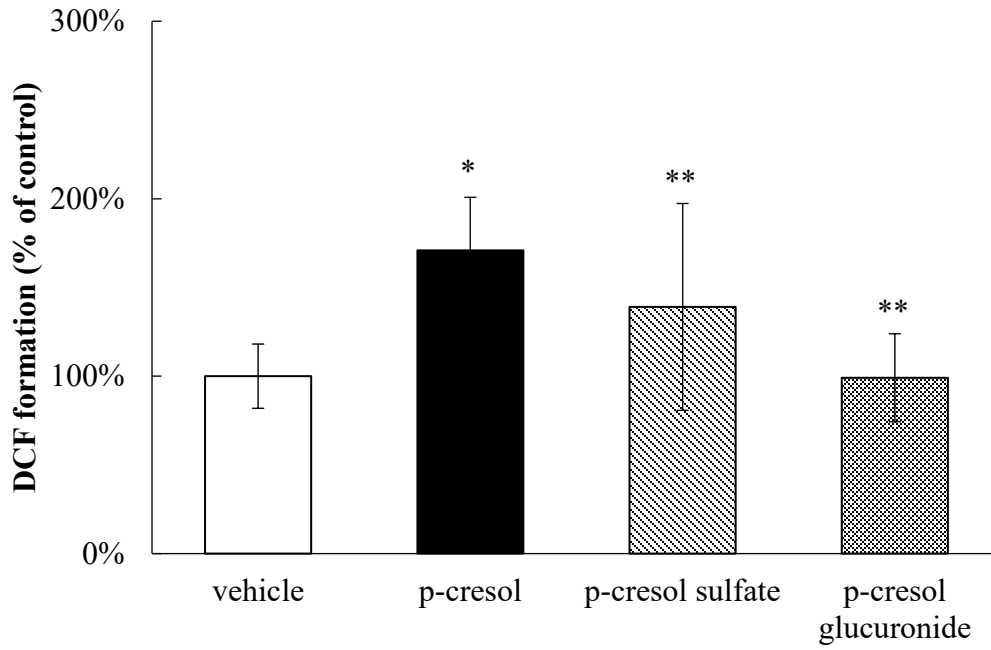
Figure 9B)
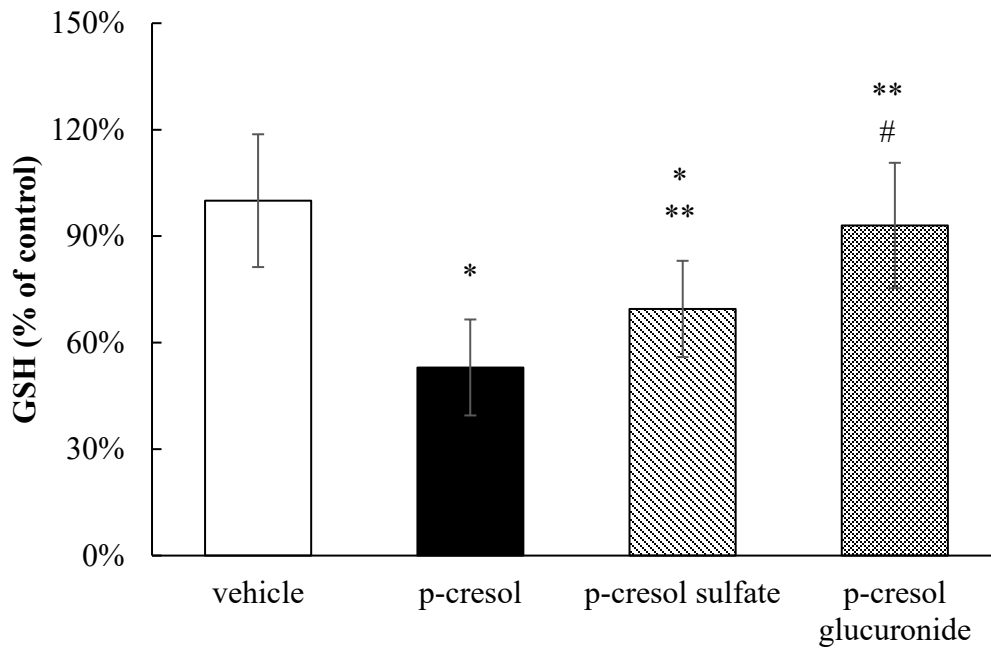
Figure 9C)
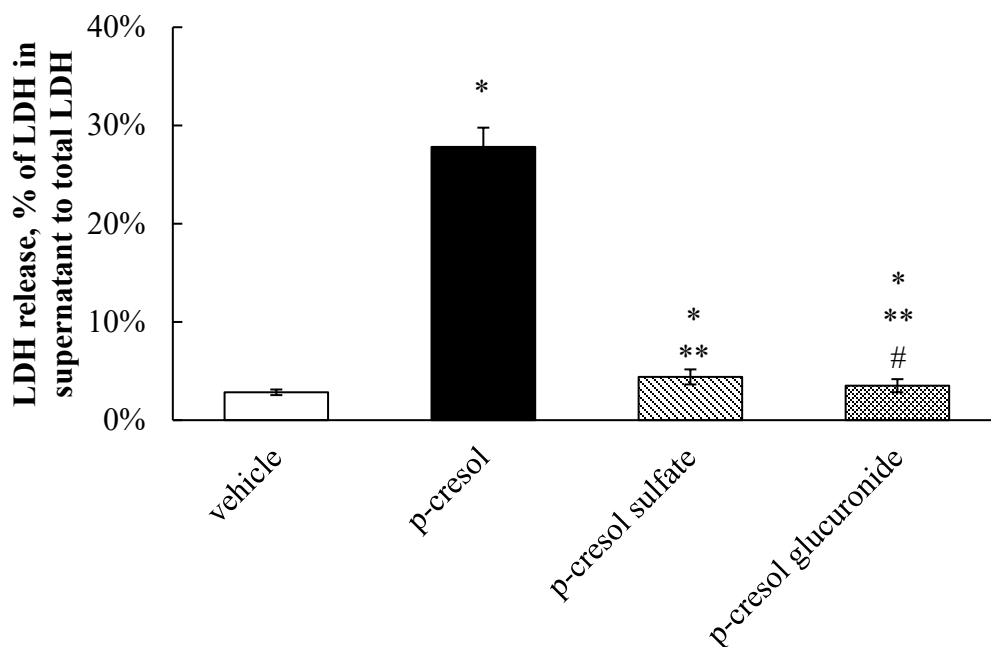
Figure 9. Relative effects of *p*-cresol conjugated metabolites in (A) DCF formation, (B) total cellular GSH depletion, and (C) LDH release in HepaRG cells (0.4 million cells/well). Cells were treated with equal-molar (i.e. 1 mM) concentrations of *p*-cresol, *p*-cresol sulfate, or *p*-cresol glucuronide for 24 hours as described in Materials and Methods. DCF formation and total cellular GSH depletion were expressed as percentages of the vehicle control (i.e. the HepaRG differentiation medium). LDH release was calculated as the percentage of activity in the cell supernatant to that of the sum of cell supernatant and cell lysates. Data are presented as mean ± standard deviation from n=6 determinations. *p<0.05 versus the vehicle control using ANOVA on ranks; **p<0.05 versus *p*-cresol; #p<0.05 versus *p*-cresol sulfate. *ANOVA, analysis of variance; DCF, 2', 7' –dichlorofluorescein; GSH, total cellular glutathione; LDH, lactate dehydrogenase.*

3.5. p-Cresol sulfate and glucuronide concentrations in HepaRG cells treated exogenously with p-cresol sulfate and p-cresol glucuronide

The concentrations of *p*-cresol sulfate and *p*-cresol glucuronide in cells treated exogenously with 1 mM of *p*-cresol sulfate or *p*-cresol glucuronide were compared to the concentrations of these metabolites generated in cells treated with 1 mM of *p*-cresol, in a time-dependent experiment. Concentrations of *p*-cresol sulfate and *p*-cresol glucuronide in the culture supernatant declined over treatment time (Figures 10A & 10B) but progressively increased in cell lysates (Figures 10C & 10D). These findings indicated evidence of cellular uptake with the attainment of maximum concentrations at 24 hours of exposure for both *p*-cresol sulfate (71.4±3.7 µM) and *p*-cresol glucuronide (128.4±6.1 µM). Compared to concentrations of *p*-cresol sulfate and *p*-cresol glucuronide generated *in situ* in cells treated with 1 mM *p*-cresol for 24 hours (Figures 8C & 8D), the intracellular concentrations of these metabolites obtained from exogenously administered *p*-cresol sulfate and *p*-cresol glucuronide were much higher at ~50-fold (*p*-cresol sulfate) and ~16-fold (*p*-cresol glucuronide). However, despite generating significantly higher intracellular concentrations of these metabolites, exogenously administered *p*-cresol sulfate and (especially) *p*-cresol glucuronide were significantly less toxic on all markers compared to *p*-cresol, as shown in Figure 9.
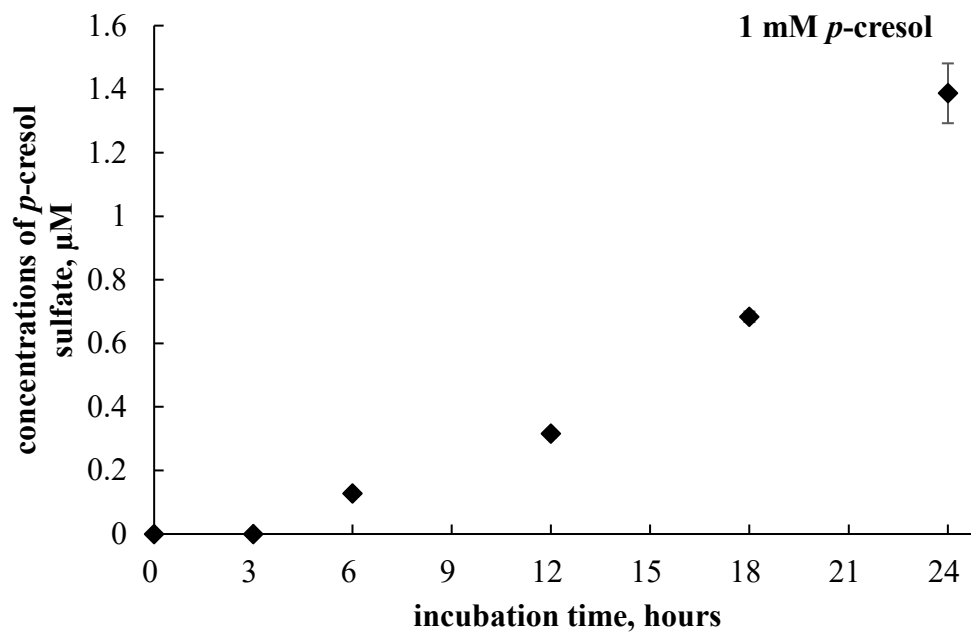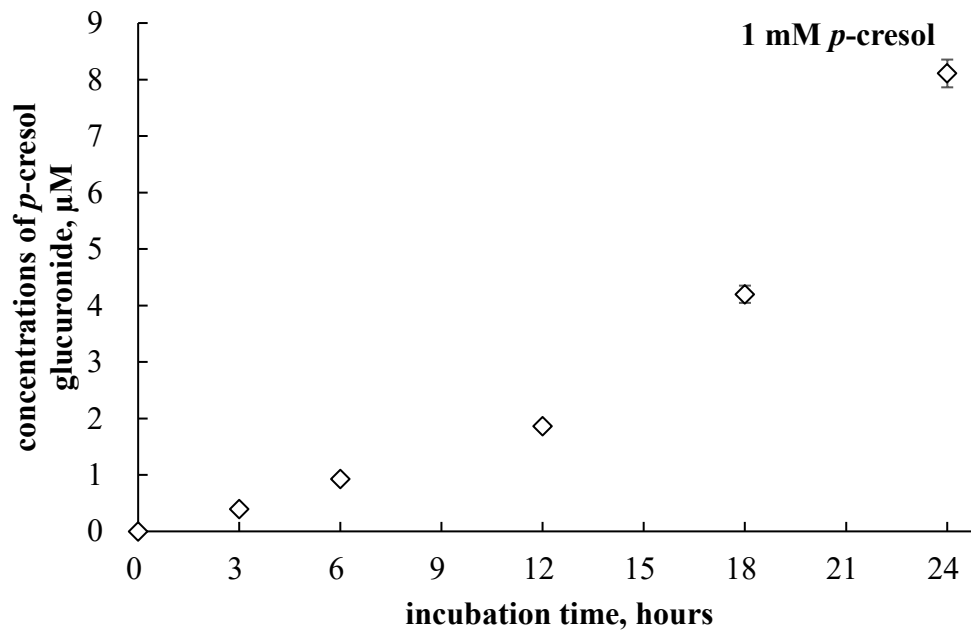
**Figure 10A)**
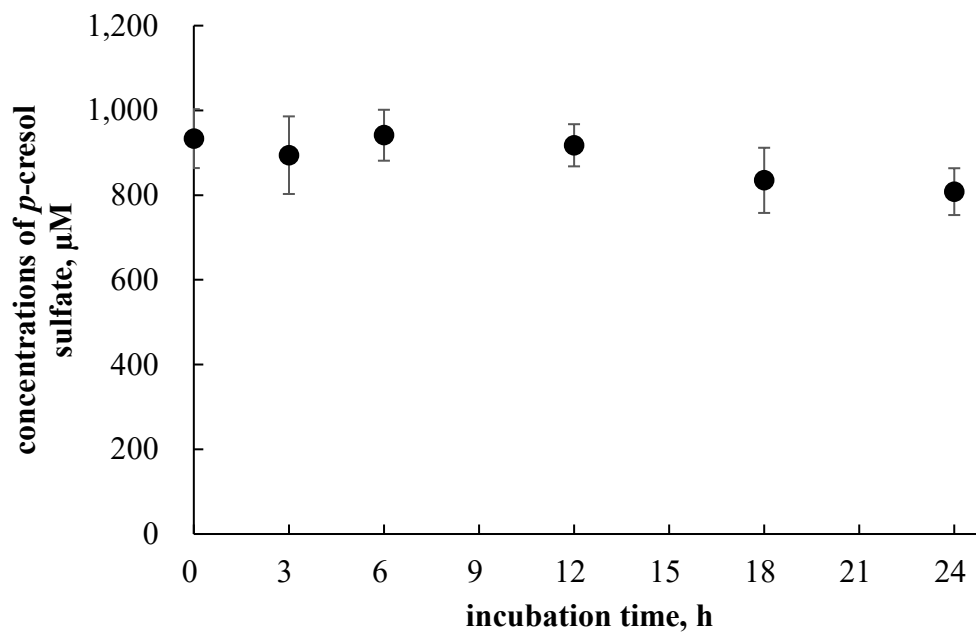
Figure 10B)
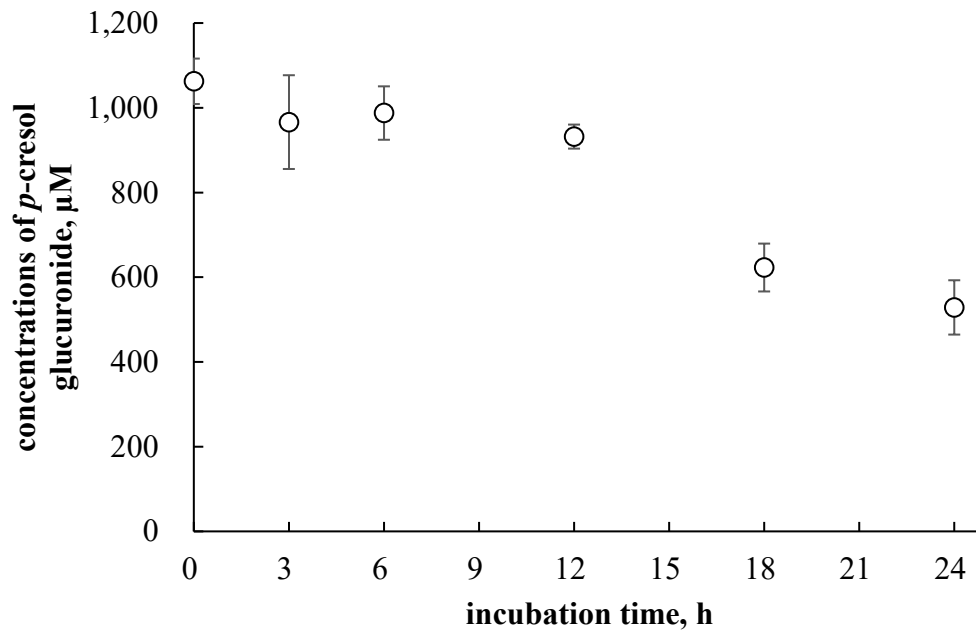
Figure 10C)
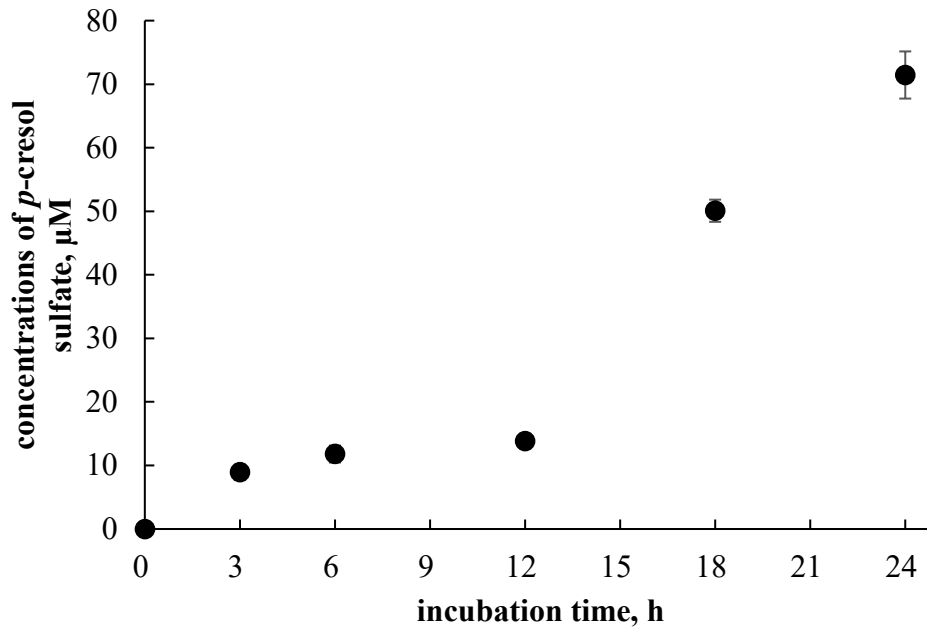
Figure 10D)
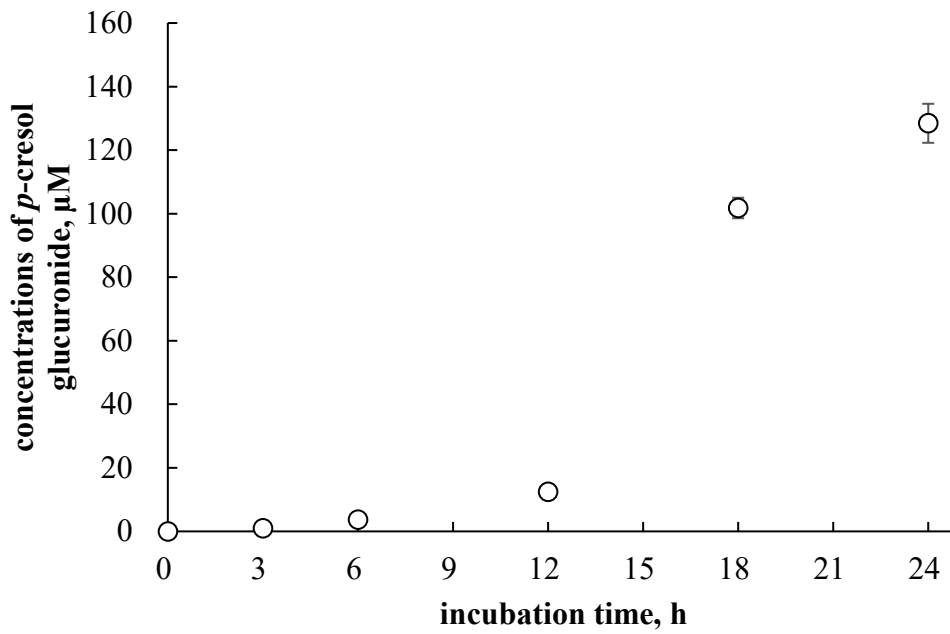
Figure 10. Concentrations of A) *p*-cresol sulfate in culture supernatant, B) *p*-cresol glucuronide in culture supernatant, C) *p*-cresol sulfate in cell lysates, and D) *p*-cresol glucuronide in cell lysates of HepaRG cells (0.4 million cells/well) treated with 1 mM *p*-cresol sulfate or *p*-cresol glucuronide from 0 to 24 hours. Concentrations of *p*-cresol sulfate and *p*-cresol glucuronide were determined in the culture supernatant and cell lysates as described in Materials and Methods. Data are presented as mean ± standard deviation from n=3 determinations.

3.6. Determination of conditions for the selective attenuation of p-cresol glucuronide formation in HepaRG cells using chemical inhibitors

The formation of *p*-cresol glucuronide in the human liver is primarily catalyzed by UGT1A6, with minor contribution from UGT1A9 (Rong and Kiang, 2020). In order to attenuate the production of *in-situ* generated *p*-cresol glucuronide, multiple inhibitors with different mechanisms of actions were utilized, including L-borneol (as UDPGA depleting agent), amentoflavone (as UGT1A6 inhibitor), and diclofenac (as UGT1A6 inhibitor) (Watkins and Klaassen, 1983,Lv et al., 2018,Uchaipichat et al., 2004,Rong and Kiang, 2020). Our preliminary experiment exposed HepaRG cells to multiple concentrations of each inhibitor alone for 24.5 hours (i.e. 0.5 hour pre-treatment and 24 hour co-treatment) and found 1 mM L-borneol (6.0±1.2%, n=9), 100 µM amentoflavone (4.2±1.5%, n=3), and 200 µM diclofenac (5.3±3.1%, n=9) to slightly increase LDH release, indicating the manifestation of low grade toxicity, compared to the vehicle control (2.1±0.8%, n=9). Therefore, our subsequent experiments tested the effects of non-toxic concentrations of L-borneol (i.e. 0.5 and 0.75 mM), amentoflavone (i.e. 10, 50, 75 µM), and diclofenac (i.e. 50 and 100 µM) on *p*-cresol glucuronide and *p*-cresol sulfate formation, with the objective to achieving a *balance* between maximum attainable inhibition of *p*-cresol glucuronide formation without affecting *p*-cresol sulfate concentrations or generating cellular necrosis (LDH). Our findings indicated that L-borneol (0.75 mM), amentoflavone (75 µM) and diclofenac (100 µM) were the optimal inhibitor conditions in this model as they selectively reduced the concentration of *p*-cresol glucuronide by 151.2±37.2 µM (i.e. by 53.9±8.2%), 147.7±62.4 µM (by 54.6±22.7%), and 63.7±44.8 µM (by 22.5±14.9%), compared to the control (i.e. 0.75 mM *p*-cresol), respectively, without affecting concentrations of *p*-cresol sulfate (Figure 11).

Figure 11A)
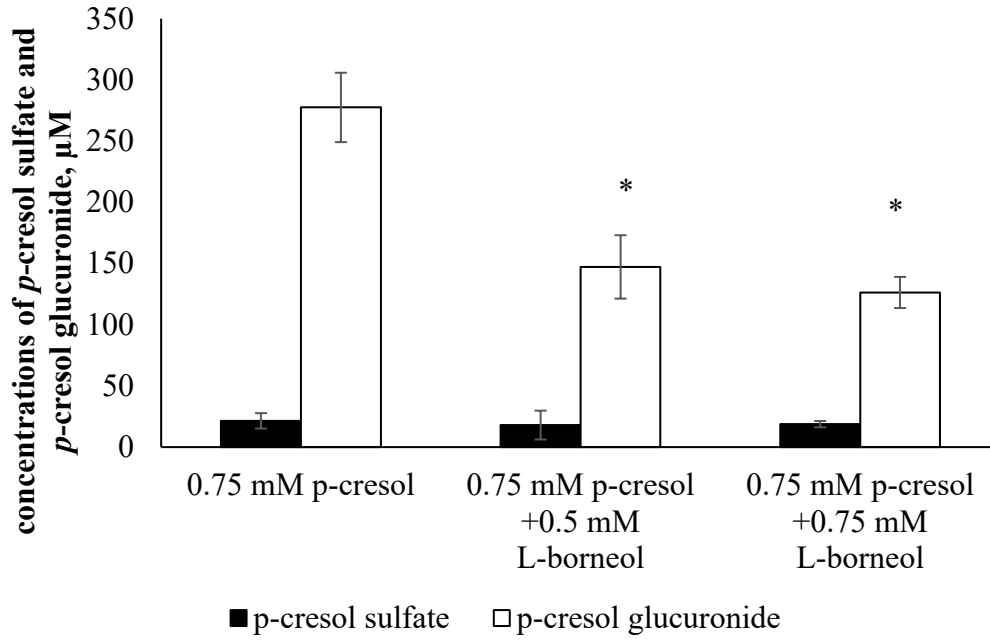
Figure 11B)
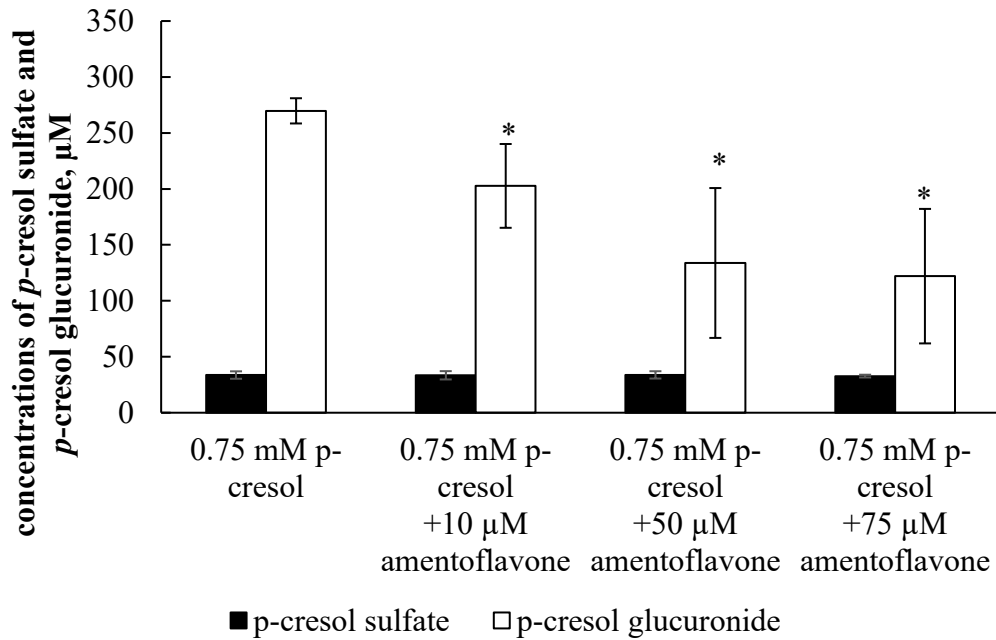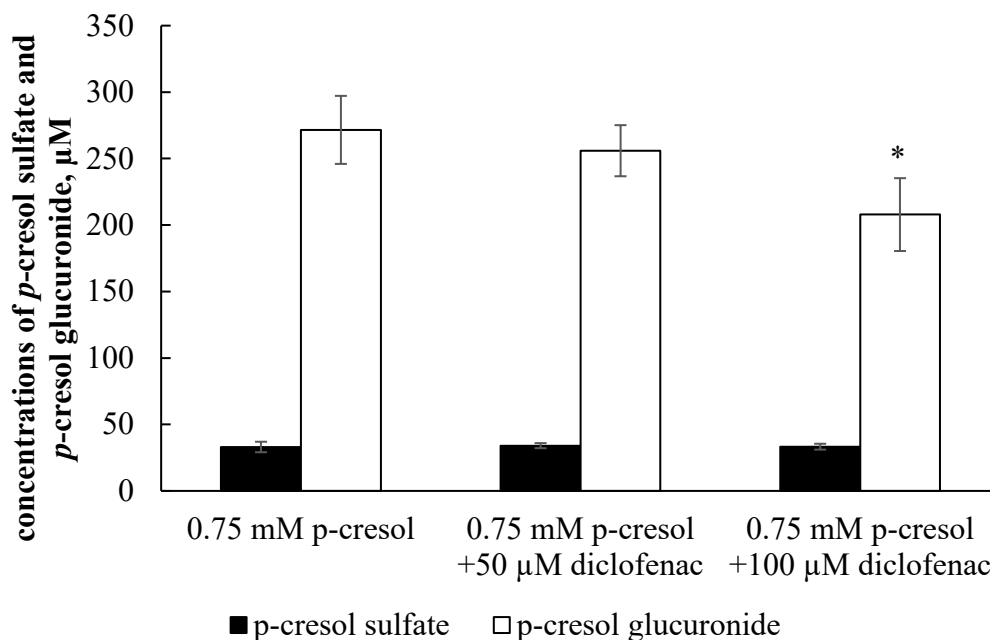
Figure 11. Effects of A) L-borneol, B) amentoflavone, and C) diclofenac on the formation of *p*-cresol sulfate and *p*-cresol glucuronide in HepaRG cells (0.4 million cells/well). Cells were pre-treated with the vehicle, and non-toxic concentrations of L-borneol (0.5, 0.75 mM), amentoflavone (10, 50, 75 µM), or diclofenac (50, 100 µM) for 30 minutes before co-treatment with 0.75 mM *p*-cresol for 24 hours. Data are presented as mean ± standard deviation from n=8 determinations. The percentages of inhibition by 0.75 mM L-borneol, 75 µM amentoflavone, and 100 µM diclofenac were 53.9±8.2%, 54.6±22.7% and 22.5±14.9% compared to the control (*p*-cresol treatment), respectively. *$p < 0.05$ versus *p*-cresol control using ANOVA on ranks. *ANOVA, analysis of variance*.

3.7. Effects of L-borneol, amentoflavone, or diclofenac on p-cresol generated cellular toxicities

To determine the role of *in-situ* generated *p*-cresol glucuronide in mediating the toxicities of *p*-cresol, cells were exposed to the vehicle, *p*-cresol, chemical inhibitor (L-borneol, amentoflavone, or diclofenac), or *p*-cresol with each individual chemical inhibitor (at non-toxic inhibitor conditions characterized to be selectively inhibitory toward the glucuronidation of *p*-cresol; please see section 3.6). The LDH marker was the primary toxicity endpoint in this mechanistic experiment because it reflected the ultimate cellular toxicity outcome in this model as evident in our time-course experiments (Figure 5) and that the chemical modulators were only optimized based on this specific marker. *p*-Cresol at 0.75 mM was utilized in this experiment as it reflected the EC_{50} values of *p*-cresol induced LDH release (Figure 4C) and generated linear metabolite formations (Figures 7&8). L-borneol (0.75 mM), amentoflavone (75 µM) or diclofenac (100 µM) alone did not affect LDH release (vs. vehicle control), but each inhibitor independently increased *p*-cresol-mediated LDH release by 28.3±5.3%, 30.0±8.2% or 27.3±6.8%, respectively, compared to *p*-cresol treatment (Figure 12). Furthermore, similar findings were observed using the DCF marker where 0.75 mM of L-borneol, which slightly reduced DCF formation, significantly increased *p*-cresol mediated DCF formation by 58.0±48.9% (Figure 13A). Although diclofenac itself did not affect DCF formation and appeared to have increased *p*-cresol mediated DCF generation, the latter effects were not statistically significant (Figure 13B). On the other hand, amentoflavone increased DCF formation by itself and L-borneol or diclofenac significantly reduced cellular GSH when used alone (please see Supplementary Material Figures S4-S6); therefore, they could not be utilized as modulators in these experiments. In contrast, amentoflavone treatment did not reduce the effects of *p*-cresol on total cellular GSH depletion (Figure 14).

Figure 12A)
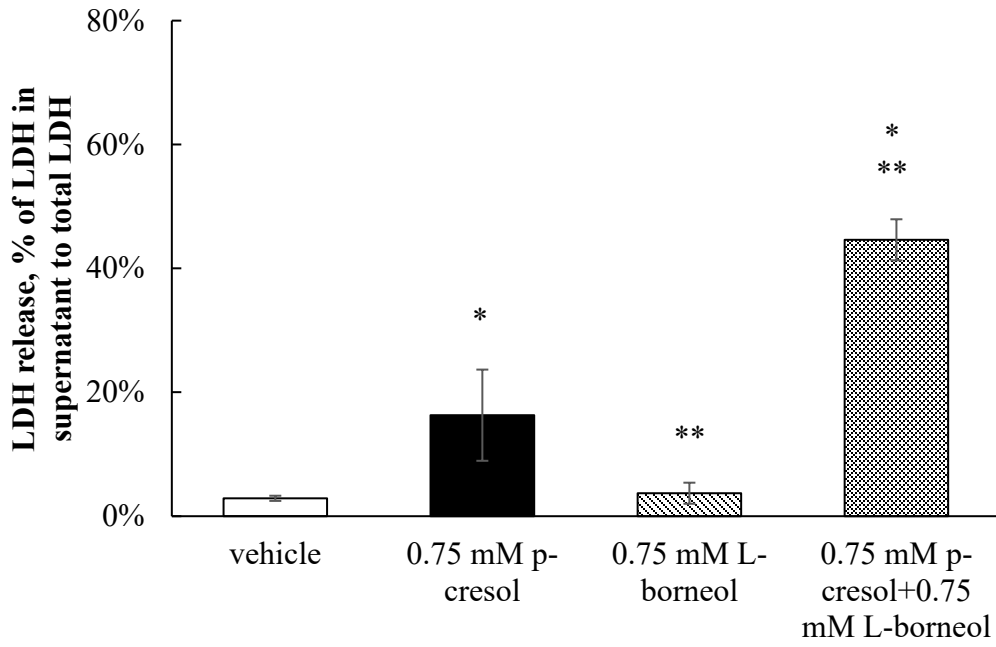
Figure 12B)
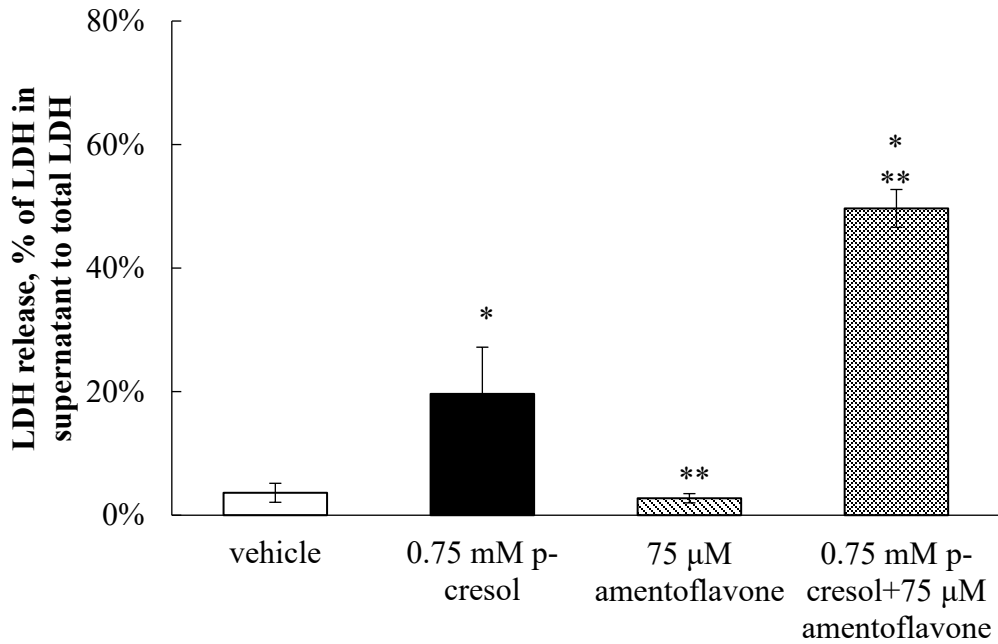
Figure 12C)
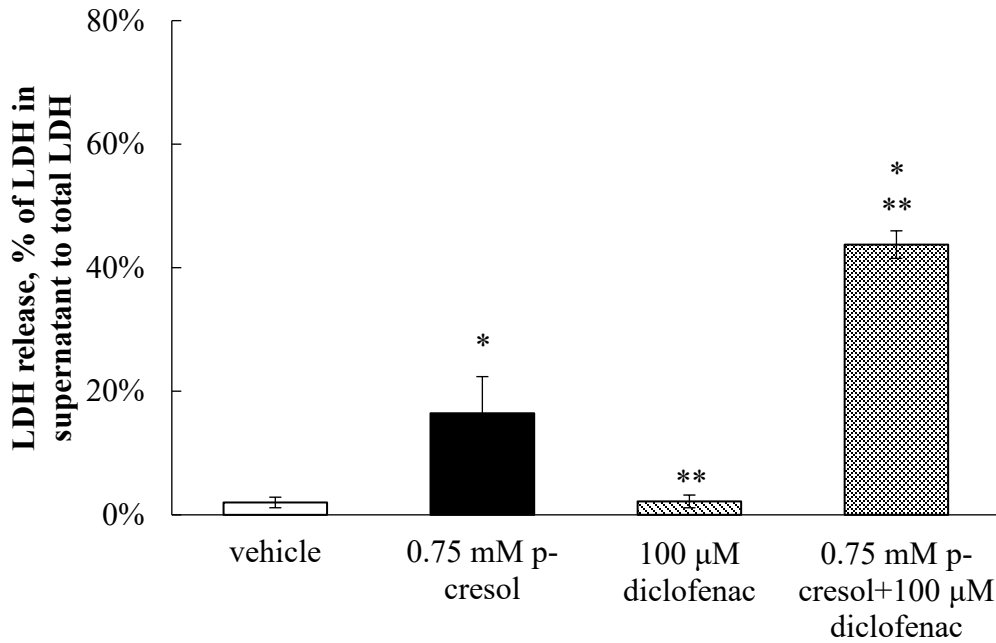
Figure 12. Effects of (A) L-borneol, (B) amentoflavone, and (C) diclofenac on *p*-cresol-mediated LDH release in HepaRG cells (0.4 million cells/well). Cells were pre-treated with vehicle or 0.75 mM L-borneol, 75 μM, amentoflavone, or 100 μM diclofenac for 30 minutes, then co-treated with vehicle or 0.75 mM *p*-cresol for 24 hours as described in Materials and Methods. LDH release was calculated as the percentage of activity in the cell supernatant to that of the sum of cell supernatant and cell lysates. Data are presented as mean ± standard deviation from n=8 determinations. *p<0.05 versus the vehicle control (i.e. the HepaRG differentiation medium) using ANOVA on ranks; **p<0.05 versus *p*-cresol. *ANOVA, analysis of variance; LDH, lactate dehydrogenase.*

Figure 13A)
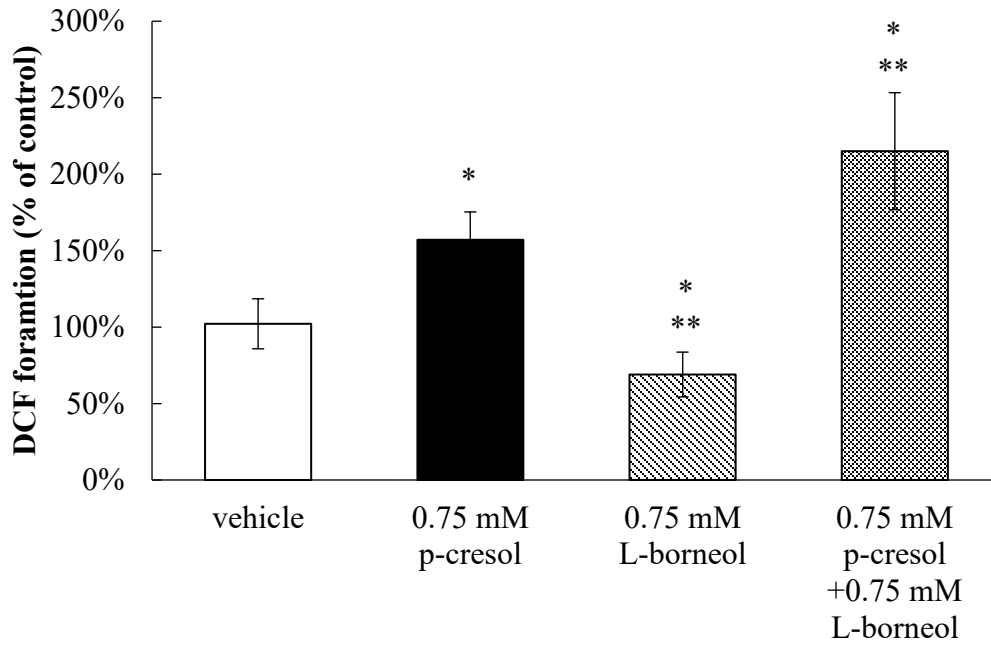
Figure 13B)
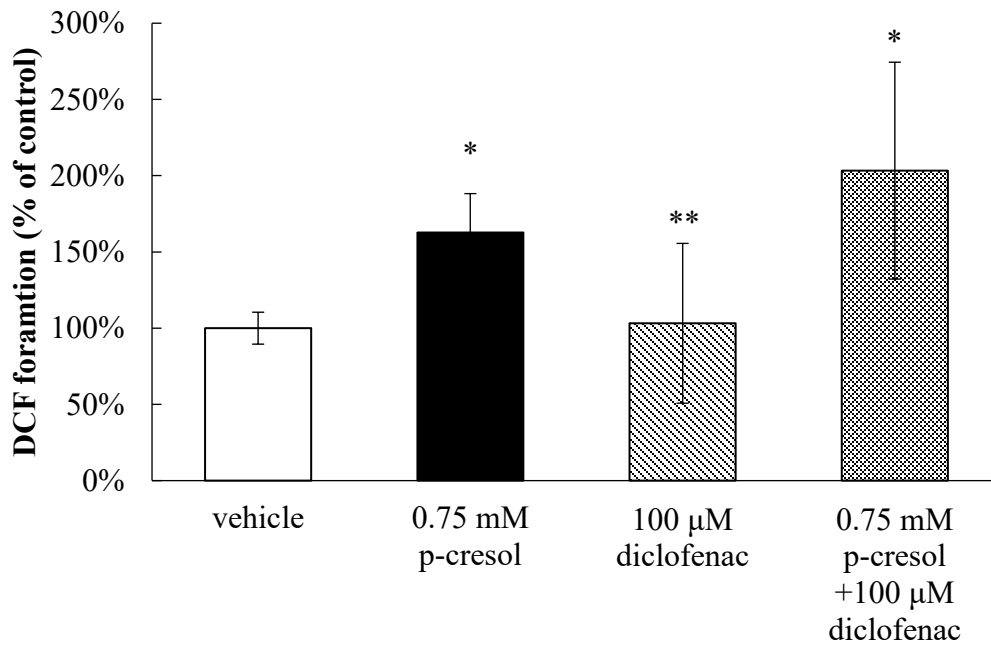
Figure 13. Effects of (A) L-borneol and (B) diclofenac on *p*-cresol-mediated DCF formation in HepaRG cells (0.4 million cells/well). Cells were pre-treated with the vehicle, 0.75 mM L-borneol, or 100 μM diclofenac for 30 minutes, then co-treated with vehicle or 0.75 mM *p*-cresol for 24 hours as described in Materials and Methods. DCF formation was expressed as the percentage of the vehicle control (i.e. the HepaRG differentiation medium). Data are presented as mean ± standard deviation from n=8 determinations. *$p<0.05$ versus the vehicle control (i.e. the HepaRG differentiation medium) using ANOVA on ranks; **$p<0.05$ versus *p*-cresol. *ANOVA, analysis of variance; DCF, 2', 7' –dichlorofluorescein.*

Figure 14
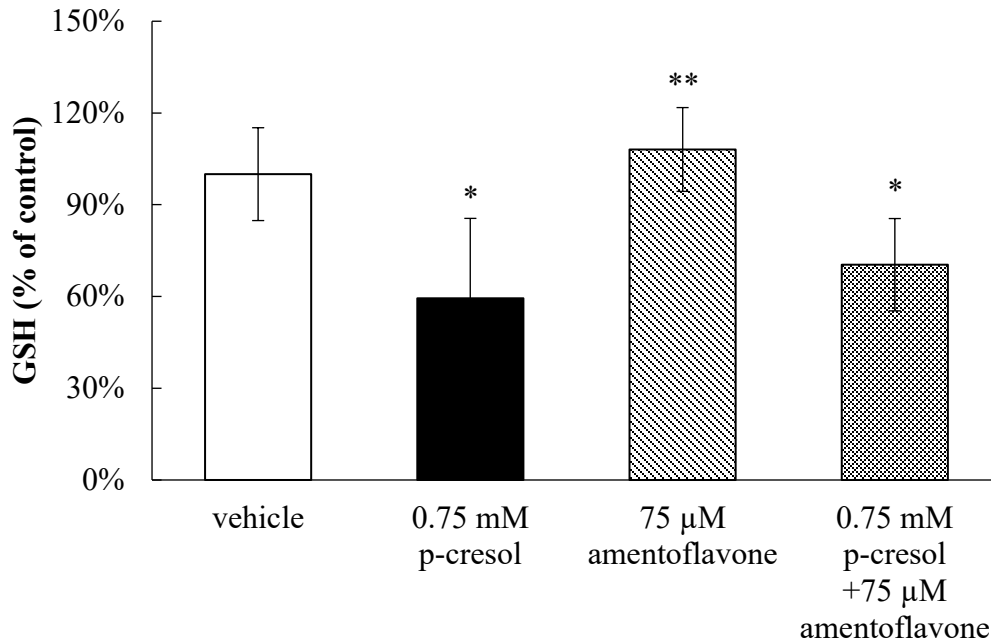
Figure 14. Effects of amentoflavone on *p*-cresol-mediated GSH depletion in HepaRG cells (0.4 million cells/well). Cells were pre-treated with the vehicle or 75 μM amentoflavone for 30 minutes, then co-treated with vehicle or 0.75 mM *p*-cresol for 24 hours as described in Materials and Methods. Total cellular GSH concentration was expressed as the percentage of the vehicle control (i.e. the HepaRG differentiation medium). Data are presented as mean ± standard deviation from n=8 determinations. *p<0.05 versus the vehicle control (i.e. the HepaRG differentiation medium) using ANOVA on ranks; **p<0.05 versus *p*-cresol. *ANOVA, analysis of variance; GSH, total cellular glutathione*

3.8. Effects of L-borneol, amentoflavone, or diclofenac on cellular p-cresol concentrations

The selective attenuation (i.e. without affecting the sulfonation) of *p*-cresol glucuronide formation resulted in increased *p*-cresol generated cellular toxicity (Figures 12-13); therefore, it was pertinent to determine if the loss of glucuronidation corresponded to increased *p*-cresol concentrations under these treatment conditions. Our findings indicated that L-borneol (0.75 mM), amentoflavone (75 µM) and diclofenac (100 µM) independently increased the concentrations of *p*-cresol (characterized in the culture supernatant) by 116.1±70.4 µM (i.e. by 209.9±50.6%,), 171.8±106.8 µM (i.e. by 212.6±31.6%), and 359.3±134.1 µM (i.e. by 356.0±57.2%), respectively (Figure 15), indicating that the inhibition of *p*-cresol glucuronidation resulted in the accumulation of the parent compound.

Figure 15A)
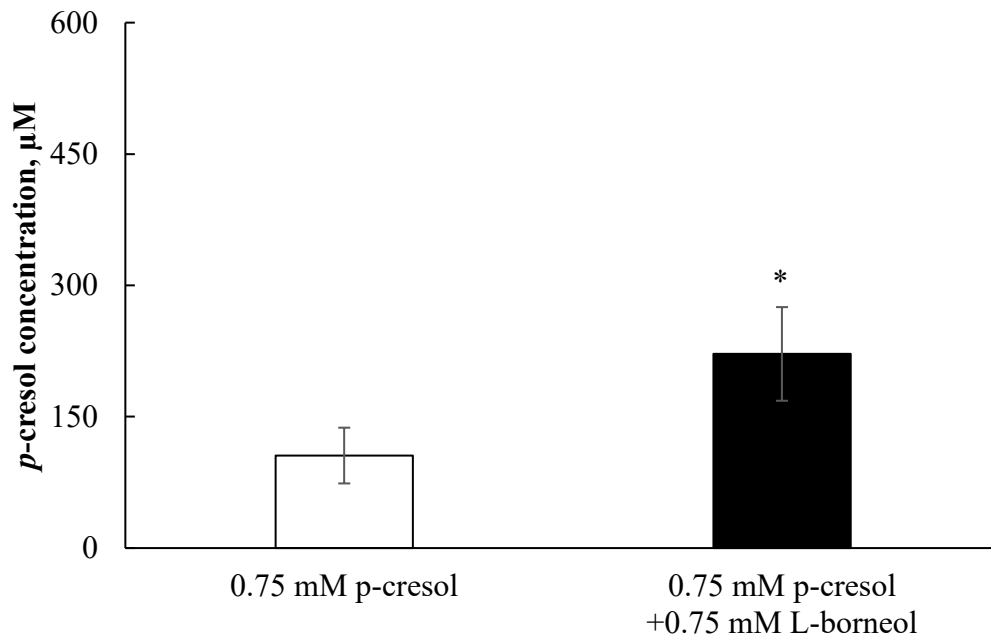
Figure 15B)
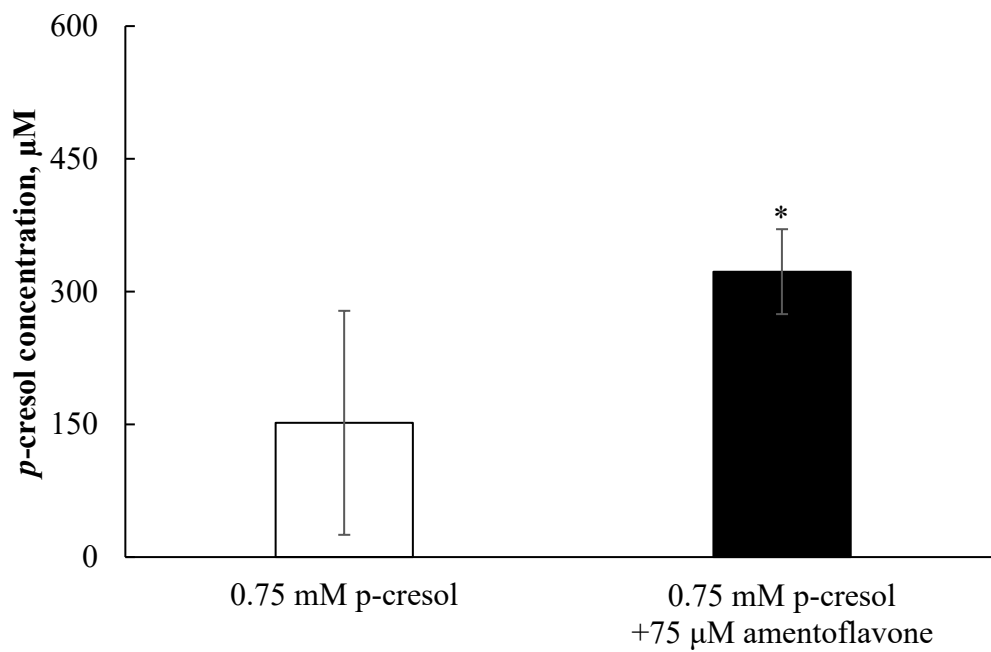
Figure 15C)
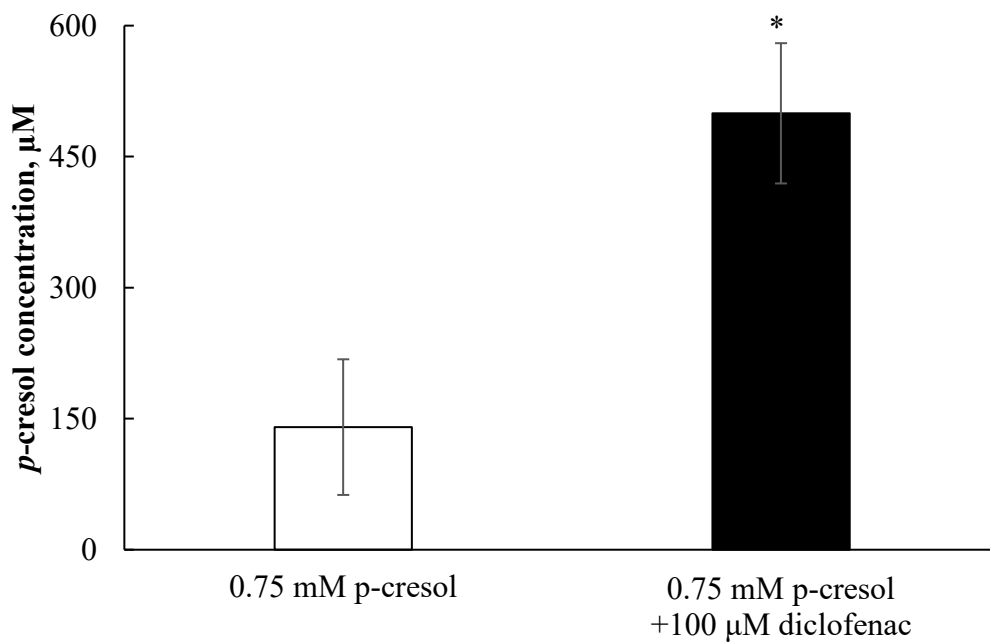
Figure 15. Effects of (A) L-borneol, (B) amentoflavone, and (C) diclofenac on p-cresol concentrations in the supernatant of HepaRG cells (0.4 million cells/well). Cells were pre-treated with 0.75 mM L-borneol, 75 μM amentoflavone, or 100 μM diclofenac for 30 minutes, then co-treated with vehicle or 0.75 mM p-cresol for 24 hours. p-Cresol concentrations were quantified as described in Materials and Methods. Data are presented as mean ± standard deviation from n=8 determinations. *p<0.05 versus p-cresol control using the Mann-Whitney rank sum test.

3.9. Validation of LC/MS/MS and UPLC assays for the quantification of p-cresol sulfate, p-cresol glucuronide, and p-cresol

The LC/MS/MS and UPLC assays used to quantify *p*-cresol sulfate, *p*-cresol glucuronide, and *p*-cresol were validated following the United States Food and Drug Administration (FDA)'s guidance document (US Food and Drug Administration., 2018). For the measurement of *p*-cresol sulfate and *p*-cresol glucuronide on the LC/MS/MS, the calibration curves were linear between 0.001 ng/mL to 80 µg/mL and 0.08 to 80 µg/mL, respectively (please see Supplementary Materials, Figures S7 & S8). The total run time was 5 minutes. The bias and imprecision of high-, mid-, and low- quality control samples were < 15% of the nominal concentrations, and that of the lower limit of quantitation quality control samples were < 20% (Supplementary Materials, Table 7). The autosampler, bench-top, freeze-thaw, and two-week storage stabilities were all within 15% with respect to bias determination using high- and low- quality control samples. (Supplementary Materials, Table 8). For the measurement of *p*-cresol on the UPLC, the calibration curve was linear between 5 to 320 µg/mL (Figure S9). The run time was 15 minutes. The bias and imprecision of all quality control samples were < 15% of the nominal concentrations (Supplementary Materials, Table 9). The autosampler, bench-top, freeze-thaw, and long-term stabilities with respect to bias determination using high- and low- quality control samples were all <15% (Supplementary Materials, Table 10). Overall, all validation parameters passed the criteria mandated by the FDA (US Food and Drug Administration., 2018).
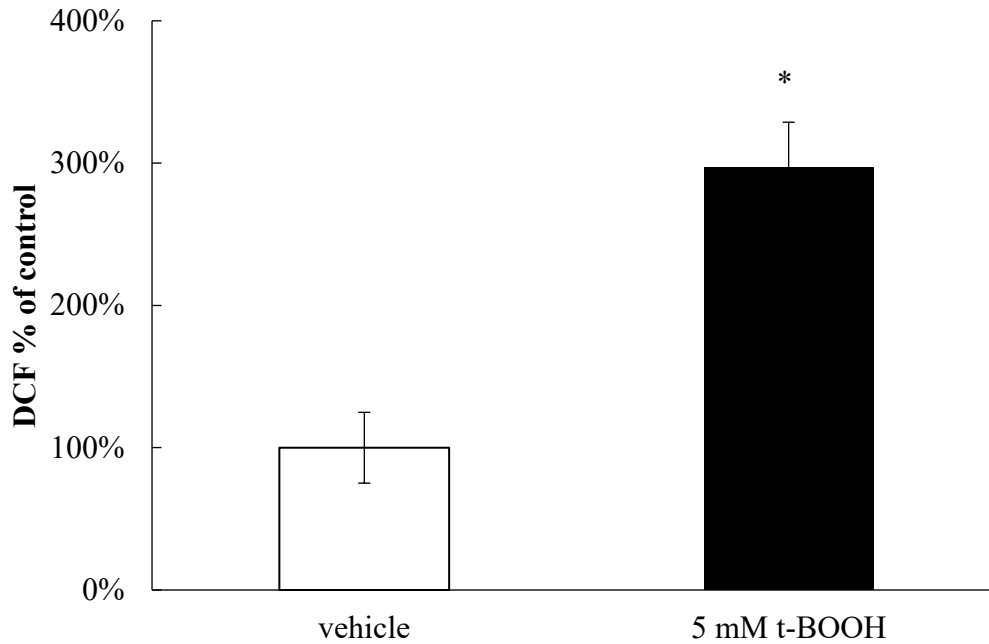
Figure S 1. Effects of t-BOOH on DCF formation in HepaRG cells (0.4 million cells/well). Cells were treated with culture medium (vehicle) or 5 mM t-BOOH for 10 minutes as described in Materials and Methods. DCF formation was expressed as percentages of the vehicle control. Data are presented as mean ± standard deviation from n=3 determinations. * $p<0.05$ versus. the vehicle control using Mann-Whitney rank sum test. *DCF, 2', 7' –dichlorofluorescein; t-BOOH, tert-Butyl hydroperoxide.*
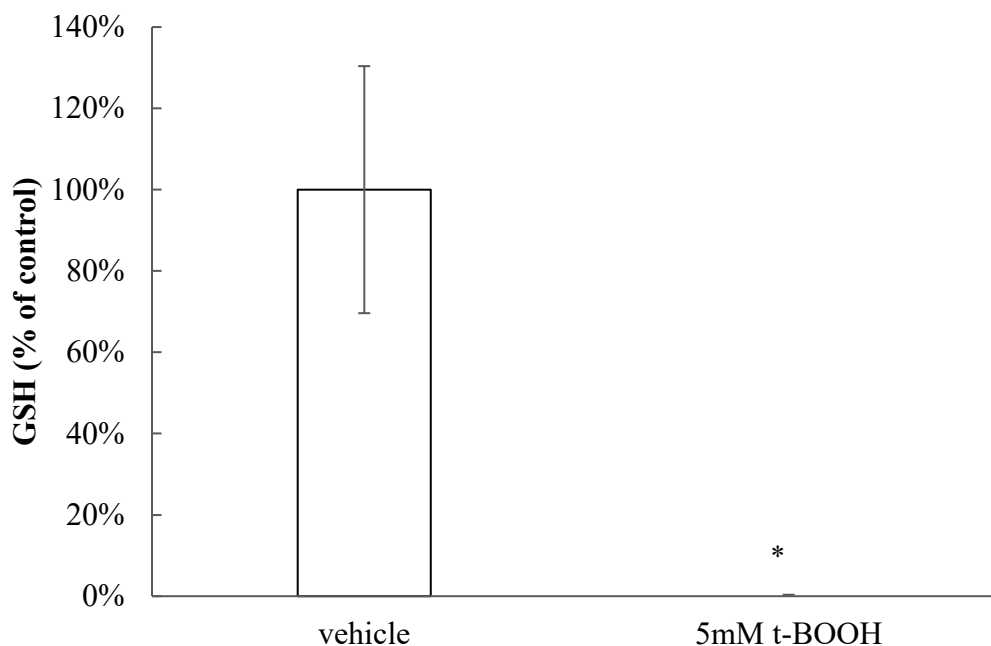
Figure S 2. Effects of t-BOOH on GSH depletion in HepaRG cells (0.4 million cells/well). Cells were treated with culture medium (vehicle) or 5 mM t-BOOH for 24 hours as described in Materials and Methods. Total cellular GSH depletion was expressed as percentages of the vehicle control. Data are presented as mean ± standard deviation from n=3 determinations. * $p < 0.05$ versus the vehicle control using Mann-Whitney rank sum test. *GSH, total cellular glutathione; t-BOOH, tert-Butyl hydroperoxide.*
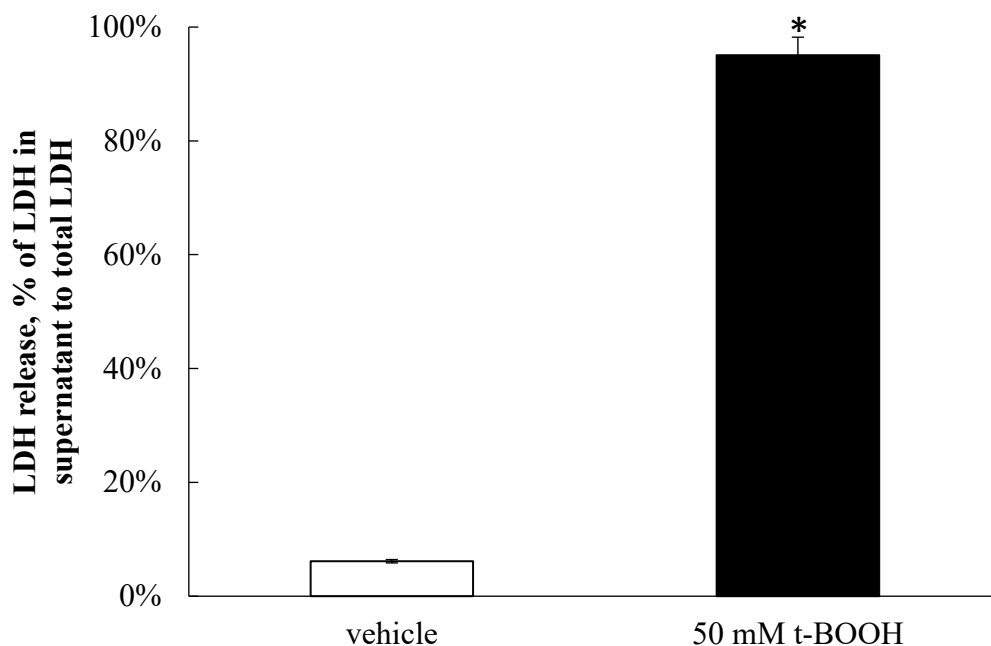
Figure S 3. Effects of t-BOOH on LDH release in HepaRG cells (0.4 million cells/well). Cells were treated with culture medium (vehicle) or 50 mM t-BOOH for 24 hours as described in Materials and Methods. LDH release was calculated as the percentage of activity in the cell supernatant to that of the sum of cell supernatant and cell lysate. Data are presented as mean ± standard deviation from n=3 determinations. * $p < 0.05$ versus the vehicle control using Mann-Whitney rank sum test. *LDH, lactate dehydrogenase; t-BOOH, tert-Butyl hydroperoxide.*
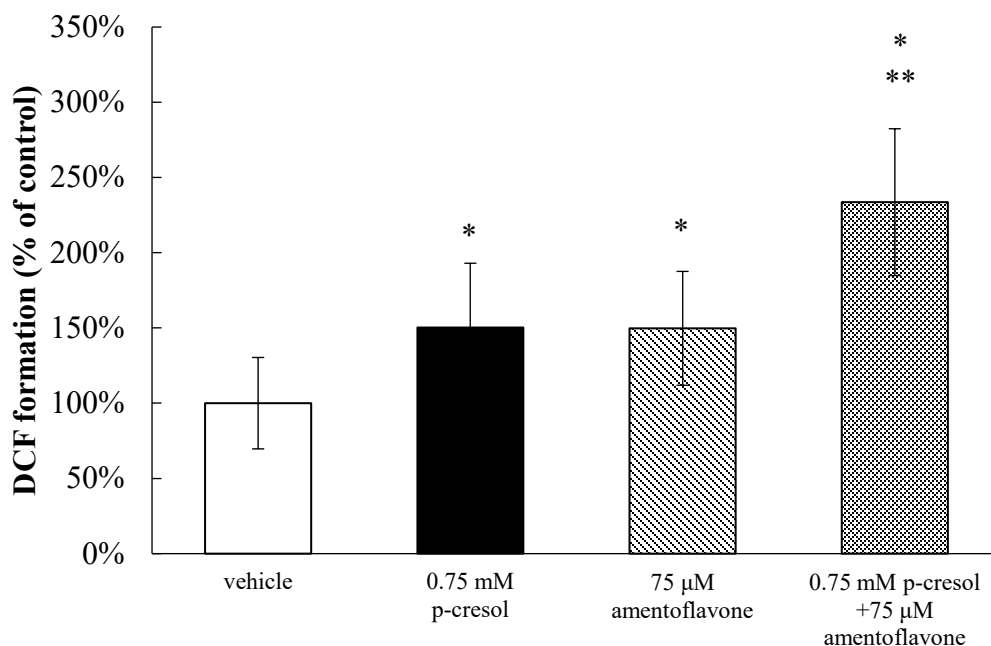
Figure S 4. Effects of amentoflavone on *p*-cresol-mediated DCF formation in HepaRG cells (0.4 million cells/well). Cells were pre-treated with the vehicle or 75 μM amentoflavone for 30 minutes, then co-treated with vehicle or 0.75 mM *p*-cresol for 24 hours as described in Materials and Methods. DCF formation was expressed as the percentage of the vehicle control (i.e. the HepaRG differentiation medium). Data are presented as mean ± standard deviation from n=8 determinations. *$p < 0.05$ versus the vehicle control (i.e. the HepaRG differentiation medium) using ANOVA on ranks; **$p < 0.05$ versus *p*-cresol. *ANOVA, analysis of variance; DCF, 2', 7' – dichlorofluorescein.*
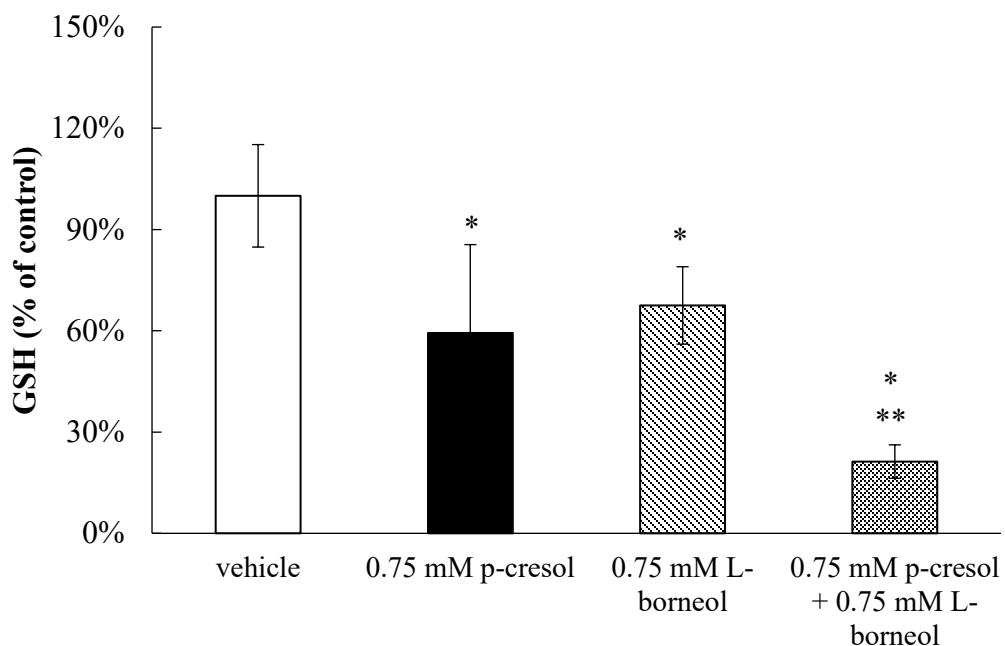
Figure S 5. Effects of L-borneol on *p*-cresol-mediated GSH depletion in HepaRG cells (0.4 million cells/well). Cells were pre-treated with the vehicle or 0.75 mM L-borneol for 30 minutes, then co-treated with vehicle or 0.75 mM *p*-cresol for 24 hours as described in Materials and Methods. Total cellular GSH concentration was expressed as the percentage of the vehicle control (i.e. the HepaRG differentiation medium). Data are presented as mean ± standard deviation from n=8 determinations. *$p < 0.05$ versus the vehicle control (i.e. the HepaRG differentiation medium) using ANOVA on ranks; **$p < 0.05$ versus *p*-cresol. *ANOVA, analysis of variance; GSH, total cellular glutathione*
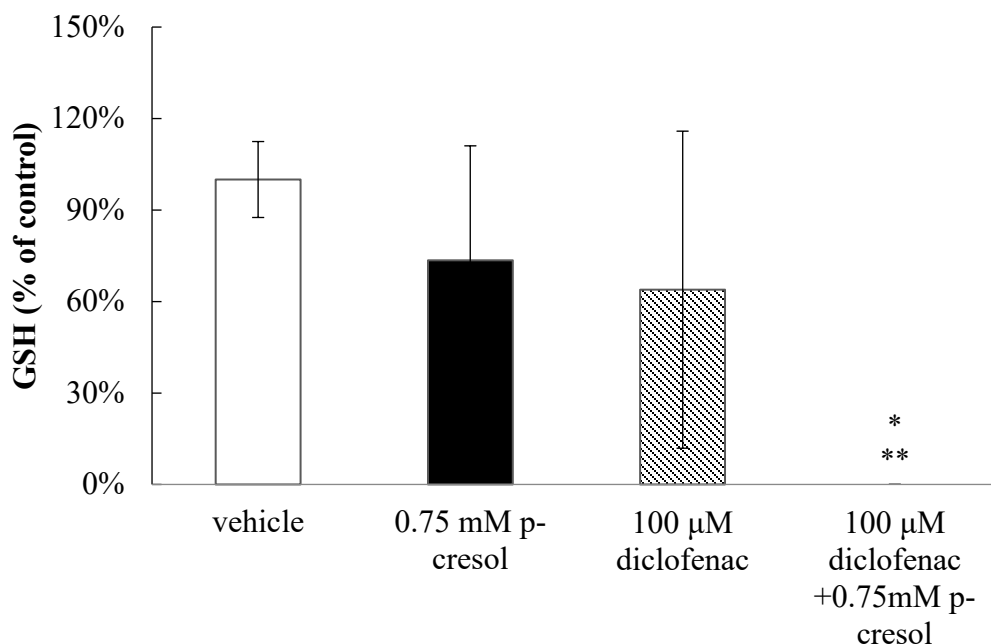
Figure S 6. Effects of diclofenac on *p*-cresol-mediated GSH depletion in HepaRG cells (0.4 million cells/well). Cells were pre-treated with the vehicle or 100 μM diclofenac for 30 minutes, then co-treated with vehicle or 0.75 mM *p*-cresol for 24 hours as described in Materials and Methods. Total cellular GSH concentration was expressed as the percentage of the vehicle control (i.e. the HepaRG differentiation medium). Data are presented as mean ± standard deviation from n=8 determinations. *p<0.05 versus the vehicle control (i.e. the HepaRG differentiation medium) using ANOVA on ranks; **p<0.05 versus *p*-cresol. *ANOVA, analysis of variance; GSH, total cellular glutathione*

Figure S 7A)
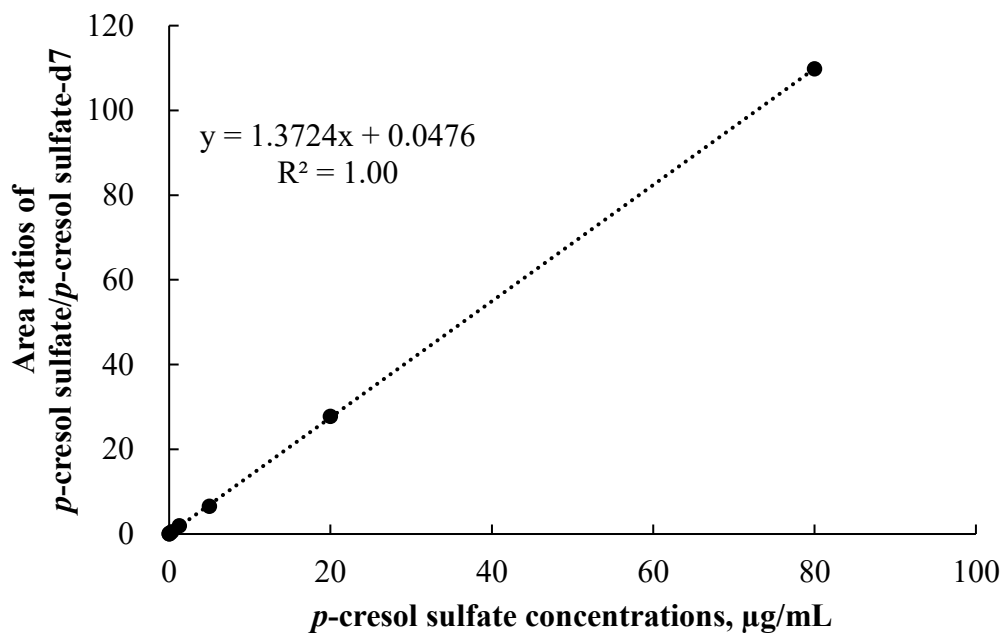
Figure S 7B)
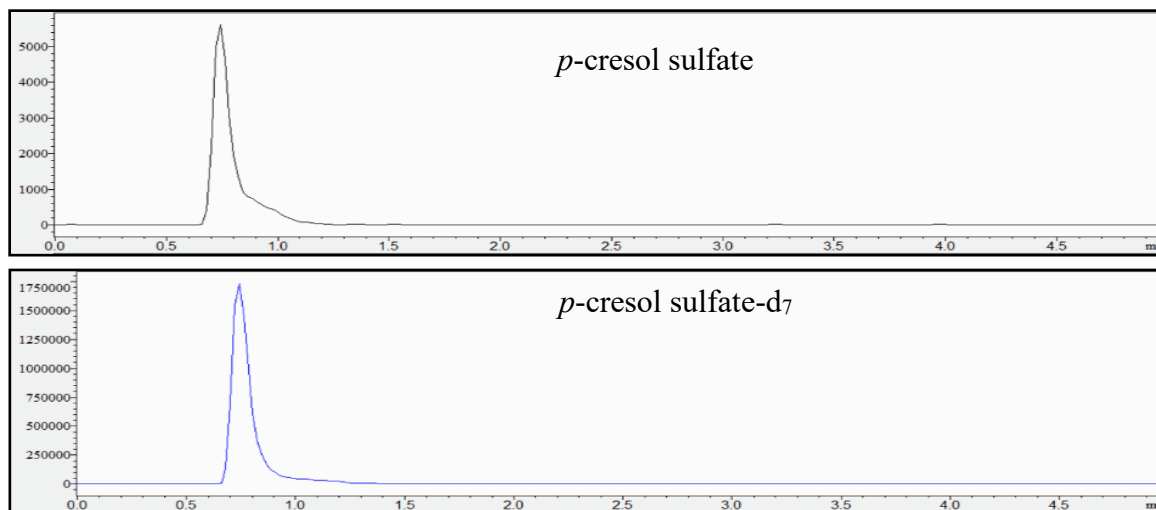
Figure S 7. A) Calibration curve of *p*-cresol sulfate based on a weighted $(1/x^2)$ least-squares regression model. **B)** Sample chromatograms of *p*-cresol sulfate and *p*-cresol sulfate-d7.

Figure S 8A)
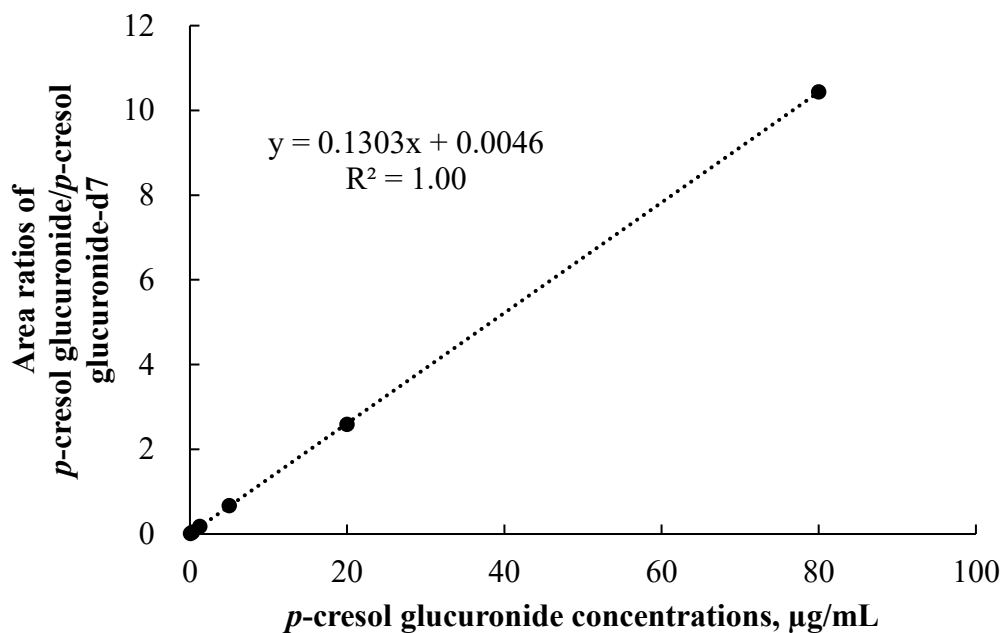
Figure S 8B)
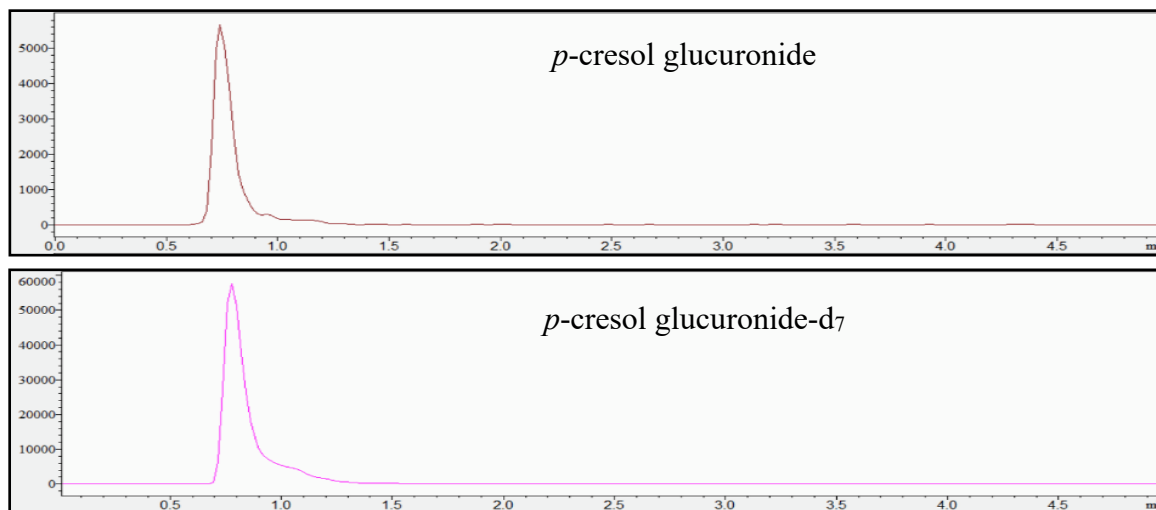
Figure S 8. A) Calibration curve of *p*-cresol glucuronide based on a weighted $(1/x^2)$ least-squares regression model. **B)** Sample chromatograms of *p*-cresol glucuronide and *p*-cresol glucuronide-d7.

Table 7. Accuracy and precision data of the UPLC/MS/MS assay for the measurement of *p*-cresol sulfate and *p*-cresol glucuronide.

	Nominal concentration	Intra-day (1), N=5		Intra-day (2), N=5		Intra-day (3), N=5		Inter-day, N=15	
p-cresol sulfate		CV (%)	Accuracy (%)	CV (%)	Accuracy (%)	CV (%)	Accuracy (%)	CV (%)	Accuracy (%)
	60 µg/mL (high QC)	4.31	102.88	5.12	95.39	7.78	98.09	6.84	106.07
	30 µg/mL (medium QC)	2.70	98.25	0.17	91.09	5.10	93.67	3.53	95.51
	0.004 ng/mL (low QC)	2.48	90.75	10.23	87.14	4.34	86.52	8.22	86.77
	0.001 ng/mL (LLOQ)	17.44	104.98	15.01	97.34	6.79	100.09	12.83	101.55
p-cresol glucuronide	60 µg/mL (high QC)	2.55	89.20	2.76	85.88	5.61	85.44	3.73	86.48
	30 µg/mL (medium QC)	3.30	95.79	6.89	92.69	5.12	88.56	4.22	92.27
	0.23 µg/mL (low QC)	7.61	113.92	1.03	111.47	0.09	108.19	2.35	111.69
	0.08 µg/mL (LLOQ)	3.47	107.59	0.87	105.21	1.41	102.04	1.53	103.94

CV, coefficient of variation; LLOQ, lower limit of quantification; QC, quality control; UPLC/MS/MS, ultra-high performance liquid chromatography-tandem mass spectrometry

Table 8. Stability data of the UPLC/MS/MS assay for the measurement of *p*-cresol sulfate and *p*-cresol glucuronide.

	p-cresol sulfate		*p*-cresol glucuronide	
Nominal concentration	0.004 ng/mL (low QC)	60 µg/mL (high QC)	0.23 µg/mL (low QC)	60 µg/mL (high QC)
	Accuracy (%)	Accuracy (%)	Accuracy (%)	Accuracy (%)
Autosampler stability	99.87	94.23	94.79	106.33
Bench-top stability	96.18	101.77	89.68	97.31
Freeze-thaw stability	113.25	91.01	92.79	104.12
Two-week stability	99.75	99.64	99.31	105.51

Various conditions were tested: 1) autosampler stability (i.e. 24 hours at 4 °C), 2) bench-top stability (i.e. 6 hours at "room temperature", 23.5 °C), 3) freeze-thaw stability (i.e. 3 cycles of freezing/thawing, where samples were frozen at -80 °C for 23.5 hours then thawed at room temperature for 0.5 hours), and 4) two-week stability (i.e. 2 weeks at -80 °C). *QC, quality control; UPLC/MS/MS, ultra-high performance liquid chromatography-tandem mass spectrometry*

Figure S 9A)
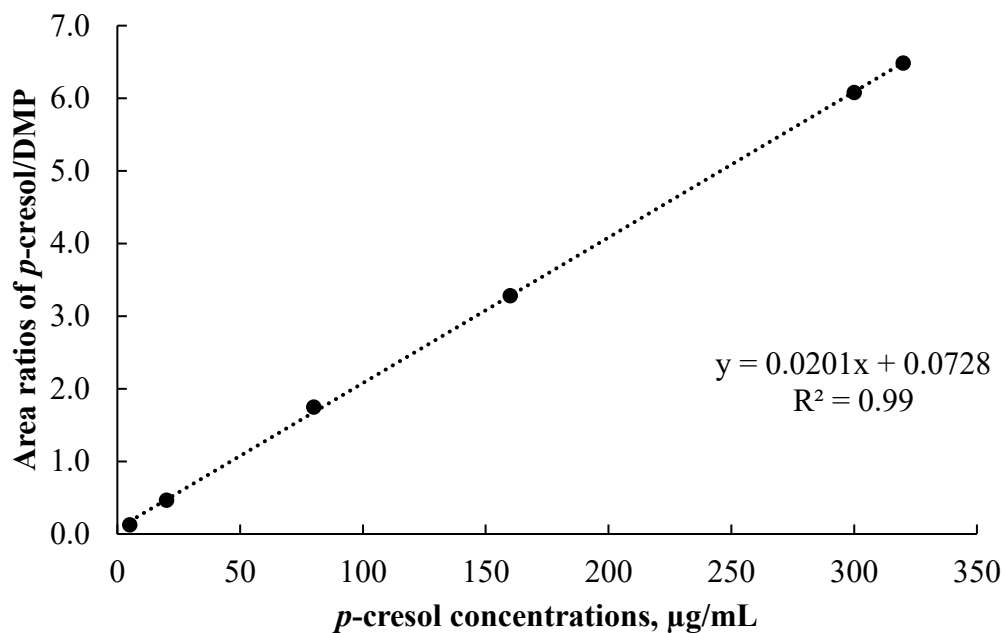
Figure S 9B)
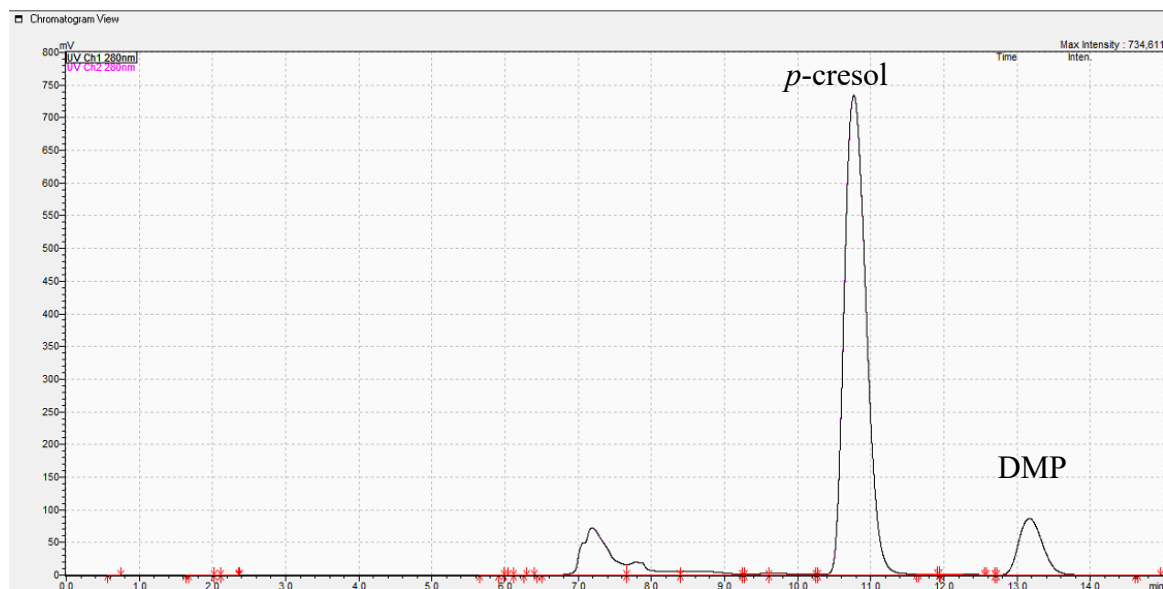
Figure S 9. A) Calibration curve of *p*-cresol based on a weighted $(1/x^2)$ least-squares regression model. **B)** Sample chromatograms of *p*-cresol and DMP. *DMP, 2,6-dimethylphenol.*

Table 9. Accuracy and precision data of the UPLC assay for the measurement of *p*-cresol.

Concentration	Intra-day (1) (N=5)		Intra-day (2) (N=5)		Intra-day (3) (N=5)		Intra-day (N=15)	
	CV (%)	Accuracy, %	CV (%)	Accuracy, %	CV (%)	Accuracy, %	CV (%)	Accuracy, %
300 µg/mL (high QC)	5.14	89.54	3.01	89.84	1.87	96.78	3.34	92.05
160 µg/mL (medium QC)	2.33	91.44	2.08	94.31	6.42	104.37	3.61	96.71
20 µg/mL (Low QC)	3.22	97.32	4.00	101.15	8.75	110.90	5.32	103.12
5 µg/mL (medium LLOQ)	6.03	102.11	5.07	102.46	8.01	98.77	6.37	101.11

CV, coefficient of variation; LLOQ, lower limit of quantification; QC, quality control; UPLC, ultra-high performance liquid chromatography

Table 10. Stability data of the UPLC assay for the measurement of *p*-cresol.

Nominal concentration (µg/mL)	20 µg/mL (low QC)	300 µg/mL (high QC)
	Accuracy (%)	Accuracy (%)
Autosampler stability (%)	85.32	93.80
Bench-top stability (%)	104.93	113.01
Freeze-thaw stability (%)	105.60	113.79
Long-term stability (%)	101.32	99.66

Various conditions were tested: 1) autosampler stability (i.e. 24 hours at 4 °C), 2) bench-top stability (i.e. 6 hours at "room temperature", 23.5 °C), 3) freeze-thaw stability (i.e. 3 cycles of freezing/thawing, where samples were frozen at -80 °C for 23.5 hours then thawed at room temperature for 0.5 hours), and 4) long-term stability (i.e. 3 days at -80 °C). *QC, quality control; UPLC, ultra-high performance liquid chromatography*

Chapter III : Discussion

1. Discussion

      p-Cresol generated concentration- and time-dependent responses on markers of oxidative stress, total cellular glutathione, and cellular necrosis in HepaRG cells. Although the toxic effects of *p*-cresol have been reported in various *in vitro* or *in vivo* animal liver models (Kitagawa, 2001,Abreo et al., 1997,Thompson et al., 1994,Thompson et al., 1996,U.S. Environmental Protection Agency, 2010), the observations of direct toxicological effects (Figures 4 & 5) in a human hepatic model are, to our knowledge, novel findings. The effects of *p*-cresol on oxidative stress induction (i.e. DCF formation, Figures 4A & 5A), glutathione depletion (Figures 4B & 5B), and cellular necrosis (Figures 4C & 5C) were consistent with its effects in other models: DCF generation in human umbilical vein endothelial and U937 mononuclear cells (e.g. (Sheu et al., 2020,Chang et al., 2014)); glutathione depletion in rat liver slices or glutathione adduct formation in GSH-fortified human liver microsomes (e.g. (Thompson et al., 1994,Yan et al., 2005)); and LDH release in rat liver slices, human colonic epithelial cells, and human bone marrow-derived mesenchymal stem cells (e.g. (Thompson et al., 1994,Wong et al., 2016,Idziak et al., 2014)). The EC_{50} values associated with *p*-cresol exposure observed of these markers in HepaRG cells (Figure 4) could be considered physiologically attainable under *toxic conditions* in humans. This is based on the documentation of relatively elevated plasma concentrations of *p*-cresol metabolites in hemodialysis patients as high as ~1.66 mM (Cuoghi et al., 2012), which may indirectly infer that similar toxic concentrations of the precursor *p*-cresol can be attainable in the liver, the primary organ of *p*-cresol metabolism and hence the direct origin of these metabolites (Gryp et al., 2017). Temporal experiments suggested the time-dependent relationships between *p*-cresol induced oxidative injury (initially evident at 6 hour of exposure), glutathione depletion (6 hour), and the

eventual manifestation of cellular necrosis (12 hours) (Figure 5). Although the role of cellular glutathione in mediating *p*-cresol induced LDH release has been demonstrated in rat liver slices (Thompson et al., 1994), further mechanistic experiments (not part of current objectives) are required to establish cause-effect relationships of these toxicity markers from *p*-cresol exposure in this human model. Furthermore, *p*-cresol was relatively more potent on each toxicity marker compared to a sample panel of toxicologically relevant protein-bound uremic solutes (Vanholder et al., 2018) (Figure 6), supporting a targeted mechanistic investigation on *p*-cresol alone in this study. The lack of substantial increases in DCF formation by indole-3-acetic acid, indoxyl-sulfate, kynurenic acid, and hippuric in our model (Figure 6A) was consistent with that reported by Weigand et al (Weigand et al., 2019) in primary cultures of human hepatocytes. However, the usage of different markers of toxicity, under different exposure conditions, in different liver cell types, and in the absence of *p*-cresol control (Weigand et al., 2019) precluded further direct comparisons between the two studies.

Both concentration-response (Figure 7) and time-course (Figure 8) experiments indicated *p*-cresol glucuronide to be the predominant, and *p*-cresol sulfate a relatively minor, *in situ*-generated metabolite from *p*-cresol exposure in HepaRG cells. While the relative concentrations of these two metabolites in our model were inconsistent with that observed in the human plasma (i.e. higher sulfate than glucuronide based on total concentrations) under typical uremic conditions (e.g. (Meert et al., 2012,Poesen et al., 2016,Liabeuf et al., 2013,Mutsaers et al., 2015,Itoh et al., 2012,Chinnappa et al., 2018)), this observation might be explained by the kinetic behaviors of the associated enzymes. Recently, it was determined that UGT1A6 was the primary enzyme contributing to the production *p*-cresol glucuronide in human liver microsomes (Rong and Kiang, 2020) and sulfotransferase (SULT)1A1 as the predominant enzyme responsible for *p*-cresol

sulfation in human liver cytosols (manuscript in preparation; (Rong, 2021)). The UGT1A6-mediated p-cresol glucuronidation in human liver microsomes (Rong and Kiang, 2020) has a much lower affinity (i.e. substrate concentration at half maximum reaction rate, $K_m=67.3\pm17.3$ μM) and higher capacity (i.e. maximum reaction rate, $V_{max}=8.5\pm0.7$ nmol/mg/min) compared to SULT1A1-mediated p-cresol sulfate formation in human liver cytosols (Rong, 2021), which is consistent with the general kinetic behaviors of UGT and SULT enzymes (James and Ambadapadi, 2013,James, 2014). Therefore, under conditions of high p-cresol concentrations required to generate toxicity in our model, the glucuronidation pathway was likely preferred over sulfonation. This general kinetic behavior is also evident in clinical studies where Poesen et al (Poesen et al., 2016) and Mutsaers et al (Mutsaers et al., 2015) both independently illustrated a shift from p-cresol sulfate to p-cresol glucuronide production in patients with more severe stages of kidney disease, possibly due to the accumulation of p-cresol. Furthermore, the level of constitutive gene expressions associated with UGT1A6 and SULT1A1 in HepaRG cells were comparable to human hepatocytes based on microarray analysis (Hart et al., 2010); thus, it was unlikely that discrepancies in metabolite generation were due to significantly altered enzyme levels in our model. However, comparisons on UGT1A6 / SULT1A1 protein expression and probe specific activities in HepaRG cells are still lacking in the literature. Collectively, these data suggested that glucuronidation is likely a quantitatively important pathway, whether it be responsible for detoxification or toxification (discussed below), in the human liver at elevated toxic concentrations of p-cresol.

Overall, our data indicated that p-cresol glucuronide or the glucuronidation pathway was likely associated with the detoxification of p-cresol in HepaRG cells, based on the following complementary findings: 1) Exogenously administered p-cresol glucuronide was significantly less toxic than p-cresol at equal molar conditions (Figure 9), despite generating much higher

concentrations of intracellular *p*-cresol glucuronide (Figure 10D) than *p*-cresol (Figure 8D). 2) Selective attenuation of *in-situ* generated *p*-cresol glucuronide (Figure 11) resulted in significantly increased LDH release from *p*-cresol exposure (Figure 12), and these findings were reproducible using multiple chemical inhibitors with independent mechanisms of actions (i.e. L-borneol being a UDPGA co-factor depletory agent; amentoflavone and diclofenac being reversible enzyme inhibitors (Watkins and Klaassen, 1983,Lv et al., 2018,Uchaipichat et al., 2004,Rong and Kiang, 2020). 3) The enhanced LDH release from reduced *in-situ p*-cresol glucuronide formation (Figure 12) was associated with the accumulation of the parent compound, *p*-cresol (Figure 15). These observations are consistent with the general assertion that the glucuronidation reaction and glucuronide metabolites are typically associated with xenobiotic detoxification (with the exception of acyl-glucuronides) (Bradshaw et al., 2020). More specifically, these findings are consistent with observations of lack of *p*-cresol glucuronide toxicity in various human cell types: *p*-cresol glucuronide (sodium or calcium salt) up to 100 µM was generally less toxic than *p*-cresol as measured by crystal violet staining in HEK293 cells (London et al., 2020); *p*-cresol glucuronide appeared less effective in reducing mitochondrial metabolism (measured by 3-4,5-dimethylthiazol-2-yl]-2,5-diphenyl tetrazolium bromide) compared to *p*-cresol in ciPTEC cells exposed to 2mM of each compound for 48 hours (Mutsaers et al., 2013); isolated whole blood from healthy human volunteers exposed to 48 mg/L of *p*-cresol glucuronide alone for 10 minutes did not exhibit enhanced oxidative burst activities compared to the vehicle control (Meert et al., 2012); and *p*-cresol glucuronide (500 µM) had minimal or no effects on mitochondrial membrane potential, lactate production, or reactive oxygen species production in primary cultures of human hepatocytes with 96 hours of exposure (Weigand et al., 2019). Although *p*-cresol glucuronide was

effective in reducing hepatocyte viability and cellular ATP (Weigand et al., 2019), comparative effects to *p*-cresol was not established in their model.

The lack of toxicity associated with *p*-cresol glucuronide formation in our model could suggest alternative pathway(s) of *p*-cresol metabolism (or metabolites) may be involved in mediating the toxicity of *p*-cresol. *p*-Cresol is known to undergo cytochrome P450 (CYP)-mediated oxidative metabolism in the production of reactive intermediates as demonstrated in GSH-fortified human liver microsomes (Yan et al., 2005) and rat liver slices (Thompson et al., 1994,Thompson et al., 1996). The potential role of toxic oxidative metabolites was demonstrated in rat liver slices where phenobarbital animal pre-treatment further increased cellular toxicity (measured by loss of potassium) associated with *p*-cresol treatment, and the effects were reduced by metyrapone, a CYP450 inhibitor (Thompson et al., 1994). The consequence of reactive intermediates was suggested by the depletion of cellular glutathione in *p*-cresol-exposed rat liver slices (Thompson et al., 1994), which was consistent with our observation of *p*-cresol associated concentration- and time-dependent reductions in total cellular glutathione in HepaRG cells (Figures 4B & 5B). However, the metabolite and *p*-cresol concentration data obtained in our model could potentially argue against the hypothesis of toxic CYP-generated metabolites (Figures 11 & 15). Specifically, the decrease in *p*-cresol glucuronide by L-borneol (a relatively specific glucuronidation inhibitor) corresponded with roughly equal increases in *p*-cresol concentration (Figures 11A & 15A), but higher increases in *p*-cresol concentrations compared to reductions in glucuronide concentrations were observed for both amentoflavone and diclofenac (Figures 11B-C & 15B-C), which may be explained by the additional inhibitory effects of these two chemicals toward CYP enzymes which may mediate the metabolism of *p*-cresol (Yan et al., 2005,Tassaneeyakul et al., 1998,Karjalainen et al., 2008,Lv et al., 2018). On the other hand,

although amentoflavone and diclofenac inhibited multiple UGT enzymes (Lv et al., 2018,Uchaipichat et al., 2004), their non-specific effects toward glucuronidation were unlikely to have contributed to this observation since *p*-cresol was primarily conjugated by a single UGT enzyme in the human liver (i.e. UGT1A6) (Rong and Kiang, 2020). However, despite potential evidence of CYP450 inhibition by amentoflavone and diclofenac in our model, all three chemical modulators affected *p*-cresol mediated LDH release to the same extent (Figure 12), suggesting that the possible CYP inhibition by amentoflavone and diclofenac did not reduce *p*-cresol generated toxicity in our model. Therefore, further control experiments (i.e. measurement of probe substrate activities and use of selective CYP450 modulators) are needed to test the toxic oxidative metabolism hypothesis. Furthermore, despite data demonstrating exogenously administered *p*-cresol sulfate was less toxic than *p*-cresol in HepaRG cells (Figure 9), *p*-cresol sulfate was consistently more toxic than the glucuronide (Figure 9). Therefore, further mechanistic experiments testing the *in situ* production of this metabolite in relation to the manifestation of toxicity are also warranted, given the significant body of literature supporting the toxicology of *p*-cresol sulfate in various clinical and experimental models (Gryp et al., 2017,Vanholder et al., 2018,Glorieux et al., 2021) (further discussed below).

The *in vitro* and/or *in vivo* evidences associated with *p*-cresol sulfate mediated cardiovascular, renal, and hepatic toxicities have been described by numerous studies in the literature (Schepers et al., 2007,Meijers et al., 2008,Gross et al., 2015,Koppe et al., 2013,Watanabe et al., 2013,Poveda et al., 2014,Mutsaers et al., 2015,Weigand et al., 2019,Lin et al., 2015,Lin et al., 2014,Rossi et al., 2014,Liabeuf et al., 2010,Wang et al., 2013,Tang et al., 2014,Chiu et al., 2010,Wang et al., 2010,Wu, I. W. et al., 2011). In our exogenously-administered *p*-cresol and *p*-cresol sulfate experiments, *p*-cresol sulfate was less toxic compared to *p*-cresol on DCF formation,

total cellular glutathione (GSH) depletion, and lactate dehydrogenase (LDH) release. However, these observations could be due to higher cellular uptake of *p*-cresol over *p*-cresol sulfate, as *p*-cresol is relatively more lipophilic compared to *p*-cresol sulfate. In terms of hepatic transporters, *p*-cresol is known not to be a substrate of organic anion-transporting polypeptide (OATP) 1B1 or OATP1B3 (Sato et al., 2014). On the other hand, to the best of our knowledge, the data on the hepatic transporters responsible for the uptake of *p*-cresol sulfate are still lacking. Assuming *p*-cresol sulfate is transported by OATP1B1 and OATP1B3 (i.e. the major uptake transporter for the liver), the HepaRG cell line only expresses minimal levels of OATP1B1 and does not express OATP1B3 (Kotani et al., 2012). Therefore, HepaRG may not be the optimal experimental model to investigate the effects of exogenously-administered *p*-cresol sulfate, due to the lack of fully-expressed uptake transporters. Alternative hepatic cellular models such as primary human hepatocytes might be more suitable to evaluate the hepatic toxicity of exogenous *p*-cresol sulfate given the existence of the full complements of hepatic uptake transporters. Furthermore, to further characterize the role of sulfonation in *p*-cresol mediated toxicity, sulfotransferase (SULT) chemical inhibitors (e.g. mefenamic acid, tolfenamic acid, and flufenamic acid (James and Ambadapadi, 2013, Rong, 2021)) selective toward SULT1A1, the primary enzyme responsible for *p*-cresol sulfonation (Rong, 2021), or siRNA knock-down of SULT1A1 gene (e.g. (Hashimoto et al., 2016)) can be utilized to modulate the *in situ* production of *p*-cresol sulfate. Furthermore, we could also attempt to induce the production of *p*-cresol sulfate using chemical inducers such as rifampin (Volpe et al., 2014) or over-expression of SULT1A1 gene by transduction. These modulation experiments can be studied in the context of already established toxicity markers in our HepaRG model (i.e. DCF formation, GSH depletion, and LDH release) or in primary cultures of human hepatocytes.

Our findings should be considered in the context of the following limitations: i) It was necessary for direct comparative purposes to utilize relatively high concentrations of metabolites or other uremic solutes in parts of our study (i.e. consistent with the approach of other investigators in this area (e.g. (Weigand et al., 2019,Mutsaers et al., 2015,London et al., 2020)), which may have exceeded typical physiological concentrations; but these were supported by further mechanistic studies involving metabolites generated *in situ* from *p*-cresol exposure (Figures 11-15). ii) While many of the recommendations proposed by the EUTox group for conducting *in vitro* studies involving uremic toxins (Cohen et al., 2007) have been considered for this investigation, some suggested conditions may not be relevant in this model. For example, our model (Guillouzo et al., 2007,Biopredic International, 2016,Gripon et al., 2002) had already been optimized for the generation of albumin and therefore it was not necessary, and may have been harmful to the cells, to add 35 g/L of albumin to the incubation medium. iii) The chemical inhibition approach in our mechanistic study was not specific (e.g. both amentoflavone and diclofenac having potential effects on CYP450 oxidation) and may have contributed to some negative findings (e.g. lack of effects of amentoflavone on *p*-cresol associated GSH reduction). However, the usage of three independent inhibitors provided consistent findings with respect to the primary toxicity endpoint (e.g. LDH release), which were supported by findings with the DCF marker, suggesting the robustness of our data. iv) The apparent lack of toxicity of exogenously administered or *in-situ* generated *p*-cresol glucuronide may be a specific observation in this hepatic model and should be further verified in other target tissues of *p*-cresol toxicity (i.e. heart and kidney cells). v) the exact reactive oxygen/nitrogen species involved and potential regulatory pathways should also be examined.

Based on our literature review, cardiac and renal tissues are the major toxicity targets of uremic toxins, which may exhibit different toxicity profiles compared to the liver. Therefore, cardiac and renal models should also be examined to fully determine the toxicology profiles of *p*-cresol, *p*-cresol sulfate, and *p*-cresol glucuronide. Given the fact that the kidney is the primary organ responsible for the excretion of *p*-cresol sulfate/glucuronide and likely one of the more important targets of toxicity based on the volume of experimental data, we will focus on the kidney model for our discussions on future experimentation. To investigate the toxicology of *p*-cresol, *p*-cresol sulfate, and *p*-cresol glucuronide, the ideal model should have adequate expressions of transporter activities (for the intracellular uptake and efflux of *p*-cresol sulfate and glucuronide) and metabolism enzyme activities (for the conjugations of *p*-cresol). With respect to transporters, *p*-cresol sulfate was identified to be a substrate for organic anion transporter (OAT)1 and OAT3 (Wu et al., 2017,Watanabe et al., 2014). In OAT1/OAT3 expressed human embryonic kidney 293 cells, the uptake of *p*-cresol sulfate can be described to be relatively high affinity and high capacity by OAT1 (i.e. half maximum substate concentration of K_m=127.8 μM, maximum uptake rate V_{max}=9.8 nmol/min/mg protein), but comparably lower affinity towards OAT3 as evident by high K_m value (i.e. >5 mM) (Watanabe et al., 2014,Wu et al., 2017). To our knowledge, the data characterizing transporters involved in the uptake of *p*-cresol glucuronide are still lacking; therefore, further experiments are needed to determine their identities. In addition, the efflux of *p*-cresol sulfate or *p*-cresol glucuronide was known to be mediated by the multidrug resistance protein 4 and breast cancer resistance protein (Mutsaers et al., 2015). On the other hand, relatively more is known of how *p*-cresol is metabolized as SULT1A1 and uridine 5'-diphospho-glucuronosyltransferase (UGT) 1A6 have recently been determined to be the major enzymes for *p*-cresol conjugation in both liver and kidney tissues, respectively ((Rong, 2021,Rong and Kiang,

2020). In order to further characterize the toxicology of *p*-cresol and its metabolites, the ideal experimental kidney cellular model must exhibit functional OAT1, OAT3, multidrug resistance protein 4, and breast cancer resistance protein, SULT1A1, UGT1A6, and other Phase I, Phase II, and Phase III enzymes normally expressed in primary human kidney epithelial tubular cells.

Conditionally immortalized human renal proximal tubule epithelial cells (ciPTEC) were obtained from renal cell materials collected in the urine from a healthy donor. In its constitutive form, it lacks the stably expressed OAT1 and OAT3 transporter activities, therefore this model was further transfected into two additional cell lines overexpressing OAT1 and OAT3 transporter activities (i.e.ciPTEC-OAT1 and ciPTEC-OAT3) (Bajaj et al., 2018,Nieskens et al., 2016). In addition, ciPTEC also expresses other renal transporters such as organic cation transporter 2, p-glycoprotein, breast cancer resistance protein, multidrug and toxin extrusion proteins, and multidrug resistance proteins 4 (Bajaj et al., 2018). Furthermore, mRNA expressions of major metabolism enzymes were also evident in the differentiated ciPTEC cell line (Mutsaers et al., 2013), such as SULT1A1, UGT1A6, UGT1A9, in addition to the full complements of CYP450 enzymes which are collectively responsible for the conjugation or oxidation of *p*-cresol. However, functional activity assays for many of these enzymes still remain to be characterized.

The usage of the ciPTEC model for investigating xenobiotic-induced toxicity based on drug uptake and/or drug metabolism is already documented in the literature. For example, Mutsaers et al. utilized ciPTEC cells to study the toxicities of *p*-cresol, *p*-cresol sulfate, and *p*-cresol glucuronide (Mutsaers et al., 2013). In their study, ciPTEC cells were incubated with 2 mM *p*-cresol, *p*-cresol sulfate, and *p*-cresol glucuronide for 48 hours at 37 °C, and cytotoxicity was determined by the 3-(4,5-dimethylthiazol-2-yl)-2,5-diphenyltetrazolium bromide (MTT) assay. It was found that *p*-cresol, *p*-cresol sulfate, and *p*-cresol glucuronide significantly decreased MTT

by 28%, 21% and 14%, respectively (p<0.005). Moreover, Mihaila et al. used ciPTEC cells to study the inhibition of OAT1 mediated substrate uptake (Mihaila et al., 2020). ciPTEC-OAT1 cells were incubated with fluorescein (probe marker) and indoxyl sulfate (110 μM), kynurenic acid (1 μM), or *p*-cresol sulfate (125 μM) (as inhibitors). The uptake of fluorescein was significantly decreased to 46.7% of the inhibitor-free control by *p*-cresol sulfate, indicating that *p*-cresol sulfate is likely to inhibit OAT-1 mediated excretion (which may lead to accumulation of toxic compounds in the cells).

Primary cultures of kidney cells express OAT1 and OAT3 and other renal transporters such as p-glycoprotein, breast cancer resistance protein, multidrug resistance proteins 2, and organic cation transporter 3 (Bajaj et al., 2018). Primary renal cells also express metabolism enzymes such as CYP450, uridine 5'-diphospho-glucuronosyltransferase, and sulfotransferases (Bajaj et al., 2018). However, primary kidney cells are generally difficult (scarcity and very costly) to obtain compared to ciPTEC cells, and therefore may not be suitable for academic research. However, the usage of primary cultures of human kidney cells can allow one to characterize inter-individual (physiological, genetic, intrinsic) variability, which is a limitation of immortalized cell lines such as the ciPTEC cells.

To further characterize the toxic effects of *p*-cresol, *p*-cresol sulfate, and *p*-cresol glucuronide in a human kidney experimental model, ciPTEC cells can be utilized as discussed above. On one hand, assuming OAT1 and/or OAT3 are responsible for the transmembrane uptake of *p*-cresol sulfate and *p*-cresol glucuronide, the uptake profiles (i.e. kinetics) can be characterized in ciPTEC, ciPTEC-OAT1 overexpressed, and ciPTEC-OAT3 overexpressed cell lines. We anticipate that ciPTEC-OAT1/3 overexpressed cells would show significantly higher intracellular concentrations of *p*-cresol sulfate and/or *p*-cresol glucuronide compared to the control ciPTEC

cells. Subsequently, we can attempt to identify the correlation between *p*-cresol sulfate / glucuronide uptake and the generation of toxicities (e.g. DCF, GSH, and LDH assays as already established in my thesis). In addition, the intracellular uptakes of *p*-cresol sulfate or *p*-cresol glucuronide can be mechanistically modulated by OAT1 and/or OAT3 inhibitors (e.g. para-aminohippuric acid, estrone sulfate, and probenecid (Nieskens et al., 2016)), and the effects of these modulations on the manifestation (or reduction) of cellular toxicities can be characterized. Furthermore, enzyme kinetic experiments should be conducted in ciPTEC cells to determine the *in situ* production of *p*-cresol sulfate and *p*-cresol glucuronide formation from *p*-cresol, as significant concentrations of *p*-cresol is still evident in the renal tissue (Ikematsu et al., 2019). Similar to our approach documented in Chapter II, one can further mechanistically modulate (through inhibition, gene-knock down, induction, or over-expression) the metabolism enzymes in order to determine the role of *in situ*-generated *p*-cresol metabolites in the manifestation of toxicities in ciPTEC cells. To our knowledge, these will be novel investigations that will likely have impacts to this field.

There is *in vitro* evidence that *p*-cresol sulfate and *p*-cresol glucuronide induce oxidative stress in human cellular models. Schepers et al. (Schepers et al., 2007) investigated the oxidative burst activities of *p*-cresol sulfate in human leucocytes using dihydrorhodamine measured by flow cytometry. *p*-Cresol sulfate was identified to significantly increase the oxidative burst activities of PMA-stimulated human granulocytes ($p < 0.05$). In addition, Meert et al. (Meert et al., 2012) studied the oxidative burst activities of *p*-cresol sulfate and glucuronide in human leucocytes using the same assay, where *p*-cresol sulfate increased the oxidative burst activities in all baseline leucocytes ($p < 0.01$), N-formyl-methionine-leucine-phenylalanine (fMLP)-stimulated lymphocytes ($p < 0.01$), E. coli-stimulated monocytes ($p < 0.05$), and phorbol-12-myristate-13-acetate (PMA)-stimulated

monocytes and granulocytes (p<0.05). On the other hand, *p*-Cresol glucuronide alone had no effects on oxidative burst activities in all baseline or stimulated leucocytes. However, the combinations of *p*-cresol sulfate and glucuronide increased oxidative burst activities in all conditions except for E. coli-stimulated lymphocytes, compared to the control; and the combination of both compounds also increased the activities in all baseline leucocytes and fMLP-stimulated granulocytes compared to *p*-cresol sulfate alone. Furthermore, *p*-cresol sulfate increased oxidative stress in human kidney 2 proximal tubular epithelial cells (as measured by DCFDA and Amplex Red assays) (Watanabe et al., 2013), human umbilical vein endothelial cells, and isolated human vascular smooth muscle cells (as measured by DCFDA assay) (Gross et al., 2015). With respect to clinical study, Rossi et al. (Rossi et al., 2014) identified that increased free *p*-cresol sulfate serum concentration was associated with decreased levels of glutathione peroxidase (p=0.022), a marker for elevated oxidative stress in the clinic. Overall, the markers utilized to quantify oxidative stress *in vitro* are overall universal indicators without specificity (to be discussed further below), and, only limited clinical data are available. Moreover, to our knowledge, very little data are available on *p*-cresol and its *in situ* generated metabolites in the generation of oxidative stress, as demonstrated in our data presented in Chapter II.

In our study and many others (summarized above), oxidative stress was determined by the DCFDA marker. The non-fluorescent DCFDA is first converted to dichlorofluorescin (DCFH) by esterases within the cell. Subsequently, DCFH reacts with a variety of reactive oxygen species to form the fluorescent DCF (Marchesi et al., 1999). However, DCFDA is a non-specific marker because it can react with free radicals including nitric oxides and reactive oxygen species such as peroxyl, alkoxyl, $NO_2\cdot$, carbonate, $OH\cdot$, and peroxynitrite (Fuloria et al., 2021,Halliwell and Whiteman, 2004). On the other hand, DCFH is not sensitive to hydrogen peroxide (Halliwell and

Whiteman, 2004). Moreover, the intermediate DCFH can also generate fluorescence signal in the absence of reactive oxygen species (Halliwell and Whiteman, 2004), and this is evident by data illustrating high concentrations of DCFDA and exposure to light could cause artefactual readings. In addition to the DCFDA assay, several other approaches can be used to measure reactive oxygen species: Amplex red can be used to measure hydrogen peroxide (Fuloria et al., 2021); chemiluminescence analysis (using dihydrorhodamine to determine $^{\cdot}OH$, $ONOO^-$, NO_2^-, and peroxidase derived species; dihydroethidine to determine O_2^- ; and luminol to determine $^{\cdot}OH$ and $ONOO^-$, (Halliwell and Whiteman, 2004)) can be utilized; electro-chemical biosensing (using polyaniline-sulfonic acid or cytochrome-c layers over gold wire electrode) may also be utilized to measure $O_2^{\cdot-}$, and chromatography (using stabilization agents such as dimethyl sulfoxide, salicylic acid, or benzoic acid) can be employed to measure $^{\cdot}OH$, and spectrophotometry (using cytochrome c, nitro blue tetrazolium, aconitase, boronates, or diaminobenzidine) may be used to measure hydrogen peroxide and $O_2^{\cdot-}$ (Fuloria et al., 2021).

Furthermore, GSH homeostasis can also be utilized as an indicator of oxidative stress. The following enzymes are involved in GSH formation, GSH conjugation, and GSH redox cycling (Aquilano et al., 2014). Briefly, GSH is a tripeptide complex of glutamate, cysteine, and glycine. Its biosynthesis is a 2-step reaction requiring energy provided by ATP. In the first step, glutamate and cysteine are combined together catalyzed by glutamate-cysteine ligase (GCL); later on, glycine binds to the complex of glutamate and cysteine under the function of glutathione synthase (GS), in the formation of GSH. Overall, GSH exhibits antioxidant properties by conjugating to electrophilic compounds, and this process is primarily mediated by glutathione-S-transferase (GST). In addition, GSH redox cycling as indicated by the ratio of reduced to oxidized GSH (i.e. glutathione disulfide [GSSG] or glutathionylated-cysteine derivative [GSSR]) can provide further

114

indication of oxidative stress (Aquilano et al., 2014). GSH redox cycling is a process that describes the conversions between reduced GSH to GSSG and/or GSSR (i.e. the oxidized forms of GSH). Under normal physiological conditions, GSH mostly exists in the reduced form; once encountering electrophilic compounds/species (e.g. H_2O_2), the reduced GSH undergoes GSH peroxidase (GPX)-mediated reaction in the formation of GSSG and/or GSSR (in the presence of "reactive cysteinyl residue"). Subsequently, GSSG and GSSR can be recycled back to reduced GSH by the GSH reductase (GR) and thioredoxin (Trx)/glutaredoxin (Grx) system, respectively, which requires nicotinamide adenine dinucleotide phosphate [NADPH) as a cofactor (Aquilano et al., 2014). As the antioxidant functions of GSH in detoxifying reactive compounds are dependent on complicated series of enzymatic reactions, the oxidative stress can be evaluated based on the enzyme expressions of these associated enzymes.

With respect to the defense mechanisms toward oxidative stress, the nuclear factor erythroid 2-related factor 2 (Nrf2) regulation pathway has been widely investigated (Ma, 2013). However, to the best of our knowledge, direct evidence indicating effects of p-cresol or its metabolites on the Nrf2 pathway is still lacking. Under normal conditions, Nrf2 is locating in the cytoplasm, bound to Kelch-like ECH-associated protein 1 (Keap1), in the form of a stable, inactivated complex (Saito, 2013). In the presence of reactive oxygen/nitrogen species (e.g. induced uremic toxins), the Nrf2-Keap1 complex undergoes conformation change, resulting in the dissociation of Keap1 from the complex and the activation of the Nrf2 (Saito, 2013). Subsequently, the activated Nrf2 translocates into the nucleus and binds to antioxidant/electrophile responsive element (ARE/EpRE) (Saito, 2013). Upon binding, the downstream "antioxidant and detoxifying molecules" including NAD(P)H:quinone oxidoreductase 1 (NQO1), heme oxygenase-1, GST,

multidrug resistance proteins, GLC, and CYP450, can be upregulated to counteract the effects of oxidative stress (Saito, 2013).

To investigate the effects of p-cresol and its metabolites in the Nrf2 regulation pathway, we first need to determine which specific reactive oxygen species are associated with p-cresol and its metabolites in HepaRG and ciPTEC cells. Chemical approaches such as dihydrorhodamine (to determine ˙OH, ONOO$^-$, NO$_2^-$, and peroxidase derived species), dihydroethidine (to determine O$_2^-$), or luminol (to determine ˙OH and ONOO$^-$) can be utilized to identify the specific reactive species involved in the oxidative stress mediated by p-cresol and its metabolites (Halliwell and Whiteman, 2004). Furthermore, the relative effects of p-cresol, p-cresol sulfate, and p-cresol glucuronide in the generation of reactive oxygen/nitrogen species can be characterized in HepaRG and/or ciPTEC cells, using exogenously-administered or *in-situ* generated p-cresol sulfate and p-cresol glucuronide. Specifically, oxidative stress can be assessed after directly administrating p-cresol, p-cresol sulfate, or p-cresol glucuronide; and chemical inhibitors or inducers for sulphation or glucuronidation can be utilized to modulate the production of p-cresol sulfate or p-cresol glucuronide in HepaRG and ciPTEC cells. Based on the known metabolic enzymes (i.e. SULT1A1 and UGT1A6 in the formation of p-cresol sulfate and p-cresol glucuronide, respectively) involved in the metabolism of p-cresol (Rong, 2021,Rong and Kiang, 2020), mefenamic acid, tolfenamic acid, and flufenamic acid can be utilized as p-cresol sulphation inhibitors; rifampin can be utilized as p-cresol sulphation/glucuronidation inducer; L-borneol, amentoflavone, and diclofenac can be utilized as p-cresol glucuronidation inhibitors; and phenobarbital can be utilized as a p-cresol glucuronidation inducer. In addition to chemical modulators, one can also knock-down or over-express SULT1A1 and UGT1A6 genes, in order to test the effects on the generation of specific oxygen and nitrogen species.

Furthermore, the roles of *p*-cresol, *p*-cresol sulfate, and *p*-cresol glucuronide in the activation of Nrf2 regulatory pathway can be characterized in human *in vitro* models as described above. First, the activation of Nrf2 regulation pathway can be verified using the electrophoretic mobility shift assay, by determining the binding of Nrf2 with ARE (Korashy and El-Kadi, 2005). Furthermore, the expressions of the downstream genetic markers can be evaluated using reverse transcription polymerase chain reaction (RT-PCR) assays. For example, increased expression of NQO1, heme oxygenase-1, GST, multidrug resistance proteins, GLC, or CYP450 might indicators illustrating the successful activation of this oxidative stress defense regulation pathway. In addition, the involvement of *p*-cresol or its metabolites in the Nrf2 pathway can be further tested in Nrf2 knock-out models or cells treated with Nrf2 enhancers/activators (e.g. The toxicity of acetaminophen was determined in Nrf2 knock-out mouse model (Ma, 2013) and dimethyl fumarate can be used as an example of Nrf2 activator (Saito, 2013)). These experiments are expected to contribute novel knowledge to the literature.

2. Overall Conclusion

Overall, the initially proposed four objectives as stated in **Chapter I** have been systematically tested in this thesis. In terms of *"Objective 1: To characterize the concentration- and temporal- effects of p-cresol on markers of oxidative stress (2', 7'-dichlorofluorescein, DCF formation), total cellular glutathione (GSH) depletion, and lactate dehydrogenase (LDH) release in HepaRG cells"*, *p*-cresol caused both concentration- and time-dependent responses on DCF formation, GSH concentration, and LDH release in HepaRG cells at potentially toxicologically relevant conditions. With respect to *"Objective 2: To compare the effects of p-cresol and other protein bound uremic toxins on toxicity markers in HepaRG cells"*, *p*-cresol was demonstrated to be relatively more toxic than other tested uremic toxins on the above toxicity markers. In response to *"Objective 3: To determine the metabolic activities of HepaRG cells in the production of major p-cresol conjugated metabolites (i.e. p-cresol sulfate and p-cresol glucuronide)"*, the generations of *p*-cresol sulfate and *p*-cresol glucuronide were both concentration- and time-dependent in HepaRG cells; in addition, *p*-cresol glucuronide was identified to be the predominant metabolite of *p*-cresol under our experimental conditions in HepaRG cells. Lastly, regarding *"Objective 4: To characterize the effects of exogenously-administered and in-situ generated p-cresol metabolites (i.e. p-cresol glucuronide) in the manifestation of toxicities in HepaRG cells"*, although the exogenous administration of *p*-cresol sulfate and *p*-cresol glucuronide resulted in relatively high intracellular concentrations of these metabolites, both metabolites were significantly less toxic compared to *p*-cresol at equal-molar conditions. Moreover, selective inhibition of the glucuronidation pathway (without affecting *p*-cresol sulfate formation, while increasing *p*-cresol accumulation) using independent chemical inhibitors (i.e. L-borneol, amentoflavone, or

diclofenac) consistently resulted in further increases in LDH release associated with *p*-cresol exposure.

These collective data addressed the overall hypothesis in my thesis. In conclusion, our novel data indicated that *p*-cresol was a relatively potent toxicant; however, glucuronidation was unlikely associated with the manifestation of its toxic effects in HepaRG cells.

Reference list

Abreo, K., Sella, M., Gautreaux, S., De Smet, R., Vogeleere, P., Ringoir, S., Vanholder, R., 1997. P-Cresol, a uremic compound, enhances the uptake of aluminum in hepatocytes. J. Am. Soc. Nephrol. 8, 935-942.

Andersen, A., 2006. Final report on the safety assessment of sodium p-chloro-m-cresol, p-chloro-m-cresol, chlorothymol, mixed cresols, m-cresol, o-cresol, p-cresol, isopropyl cresols, thymol, o-cymen-5-ol, and carvacrol. Int. J. Toxicol. 25 Suppl 1, 29-127.

Aquilano, K., Baldelli, S., Ciriolo, M.R., 2014. Glutathione: new roles in redox signaling for an old antioxidant. Front. Pharmacol. 5, 196.

Ashraf, M.N., Asghar, M.W., Rong, Y., Doschak, M.R., Kiang, T.K.L., 2019. Advanced In Vitro HepaRG Culture Systems for Xenobiotic Metabolism and Toxicity Characterization. Eur. J. Drug Metab. Pharmacokinet. 44, 437-458.

Bajaj, P., Chowdhury, S.K., Yucha, R., Kelly, E.J., Xiao, G., 2018. Emerging Kidney Models to Investigate Metabolism, Transport, and Toxicity of Drugs and Xenobiotics. Drug Metab. Dispos. 46, 1692-1702.

Biopredic International, 2016. HepaRG Cell Line Specifications. https://www.biopredic.com/ (accessed 03 February 2021).

Bradshaw, P.R., Athersuch, T.J., Stachulski, A.V., Wilson, I.D., 2020. Acyl glucuronide reactivity in perspective. Drug Discov. Today 25, 1639-1650.

Cayman Chemical, 2016. Glutathione Assay Kit Booklet. https://www.caymanchem.com/product/703002/glutathione-assay-kit (accessed 03 February 2021)
.

Chang, M.C., Chang, H.H., Chan, C.P., Yeung, S.Y., Hsien, H.C., Lin, B.R., Yeh, C.Y., Tseng, W.Y., Tseng, S.K., Jeng, J.H., 2014. p-Cresol affects reactive oxygen species generation, cell cycle arrest, cytotoxicity and inflammation/atherosclerosis-related modulators production in endothelial cells and mononuclear cells. PLoS One 9, e114446.

Chen, X., Zhong, Z., Xu, Z., Chen, L., Wang, Y., 2010. 2',7'-Dichlorodihydrofluorescein as a fluorescent probe for reactive oxygen species measurement: Forty years of application and controversy. Free Radic. Res. 44, 587-604.

Chinnappa, S., Tu, Y.K., Yeh, Y.C., Glorieux, G., Vanholder, R., Mooney, A., 2018. Association between Protein-Bound Uremic Toxins and Asymptomatic Cardiac Dysfunction in Patients with Chronic Kidney Disease. Toxins (Basel) 10, 520.

Cohen, G., Glorieux, G., Thornalley, P., Schepers, E., Meert, N., Jankowski, J., Jankowski, V., Argiles, A., Anderstam, B., Brunet, P., Cerini, C., Dou, L., Deppisch, R., Marescau, B., Massy, Z., Perna, A., Raupachova, J., Rodriguez, M., Stegmayr, B., Vanholder, R., Hörl, W.H., European Uremic Toxin Work Group (EUTox), 2007. Review on uraemic toxins III: recommendations for handling uraemic retention solutes in vitro--towards a standardized approach for research on uraemia. Nephrol. Dial. Transplant. 22, 3381-3390.

Cuoghi, A., Caiazzo, M., Bellei, E., Monari, E., Bergamini, S., Palladino, G., Ozben, T., Tomasi, A., 2012. Quantification of p-cresol sulphate in human plasma by selected reaction monitoring. Anal. Bioanal Chem. 404, 2097-2104.

de Loor, H., Bammens, B., Evenepoel, P., De Preter, V., Verbeke, K., 2005. Gas chromatographic-mass spectrometric analysis for measurement of p-cresol and its conjugated metabolites in uremic and normal serum. Clin. Chem. 51, 1535-1538.

De Smet, R., David, F., Sandra, P., Van Kaer, J., Lesaffer, G., Dhondt, A., Lameire, N., Vanholder, R., 1998. A sensitive HPLC method for the quantification of free and total p-cresol in patients with chronic renal failure. Clin. Chim. Acta 278, 1-21.

Fuloria, S., Subramaniyan, V., Karupiah, S., Kumari, U., Sathasivam, K., Meenakshi, D.U., Wu, Y.S., Sekar, M., Chitranshi, N., Malviya, R., Sudhakar, K., Bajaj, S., Fuloria, N.K., 2021. Comprehensive Review of Methodology to Detect Reactive Oxygen Species (ROS) in Mammalian Species and Establish Its Relationship with Antioxidants and Cancer. Antioxidants (Basel) 10, 128. doi: 10.3390/antiox10010128.

Glorieux, G., Vanholder, R., Van Biesen, W., Pletinck, A., Schepers, E., Neirynck, N., Speeckaert, M., De Bacquer, D., Verbeke, F., 2021. Free P-Cresyl Sulfate Shows The Highest Association With Cardiovascular Outcome In Chronic Kidney Disease. Nephrol. Dial. Transplant.

Graboski, A.L., Redinbo, M.R., 2020. Gut-Derived Protein-Bound Uremic Toxins. Toxins (Basel) 12, 590. doi: 10.3390/toxins12090590.

Gripon, P., Rumin, S., Urban, S., Le Seyec, J., Glaise, D., Cannie, I., Guyomard, C., Lucas, J., Trepo, C., Guguen-Guillouzo, C., 2002. Infection of a human hepatoma cell line by hepatitis B virus. Proc. Natl. Acad. Sci. U. S. A. 99, 15655-15660.

Gross, P., Massy, Z.A., Henaut, L., Boudot, C., Cagnard, J., March, C., Kamel, S., Drueke, T.B., Six, I., 2015. Para-cresyl sulfate acutely impairs vascular reactivity and induces vascular remodeling. J. Cell. Physiol. 230, 2927-2935.

Gryp, T., Vanholder, R., Vaneechoutte, M., Glorieux, G., 2017. p-Cresyl Sulfate. Toxins (Basel) 9, 52.

Guillouzo, A., Corlu, A., Aninat, C., Glaise, D., Morel, F., Guguen-Guillouzo, C., 2007. The human hepatoma HepaRG cells: a highly differentiated model for studies of liver metabolism and toxicity of xenobiotics. Chem. Biol. Interact. 168, 66-73.

Halliwell, B., Whiteman, M., 2004. Measuring reactive species and oxidative damage in vivo and in cell culture: how should you do it and what do the results mean? Br. J. Pharmacol. 142, 231-255.

Hart, S.N., Li, Y., Nakamoto, K., Subileau, E.A., Steen, D., Zhong, X.B., 2010. A comparison of whole genome gene expression profiles of HepaRG cells and HepG2 cells to primary human hepatocytes and human liver tissues. Drug Metab. Dispos. 38, 988-994.

Hashimoto, K., Zaitseva, I.N., Bonala, R., Attaluri, S., Ozga, K., Iden, C.R., Johnson, F., Moriya, M., Grollman, A.P., Sidorenko, V.S., 2016. Sulfotransferase-1A1-dependent bioactivation of aristolochic acid I and N-hydroxyaristolactam I in human cells. Carcinogenesis 37, 647-655.

Idziak, M., Pędzisz, P., Burdzińska, A., Gala, K., Pączek, L., 2014. Uremic toxins impair human bone marrow-derived mesenchymal stem cells functionality in vitro. Exp. Toxicol. Pathol. 66, 187-194.

Ikematsu, N., Kashiwagi, M., Hara, K., Waters, B., Matsusue, A., Takayama, M., Kubo, S.I., 2019. Organ distribution of endogenous p-cresol in hemodialysis patients. J. Med. Invest. 66, 81-85.

Itoh, Y., Ezawa, A., Kikuchi, K., Tsuruta, Y., Niwa, T., 2012. Protein-bound uremic toxins in hemodialysis patients measured by liquid chromatography/tandem mass spectrometry and their effects on endothelial ROS production. Anal. Bioanal Chem. 403, 1841-1850.

James, M.O., 2014. Enzyme kinetics of conjugating enzymes: PAPS sulfotransferase. Methods Mol. Biol. 1113, 187-201.

James, M.O., Ambadapadi, S., 2013. Interactions of cytosolic sulfotransferases with xenobiotics. Drug Metab. Rev. 45, 401-414.

Jourde-Chiche, N., Burtey, S., 2020. Accumulation of protein-bound uremic toxins: the kidney remains the leading culprit in the gut-liver-kidney axis. Kidney Int. 97, 1102-1104.

Karjalainen, M.J., Neuvonen, P.J., Backman, J.T., 2008. In vitro inhibition of CYP1A2 by model inhibitors, anti-inflammatory analgesics and female sex steroids: predictability of in vivo interactions. Basic Clin. Pharmacol. Toxicol. 103, 157-165.

Kiang, T.K., Teng, X.W., Karagiozov, S., Surendradoss, J., Chang, T.K., Abbott, F.S., 2010. Role of oxidative metabolism in the effect of valproic acid on markers of cell viability, necrosis, and oxidative stress in sandwich-cultured rat hepatocytes. Toxicol. Sci. 118, 501-509.

Kiang, T.K., Teng, X.W., Surendradoss, J., Karagiozov, S., Abbott, F.S., Chang, T.K., 2011. Glutathione depletion by valproic acid in sandwich-cultured rat hepatocytes: Role of biotransformation and temporal relationship with onset of toxicity. Toxicol. Appl. Pharmacol. 252, 318-324.

Kitagawa, A., 2001. Effects of cresols (o-, m-, and p-isomers) on the bioenergetic system in isolated rat liver mitochondria. Drug Chem. Toxicol. 24, 39-47.

Knights, K.M., Spencer, S.M., Fallon, J.K., Chau, N., Smith, P.C., Miners, J.O., 2016. Scaling factors for the in vitro-in vivo extrapolation (IV-IVE) of renal drug and xenobiotic glucuronidation clearance. Br. J. Clin. Pharmacol. 81, 1153-1164.

Koppe, L., Pillon, N.J., Vella, R.E., Croze, M.L., Pelletier, C.C., Chambert, S., Massy, Z., Glorieux, G., Vanholder, R., Dugenet, Y., Soula, H.A., Fouque, D., Soulage, C.O., 2013. p-Cresyl sulfate promotes insulin resistance associated with CKD. J. Am. Soc. Nephrol. 24, 88-99.

Korashy, H.M., El-Kadi, A.O., 2005. Regulatory mechanisms modulating the expression of cytochrome P450 1A1 gene by heavy metals. Toxicol. Sci. 88, 39-51.

Korytowska, N., Wyczałkowska-Tomasik, A., Wiśniewska, A., Pączek, L., Giebułtowicz, J., 2019. Development of the LC-MS/MS method for determining the p-cresol level in plasma. J. Pharm. Biomed. Anal. 167, 149-154.

Kotani, N., Maeda, K., Debori, Y., Camus, S., Li, R., Chesne, C., Sugiyama, Y., 2012. Expression and transport function of drug uptake transporters in differentiated HepaRG cells. Mol. Pharm. 9, 3434-3441.

Krieter, D.H., Hackl, A., Rodriguez, A., Chenine, L., Moragues, H.L., Lemke, H.D., Wanner, C., Canaud, B., 2010. Protein-bound uraemic toxin removal in haemodialysis and post-dilution haemodiafiltration. Nephrol. Dial. Transplant. 25, 212-218.

Levey, A.S., Eckardt, K.U., Tsukamoto, Y., Levin, A., Coresh, J., Rossert, J., De Zeeuw, D., Hostetter, T.H., Lameire, N., Eknoyan, G., 2005. Definition and classification of chronic kidney disease: a position statement from Kidney Disease: Improving Global Outcomes (KDIGO). Kidney Int. 67, 2089-2100.

Liabeuf, S., Barreto, D.V., Barreto, F.C., Meert, N., Glorieux, G., Schepers, E., Temmar, M., Choukroun, G., Vanholder, R., Massy, Z.A., European Uraemic Toxin Work Group (EUTox), 2010. Free p-cresylsulphate is a predictor of mortality in patients at different stages of chronic kidney disease. Nephrol. Dial. Transplant. 25, 1183-1191.

Liabeuf, S., Glorieux, G., Lenglet, A., Diouf, M., Schepers, E., Desjardins, L., Choukroun, G., Vanholder, R., Massy, Z.A., European Uremic Toxin (EUTox) Work Group, 2013. Does p-cresylglucuronide have the same impact on mortality as other protein-bound uremic toxins? PLoS One 8, e67168.

Liang, F., Fang, Y., Cao, W., Zhang, Z., Pan, S., Xu, X., 2018. Attenuation of tert-Butyl Hydroperoxide (t-BHP)-Induced Oxidative Damage in HepG2 Cells by Tangeretin: Relevance of the Nrf2-ARE and MAPK Signaling Pathways. J. Agric. Food Chem. 66, 6317-6325.

London, J.A., Wang, E.C.S., Barsukov, I.L., Yates, E.A., Stachulski, A.V., 2020. Synthesis and toxicity profile in 293 human embryonic kidney cells of the β D-glucuronide derivatives of ortho-, meta- and para-cresol. Carbohydr. Res. , 108225.

Lv, X., Zhang, J.B., Wang, X.X., Hu, W.Z., Shi, Y.S., Liu, S.W., Hao, D.C., Zhang, W.D., Ge, G.B., Hou, J., Yang, L., 2018. Amentoflavone is a potent broad-spectrum inhibitor of human UDP-glucuronosyltransferases. Chem. Biol. Interact. 284, 48-55.

Ma, Q., 2013. Role of nrf2 in oxidative stress and toxicity. Annu. Rev. Pharmacol. Toxicol. 53, 401-426.

Marchesi, E., Rota, C., Fann, Y.C., Chignell, C.F., Mason, R.P., 1999. Photoreduction of the fluorescent dye 2'-7'-dichlorofluorescein: a spin trapping and direct electron spin resonance study with implications for oxidative stress measurements. Free Radic. Biol. Med. 26, 148-161.

Martinez, A.W., Recht, N.S., Hostetter, T.H., Meyer, T.W., 2005. Removal of P-Cresol Sulfate by Hemodialysis. J. Am. Soc. Nephrol. 16, 3430-3436.

Meert, N., Beerenhout, C., Schepers, E., Glorieux, G., Kooman, J., Vanholder, R., 2009. Evolution of protein-bound uraemic solutes during predilution haemofiltration. J. Nephrol. 22, 352-357.

Meert, N., Schepers, E., De Smet, R., Argiles, A., Cohen, G., Deppisch, R., Drüeke, T., Massy, Z., Spasovski, G., Stegmayr, B., Zidek, W., Jankowski, J., Vanholder, R., 2007. Inconsistency of reported uremic toxin concentrations. Artif. Organs 31, 600-611.

Meert, N., Schepers, E., Glorieux, G., Van Landschoot, M., Goeman, J.L., Waterloos, M.A., Dhondt, A., Van der Eycken, J., Vanholder, R., 2012. Novel method for simultaneous determination of p-cresylsulphate and p-cresylglucuronide: clinical data and pathophysiological implications. Nephrol. Dial. Transplant. 27, 2388-2396.

Meijers, B., Bammens, B., De Moor, B., Verbeke, K., Vanrenterghem, Y., Evenepoel, P., 2008. Free p-cresol is associated with cardiovascular disease in hemodialysis patients. Kidney Int. 73, 1174-1180.

Mihaila, S.M., Faria, J., Stefens, M.F.J., Stamatialis, D., Verhaar, M.C., Gerritsen, K.G.F., Masereeuw, R., 2020. Drugs Commonly Applied to Kidney Patients May Compromise Renal Tubular Uremic Toxins Excretion. Toxins (Basel) 12, 391. doi: 10.3390/toxins12060391.

Mutsaers, H.A., Caetano-Pinto, P., Seegers, A.E., Dankers, A.C., van den Broek, P. H., Wetzels, J.F., van den Brand, J. A., van den Heuvel, L. P., Hoenderop, J.G., Wilmer, M.J., Masereeuw, R., 2015. Proximal tubular efflux transporters involved in renal excretion of p-cresyl sulfate and p-

cresyl glucuronide: Implications for chronic kidney disease pathophysiology. Toxicol. In. Vitro. 29, 1868-1877.

Mutsaers, H.A., Wilmer, M.J., Reijnders, D., Jansen, J., van den Broek, P. H., Forkink, M., Schepers, E., Glorieux, G., Vanholder, R., van den Heuvel, L. P., Hoenderop, J.G., Masereeuw, R., 2013. Uremic toxins inhibit renal metabolic capacity through interference with glucuronidation and mitochondrial respiration. Biochim. Biophys. Acta 1832, 142-150.

Nieskens, T.T., Peters, J.G., Schreurs, M.J., Smits, N., Woestenenk, R., Jansen, K., van der Made, T. K., Röring, M., Hilgendorf, C., Wilmer, M.J., Masereeuw, R., 2016. A Human Renal Proximal Tubule Cell Line with Stable Organic Anion Transporter 1 and 3 Expression Predictive for Antiviral-Induced Toxicity. AAPS J. 18, 465-475.

Niwa, T., 1993. Phenol and p-cresol accumulated in uremic serum measured by HPLC with fluorescence detection. Clin. Chem. 39, 108-111.

Pham, N.M., Recht, N.S., Hostetter, T.H., Meyer, T.W., 2008. Removal of the protein-bound solutes indican and p-cresol sulfate by peritoneal dialysis. Clin. J. Am. Soc. Nephrol. 3, 85-90.

Poesen, R., Evenepoel, P., de Loor, H., Kuypers, D., Augustijns, P., Meijers, B., 2016. Metabolism, Protein Binding, and Renal Clearance of Microbiota-Derived p-Cresol in Patients with CKD. Clin. J. Am. Soc. Nephrol. 11, 1136-1144.

Poveda, J., Sanchez-Niño, M.D., Glorieux, G., Sanz, A.B., Egido, J., Vanholder, R., Ortiz, A., 2014. P-Cresyl Sulphate has Pro-Inflammatory and Cytotoxic Actions on Human Proximal Tubular Epithelial Cells. Nephrol. Dial. Transplant. 29, 56-64.

Prokopienko, A.J., West, R.E.,3rd, Stubbs, J.R., Nolin, T.D., 2019. Development and validation of a UHPLC-MS/MS method for measurement of a gut-derived uremic toxin panel in human serum: An application in patients with kidney disease. J. Pharm. Biomed. Anal. 174, 618-624.

Prokopienko, A.J., Nolin, T.D., 2018. Microbiota-derived uremic retention solutes: perpetrators of altered nonrenal drug clearance in kidney disease. Expert Rev. Clin. Pharmacol. 11, 71-82.

Riches, Z., Stanley, E.L., Bloomer, J.C., Coughtrie, M.W., 2009. Quantitative evaluation of the expression and activity of five major sulfotransferases (SULTs) in human tissues: the SULT "pie". Drug Metab. Dispos. 37, 2255-2261.

Roche, 2016. Cytotoxicity Detection Kit (LDH) Protocol. https://www.sigmaaldrich.com/content/dam/sigma-aldrich/docs/Roche/Bulletin/1/11644793001bul.pdf (accessed 03 Feruary 2021)
.

Rong, Y., 2021. Characterization of Human Sulfotransferases Catalyzing the Formation of p-cresol Sulfate and Identification of Potent Metabolism Inhibitors as Potential Therapeutic Agents

for Detoxification. The Society of Toxicology Virtual Annual Meeting, March 2021, Online, Abstract number: 3051 .

Rong, Y., Kiang, T.K.L., 2020. Characterizations of Human UDP-Glucuronosyltransferase Enzymes in the Conjugation of p-Cresol. Toxicol. Sci. 176, 285-296.

Rong, Y., Kiang, T.K.L., 2019. Development and validation of a sensitive liquid-chromatography tandem mass spectrometry assay for mycophenolic acid and metabolites in HepaRG cell culture: Characterization of metabolism interactions between p-cresol and mycophenolic acid. Biomed. Chromatogr. 33, e4549.

Rossi, M., Campbell, K.L., Johnson, D.W., Stanton, T., Vesey, D.A., Coombes, J.S., Weston, K.S., Hawley, C.M., McWhinney, B.C., Ungerer, J.P., Isbel, N., 2014. Protein-bound uremic toxins, inflammation and oxidative stress: a cross-sectional study in stage 3-4 chronic kidney disease. Arch. Med. Res. 45, 309-317.

Saito, H., 2013. Toxico-pharmacological perspective of the Nrf2-Keap1 defense system against oxidative stress in kidney diseases. Biochem. Pharmacol. 85, 865-872.

Sato, T., Yamaguchi, H., Kogawa, T., Abe, T., Mano, N., 2014. Organic anion transporting polypeptides 1B1 and 1B3 play an important role in uremic toxin handling and drug-uremic toxin interactions in the liver. J. Pharm. Pharm. Sci. 17, 475-484.

Schepers, E., Meert, N., Glorieux, G., Goeman, J., Van der Eycken, J., Vanholder, R., 2007. P-cresylsulphate, the main in vivo metabolite of p-cresol, activates leucocyte free radical production. Nephrol. Dial. Transplant. 22, 592-596.

Sheu, J.J., Yang, C.C., Wallace, C.G., Chen, K.H., Shao, P.L., Sung, P.H., Li, Y.C., Chu, Y.C., Guo, J., Yip, H.K., 2020. Uremic toxic substances are essential elements for enhancing carotid artery stenosis after balloon-induced endothelial denudation: worsening role of the adventitial layer. Am. J. Transl. Res. 12, 7144-7159.

Surendradoss, J., Chang, T.K., Abbott, F.S., 2014. Evaluation of in situ generated valproyl 1-O-beta-acyl glucuronide in valproic acid toxicity in sandwich-cultured rat hepatocytes. Drug Metab. Dispos. 42, 1834-1842.

Tassaneeyakul, W., Birkett, D.J., Miners, J.O., 1998. Inhibition of human hepatic cytochrome P4502E1 by azole antifungals, CNS-active drugs and non-steroidal anti-inflammatory agents. Xenobiotica 28, 293-301.

Thompson, D.C., Perera, K., Fisher, R., Brendel, K., 1994. Cresol isomers: comparison of toxic potency in rat liver slices. Toxicol. Appl. Pharmacol. 125, 51-58.

Thompson, D.C., Perera, K., London, R., 1996. Studies on the mechanism of hepatotoxicity of 4-methylphenol (p-cresol): effects of deuterium labeling and ring substitution. Chem. Biol. Interact. 101, 1-11.

U.S. Environmental Protection Agency, 2010. Provisional Peer-Reviewed Toxicity Values for 4-Methylphenol (p-Cresol). https://cfpub.epa.gov/ncea/pprtv/documents/Methylphenol4.pdf (accessed 03 February 2021). 2021.

Uchaipichat, V., Mackenzie, P.I., Guo, X.H., Gardner-Stephen, D., Galetin, A., Houston, J.B., Miners, J.O., 2004. Human udp-glucuronosyltransferases: isoform selectivity and kinetics of 4-methylumbelliferone and 1-naphthol glucuronidation, effects of organic solvents, and inhibition by diclofenac and probenecid. Drug Metab. Dispos. 32, 413-423.

US Food and Drug Administration., 2018. Bioanalytical Method Validation Guidance for Industry. https://www.fda.gov/files/drugs/published/Bioanalytical-Method-Validation-Guidance-for-Industry.pdf (accessed February 2021).

Vanholder, R., De Smet, R., Glorieux, G., Argiles, A., Baurmeister, U., Brunet, P., Clark, W., Cohen, G., De Deyn, P.P., Deppisch, R., Descamps-Latscha, B., Henle, T., Jorres, A., Lemke, H.D., Massy, Z.A., Passlick-Deetjen, J., Rodriguez, M., Stegmayr, B., Stenvinkel, P., Tetta, C., Wanner, C., Zidek, W., European Uremic Toxin Work Group (EUTox), 2003. Review on uremic toxins: classification, concentration, and interindividual variability. Kidney Int. 63, 1934-1943.

Vanholder, R., De Smet, R., Lesaffer, G., 1999. P-Cresol: a Toxin Revealing Many Neglected but Relevant Aspects of Uraemic Toxicity. Nephrol. Dial. Transplant. 14, 2813-2815.

Vanholder, R., Pletinck, A., Schepers, E., Glorieux, G., 2018. Biochemical and Clinical Impact of Organic Uremic Retention Solutes: A Comprehensive Update. Toxins (Basel) 10, pii: E33.

Vanholder, R., Schepers, E., Pletinck, A., Nagler, E.V., Glorieux, G., 2014. The uremic toxicity of indoxyl sulfate and p-cresyl sulfate: a systematic review. J. Am. Soc. Nephrol. 25, 1897-1907.

Volpe, D.A., Tobin, G.A., Tavakkoli, F., Dowling, T.C., Light, P.D., Parker, R.J., 2014. Effect of uremic serum and uremic toxins on drug metabolism in human microsomes. Regul. Toxicol. Pharmacol. 68, 297-303.

Watanabe, H., Miyamoto, Y., Honda, D., Tanaka, H., Wu, Q., Endo, M., Noguchi, T., Kadowaki, D., Ishima, Y., Kotani, S., Nakajima, M., Kataoka, K., Kim-Mitsuyama, S., Tanaka, M., Fukagawa, M., Otagiri, M., Maruyama, T., 2013. p-Cresyl sulfate causes renal tubular cell damage by inducing oxidative stress by activation of NADPH oxidase. Kidney Int. 83, 582-592.

Watanabe, H., Sakaguchi, Y., Sugimoto, R., Kaneko, K., Iwata, H., Kotani, S., Nakajima, M., Ishima, Y., Otagiri, M., Maruyama, T., 2014. Human organic anion transporters function as a high-capacity transporter for p-cresyl sulfate, a uremic toxin. Clin. Exp. Nephrol. 18, 814-820.

Watkins, J.B., Klaassen, C.D., 1983. Chemically-induced alteration of UDP-glucuronic acid concentration in rat liver. Drug Metab. Dispos. 11, 37-40.

Weigand, K.M., Schirris, T.J.J., Houweling, M., van den Heuvel, J. J. M. W., Koenderink, J.B., Dankers, A.C.A., Russel, F.G.M., Greupink, R., 2019. Uremic solutes modulate hepatic bile acid handling and induce mitochondrial toxicity. Toxicol. In. Vitro. 56, 52-61.

Wong, X., Carrasco-Pozo, C., Escobar, E., Navarrete, P., Blachier, F., Andriamihaja, M., Lan, A., Tomé, D., Cires, M.J., Pastene, E., Gotteland, M., 2016. Deleterious Effect of p-Cresol on Human Colonic Epithelial Cells Prevented by Proanthocyanidin-Containing Polyphenol Extracts from Fruits and Proanthocyanidin Bacterial Metabolites. J. Agric. Food Chem. 64, 3574-3583.

Wu, W., Bush, K.T., Nigam, S.K., 2017. Key Role for the Organic Anion Transporters, OAT1 and OAT3, in the in vivo Handling of Uremic Toxins and Solutes. Sci. Rep. 7, 4939-2.

Yan, Z., Zhong, H.M., Maher, N., Torres, R., Leo, G.C., Caldwell, G.W., Huebert, N., 2005. Bioactivation of 4-methylphenol (p-cresol) via cytochrome P450-mediated aromatic oxidation in human liver microsomes. Drug Metab. Dispos. 33, 1867-1876.

Yokoyama, Y., Sasaki, Y., Terasaki, N., Kawataki, T., Takekawa, K., Iwase, Y., Shimizu, T., Sanoh, S., Ohta, S., 2018. Comparison of Drug Metabolism and Its Related Hepatotoxic Effects in HepaRG, Cryopreserved Human Hepatocytes, and HepG2 Cell Cultures. Biol. Pharm. Bull. 41, 722-732.